

# AD-A251 463



## ATTACHMENT PAGE

Form Approved  
OMB No. 0704-0188

2

Estimated to average 1 hour per response, including the time for reviewing instructions, searching existing data sources, gathering the collection of information, reviewing the collection of information. Send comments regarding this burden estimate or any other aspect of this collection of information, including suggestions for reducing the burden, to Washington Headquarters Services, Directorate for Information Operations and Reports, 1215 Jefferson Avenue, Washington, DC 20540, and to the Office of Management and Budget, Paperwork Reduction Project (0704-0188), Washington, DC 20503.

1. AGENCY USE ONLY (Leave blank)		2. REPORT DATE May 92	3. REPORT TYPE AND DATES COVERED Graduate Thesis	
4. TITLE AND SUBTITLE A Methodology for Selecting an Electromagnetic Gun System			5. FUNDING NUMBERS	
6. AUTHOR(S) Karl E. Reinhard, CPT, US Army			8. PERFORMING ORGANIZATION REPORT NUMBER <b>SELECTED</b> MAY 23 1992	
7. PERFORMING ORGANIZATION NAME(S) AND ADDRESS(ES) Thesis written for the Graduate School University of Texas at Austin				
9. SPONSORING/MONITORING AGENCY NAME(S) AND ADDRESS(ES)			10. SPONSORING/MONITORING AGENCY REPORT NUMBER	
11. SUPPLEMENTARY NOTES				
12a. DISTRIBUTION/AVAILABILITY STATEMENT <div style="border: 1px solid black; padding: 5px; display: inline-block;"> <p>This document has been approved for public release and sale; its distribution is unlimited.</p> </div> <div style="text-align: center; margin-top: 10px;"> <p>DEFENSE TECHNICAL INFORMATION CENTER</p>   <p>9213045</p> </div>				
13. ABSTRACT (Maximum 200 words)  <p>This thesis proposes a methodology for selecting an electromagnetic launcher (EML) based upon mission requirements and available technology. The intent of the study is twofold. First, it reviews electromagnetic launcher applications, the principles of electromagnetic launch, and major EML system components. The review shows a wide range of potential applications and many divergent system concepts. Second, the study outlines a systematic procedure for selecting an EML system. The methodology can be used either to select the best launcher given existing technology or to project system technology requirements. The methodology does not specify analytic procedures -- the engineer must select analytic techniques appropriate for the system being studied. As an illustration of the procedure, the methodology is applied to the selection of a high performance electromagnetic tank gun.</p>				
14. SUBJECT TERMS Electromagnetic Launcher, Electromagnetic gun, Railgun, Coilgun, Coaxial launcher,			15. NUMBER OF PAGES 202	
			16. PRICE CODE	
17. SECURITY CLASSIFICATION OF REPORT Unclassified	18. SECURITY CLASSIFICATION OF THIS PAGE Unclassified	19. SECURITY CLASSIFICATION OF ABSTRACT Unclassified	20. LIMITATION OF ABSTRACT	

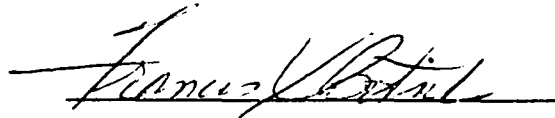
A METHODOLOGY FOR SELECTING AN  
ELECTROMAGNETIC GUN SYSTEM

APPROVED:

Supervisor:



Professor William F. Weldon



Professor Francis X. Bostick

A METHODOLOGY FOR SELECTING AN  
ELECTROMAGNETIC GUN SYSTEM

by

KARL EDWARD REINHARD, B.S.

THESIS

Presented to the Faculty of the Graduate School of

The University of Texas at Austin

in Partial Fulfillment

of the Requirements

for the Degree of

MASTER OF SCIENCE IN ENGINEERING

THE UNIVERSITY OF TEXAS AT AUSTIN

May, 1992



Statement A per telecon  
Capt Jim Creighton TAPC/OPB-D  
Alexandria, VA 22332-0411

NWW 5/27/92

Accession For	
NTIS CRA&I	<input checked="" type="checkbox"/>
DTIC TAB	<input type="checkbox"/>
Unannounced	<input type="checkbox"/>
Justification	
By	
Distribution/	
Availability Codes	
Dist	Availability or Special
A-1	

## Acknowledgments

I wish to thank my supervisor Professor William F. Weldon for generously sharing his knowledge, time, and resources. His guidance was invaluable in the preparation of this thesis and throughout the course of my studies. His engineering insights laid a foundation for my continued growth as an engineer. I also wish to thank Professor Bostick for his patient help through several courses and the insights that he provided.

I owe a debt of gratitude to my fellow graduate student Sunil Murthy who was always willing and able to discuss any and every aspect of electromechanics and electrical engineering in general. Kip Ingram provided helpful insight into the physics of electromagnetic launchers. I also wish to thank the many other engineers and staff at the Center for Electromechanics who helped me so willingly.

My deepest thanks go to my wife and best friend, Sally, for her love, patience, and sacrifice during my graduate studies. Without her help, I would not have succeeded.

Finally, Jesus Christ has been faithful to me in this endeavor. I pray that I might use my new knowledge to further his kingdom.

## TABLE OF CONTENTS

Acknowledgments .....	iii
Table of Contents .....	iv
List of Tables .....	vi
List of Figures .....	viii
Symbol Definitions .....	xi
Chapter 1. Introduction .....	1
Conventional Guns and Rockets .....	2
Military Applications .....	5
Space Applications .....	7
Other Applications .....	8
Chapter 2. Electromagnetic Gun Systems .....	10
Energy Conversion .....	10
The Railgun .....	17
The Coilgun .....	22
Chapter 3. Power Conditioning .....	43
Energy Storage .....	45
Switches .....	63
Buswork .....	69

<b>Chapter 4. Electromagnetic Gun Selection Methodology</b>	<b>70</b>
Mission Profile	72
Barrel Length and Average Acceleration	73
Decision: Railgun or Coilgun?	77
Power Supply Selection	78
Railgun Design	80
Coilgun Design	83
Switches and Buswork	90
<b>Chapter 5. Methodology Application</b>	<b>93</b>
Force and Energy Profiles	93
Select a Coilgun	96
Power Supply Selection	96
Coilgun Design	99
Computer Simulation	109
<b>Chapter 6. Conclusions and Recommendations</b>	<b>127</b>
<b>Appendix A. Mutual Inductance of Finite Coaxial Coils</b>	<b>130</b>
<b>Appendix B. Coilgun Computer Simulation</b>	<b>135</b>
<b>Appendix C. Tabulated Results</b>	<b>155</b>
<b>Endnotes</b>	<b>164</b>
<b>Bibliography</b>	<b>179</b>

## LIST OF TABLES

Table 1-1: Electric energy gun missions .....	6
Table 2-1: Coilgun Classification .....	32
Table 2-2: Summary of Proposed Coilguns .....	41
Table 3-1: Typical Characteristics of Pulsed Power Systems .....	46
Table 3-2: Battery Technology Under Development .....	47
Table 3-3: Electromagnetic Launcher Switching Requirements .....	63
Table 3-4: Typical Closing Switch Characteristics .....	65
Table 4-1: Mission Profile .....	72
Table 4-2: Major Coilgun Parameters .....	85
Table 5-1: Mission 7 Profile: Tank Main Gun .....	94
Table 5-2: M1A1 Main Battle Tank Characteristics .....	94
Table 5-3: Proposed EML System Constraints .....	94
Table 5-4: Proposed EML Component Masses and Volumes .....	97
Table 5-5: State of the Art Capacitor .....	97
Table 5-6: Conductor Properties .....	99
Table 5-7: Comparison of Stator Coil Lengths .....	102
Table 5-8: Coilgun Design Summary .....	109
Table 5-9: Initial Armature Velocity .....	111
Table 5-10: Armature and Stator Coil Self Inductances .....	111
Table 5-11: Coil Conductor Resistances .....	112
Table 5-12: Coil Conductor Masses .....	122
Table 5-13: Conductor Temperature Change .....	122
Table 5-14: Upper Bound Radial Stress Estimates .....	124

<b>Table 5-15: Estimated Switch Requirements .....</b>	<b>125</b>
<b>Table B-1: Coil 1 Simulation Parameters .....</b>	<b>155</b>
<b>Table B-2: Coil 1 Kinematic Data .....</b>	<b>156</b>
<b>Table B-3: Coil 1 Current Data .....</b>	<b>157</b>
<b>Table B-4: Coil 46 Simulation Parameters .....</b>	<b>158</b>
<b>Table B-5: Coil 46 Kinematic Data .....</b>	<b>159</b>
<b>Table B-6: Coil 46 Current Data .....</b>	<b>160</b>
<b>Table B-7: Coil 91 Simulation Parameters .....</b>	<b>161</b>
<b>Table B-8: Coil 91 Kinematic Data .....</b>	<b>162</b>
<b>Table B-9: Coil 91 Current Data .....</b>	<b>163</b>

## LIST OF FIGURES

Figure 1.1: Typical gun barrel .....	3
Figure 1.2: Rocket in flight .....	5
Figure 2.1: A path of integration to determine the energy of system .....	14
Figure 2.2: Railgun diagram .....	17
Figure 2.3: Idealized railgun .....	18
Figure 2.4: Railgun diagram .....	20
Figure 2.5: Coilgun diagram .....	23
Figure 2.6: Mutual inductance relationships between a 10 cm radius stator filament and a range of armature filament radii .....	26
Figure 2.7: Forces that exist on stator and armature coaxial coils ....	27
Figure 2.8: Traveling wave generated by sequenced closing of discrete coil switches .....	34
Figure 2.9: Pull and push modes .....	35
Figure 2.10: Traveling wave generated by multi-phase excitation of series coils with increasing pitch .....	36
Figure 2.11: Traveling wave generated by increasing frequency, multi-phase excitation of series coils .....	37
Figure 2.12: Coilgun modes of operation .....	40
Figure 3.1: Typical power supply options .....	44
Figure 3.2: Schematic of a battery circuit .....	45
Figure 3.3: Typical use of an inductor as an intermediate energy storage device .....	49
Figure 3.4: Capacitor circuit .....	51

Figure 3.5: Homopolar Generator (Faraday Disk) .....	53
Figure 3.6: Alternator Representation .....	55
Figure 3.7: Compensation .....	56
Figure 3.8: Passive compulsator .....	57
Figure 3.9: Selective passive compulsator .....	58
Figure 3.10: Active compulsator .....	59
Figure 3.11: Active compensation .....	60
Figure 3.12: Compulsator circuit .....	61
Figure 3.13: Rising Frequency Generator .....	61
Figure 3.14: Projected energy densities of Pulsed Power Sources ...	62
Figure 3.15: Closing Switches .....	66
Figure 4.1: Electromagnetic launcher selection methodology .....	71
Figure 4.2: Electromagnetic launch system diagram .....	70
Figure 4.3: Mutual inductance gradient curves for a specified armature length and various stator lengths .....	88
Figure 5.1: Mutual inductance gradient curves for the desired armature length and various stator lengths .....	101
Figure 5.2: Armature transit time through the peak gradient length .....	103
Figure 5.3: Coilgun equivalent circuit .....	105
Figure 5.4: Dimensions for determining coil self inductance .....	106
Figure 5.5: Equivalent circuit current rise time as a function of stator coil turns .....	108
Figure 5.6: Coilgun Design .....	109
Figure 5.7: Coilgun circuit model to be evaluated .....	110
Figure 5.8: Mutual inductance and mutual inductance gradient curves for stator coil 1 .....	113

Figure 5.9: Force and acceleration stator coil 1 .....	114
Figure 5.10: Armature velocity through stator coil 1 .....	114
Figure 5.11: Stator and armature currents stator coil 1 .....	115
Figure 5.12: Mutual inductance and mutual inductance gradient curves for stator coils 46 and 91 .....	116
Figure 5.13: Force and acceleration stator coil 46 .....	116
Figure 5.14: Armature velocity through stator coil 46 .....	117
Figure 5.15: Stator and armature currents stator coil 46 .....	117
Figure 5.16: Force and acceleration stator coil 91 .....	119
Figure 5.17: Armature velocity through stator coil 91 .....	119
Figure 5.18: Stator and armature currents stator coil 91 .....	120
Figure 5.19: Stator and armature currents squared -- stator coil 1 .....	121
Figure A.1: Coil geometry showing central filaments used for first order estimate of mutual inductance and mutual inductance gradient .....	131
Figure A.2: Coil geometry for stator coil 1 of example in chapter 5 .....	133
Figure A.3: Mutual Inductance computed with different numbers of filaments .....	133
Figure A.4: Mutual Inductance gradient computed with the indicated numbers of filaments .....	134

## SYMBOL DEFINITIONS

<b>A</b>	area	area	$m^2$
$\mathbf{a}_n, \mathbf{a}_x, \mathbf{a}_y,$ $\mathbf{a}_z, \mathbf{a}_r, \mathbf{a}_\phi$	unit vectors		
<b>B</b>	magnetic flux density	Webers per square meter	$Wb/m^2$
<b>C</b>	capacitance	Farads	<b>F</b>
$C_v$	specific heat capacity	Joules per gram-Kelvin	$J/(g^\circ K)$
$\delta$	mass density	kilograms per meter	$kg/m^3$
<b>d</b>	depth	meters	<b>m</b>
<b>E</b>	electric field intensity	Volts per meter	$V/m$
$\epsilon$	electric permittivity	Farads per meter	$F/m$
<b>F</b>	force	Newtons	<b>N</b>
$f$	force density	Newtons per cubic meter	$N/m^3$
<b>f</b>	frequency	Hertz (cycles per second)	$1/s$
$F^e$	electric force	Newtons	<b>N</b>
<b>H</b>	magnetic field intensity	Amps per meter	$A/m$

h	height	meters	m
I, i	current	Amps	A
J	polar moment of inertia		kg m <sup>2</sup>
<b>J</b>	current density	Amps per square meter	J/m <sup>2</sup>
K	sheet current	Amps per meter	A/m
KE	kinetic energy	Joules	J
L	inductance	Henrys	H
$\lambda$	flux linkage	Weber turns	
M	mutual inductance	Henrys	H
m	mass	kilograms	kg
$\mu$	magnetic permeability	Henrys per meter	H/m
P	power	Watt (Joules per second)	W (J/s)
q	charge	Coulombs	C
R	Resistance	Ohms	$\Omega$
r	radius	meters	m
$\rho$	resistivity	ohms per meter	$\Omega/m$
$\sigma$	conductivity	1/(ohm cm)	1/( $\Omega$ cm)

T	temperature	degrees	°K, °C
t	time	seconds	s
$\tau$	pole pitch	meter per winding	
$t_r$	current rise time	time	s
v	velocity	meters per second	m/s
V, v	electric potential	volts	V
W	energy	Joules	J
$\omega$	radial velocity	radians per second	rad/s
$W_m$	magnetic energy	Joules	J
$W_t$	thermal energy	joules	J
x, z	position	meters	m

## Chapter 1

### INTRODUCTION

In the past decade, the United States Government and industry have committed considerable resources to the development of electromagnetic launch technology. The effort has been spurred by the need to accelerate projectiles to velocities that exceed the fundamental capabilities of conventional chemical propellant guns and to replace rockets in some applications. Electromagnetic propulsion is one of the most promising technologies for meeting short and long term launch requirements. Electromagnetic launch technology has been proposed for application to advanced weapons systems, space launch and propulsion, nuclear fusion, and various industrial processes.

The possibility of using electromagnetic forces to launch projectiles was recognized early in the 20th century; but until 1976 with the work of S. C. Rashleigh and R. A. Marshall at the Australian National University,<sup>1-1</sup> the various efforts to build electromagnetic launchers had enjoyed only limited success. The early attempts to develop launchers never approached the capabilities of conventional guns due to the inadequacy of the available technology.<sup>1-2</sup> Today, the technologies are available and have been demonstrated in the laboratory to launch projectiles to velocities substantially beyond the capabilities of conventional guns. The next step in electromagnetic launcher (EML) development is to advance technology to the point that reasonably sized and reliable systems can be built and used outside of the laboratory environment.

At the most basic level, the electromagnetic launcher consists of the launcher (the barrel) and a power supply system. The railgun and coilgun are the principle electromagnetic launcher concepts being

developed. Both launchers convert very large amounts of electrical energy to mechanical energy (projectile kinetic energy) in very short time periods. The physical principles responsible for the driving force in each gun concept are different; thus, one launcher concept or the other may be more suitable for a particular application. Just as there are different launcher types, each launcher can be driven by several different power supply configurations. While both launchers have been demonstrated in the laboratory, launcher and power supply technologies are far from mature. Each launcher and power supply system has technological obstacles that prevent the system from being put in the field today. These factors complicate the process of selecting an appropriate launcher and power supply system for a given application and technology level.

The purpose of this study is to propose a methodology for selecting an electromagnetic launch system that is appropriate for a given mission and technology level. The remainder of this chapter briefly examines important aspects of conventional gun and rocket systems and explores the proposed applications for electromagnetic launchers. Chapters two and three examine the fundamental components that make up EML systems. Chapter two examines the principles of electromechanical energy conversion and then applies those principles to the railgun and coilgun. Chapter three examines power supply and conditioning including energy storage devices, switches, and buswork. Chapter four presents the methodology. In chapter five, the methodology is applied to a particular application given present and projected technologies.

### Conventional Guns and Rockets

The conventional gun is a simple machine that converts energy stored chemically in the propellant into mechanical energy via

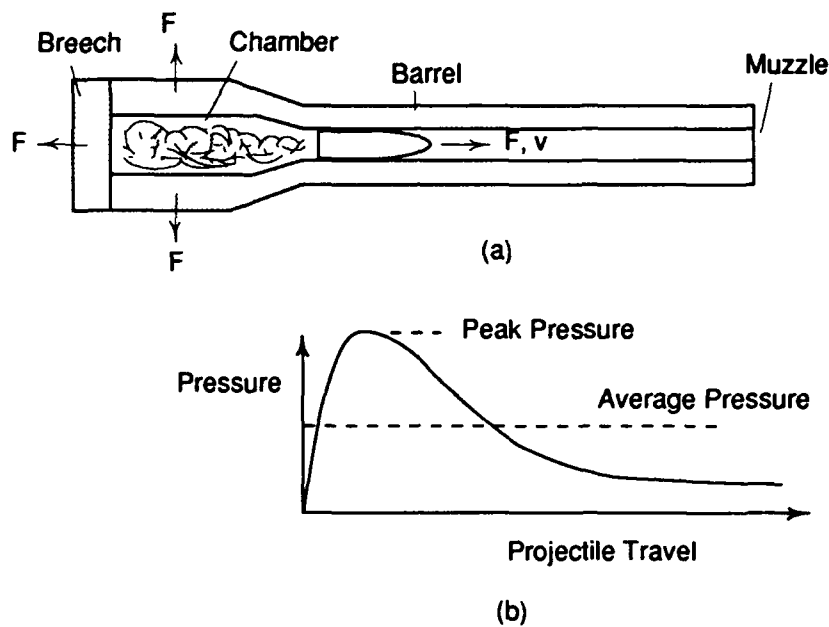


Figure 1.1<sup>1-5</sup> (a) Typical gun barrel. (b) Pressure Travel Curve.

thermodynamic action (figure 1.1(a)). Conventional propellants store energy very compactly and can release their stored energy very rapidly with relative ease. The common measure of the useful energy stored is the propellant's impetus,  $I$ , which is defined by the expression

$$I = \frac{RT_f}{M} \left( \frac{\text{J}}{\text{g}} \right)$$

where,

$$R = \text{universal gas constant} \left( \frac{\text{J}}{\text{g-mole } ^\circ\text{K}} \right)$$

$$T_f = \text{adiabatic flame temperature} (^\circ\text{K})$$

$$M = \text{molecular weight of product gases} \left( \frac{\text{g}}{\text{g-mole}} \right)$$

Today's state of the art propellants have impetus values on the order of 1 MJ/kg.<sup>1-3</sup> When the propellant is ignited, the ensuing combustion process releases the stored energy as very hot, expanding gases. The gases exert tremendous pressure ( $10^5$  pounds per square inch<sup>1-4</sup>) on the surfaces that enclose the chamber. The pressure causes the projectile to rapidly accelerate so that it leaves the muzzle with high velocity.

The pressure-travel curve, shown in figure 1.1(b), is helpful in examining the pressure applied to the projectile as a function of position during launch. The work done by the gun on the projectile is the product of the area under the curve and the projectile base cross sectional area. Piezometric efficiency is the ratio of the average to peak barrel pressure; typical efficiencies are 40 percent for artillery and 60 percent for tank guns. Piezometric efficiency is a measure of the constancy of the pressure applied to the projectile. The least stress is placed upon the barrel and projectile when the piezometric efficiency is high -- implying consistent pressure throughout the launch.<sup>1-5</sup>

The performance of a conventional gun is fundamentally limited by the breech and barrel materials and the dynamic properties of the propellant gases. The breech and barrel materials determine the maximum allowable pressure. The projectile muzzle velocity is limited by the rate at which the combustion gases expand. Force results from gas molecules contacting the projectile base. At velocities approaching the gas expansion rate, the contact between the expanding gases and projectile base diminishes reducing the force on the projectile. The expansion rate is proportional to the speed of sound in the gas which is proportional to the square root of the quotient of the gas temperature and molecular weight. The gas temperature is limited by the temperature that the bore materials can withstand without damage.<sup>1-6</sup>

The rocket, in contrast to the gun, carries its propellant

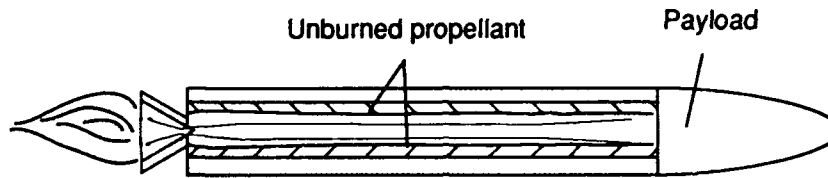


Figure 1.2 Rocket in flight. The rocket carries its fuel internally resulting in low payload fraction of total rocket mass.

internally (figure 1.2). This increases the time that the propellant can burn; thus, the rocket can be accelerated for seconds to minutes and achieve velocities of tens of kilometers per second. Rocket velocity is not limited by the gas expansion rate since the reaction takes place in the rocket's frame of reference. The penalty is that propellant adds to the mass that must be accelerated and as a consequence reduces the allowable payload. The energy densities of rocket propellants are of the same order as gun propellants and have remained fairly constant for some time despite research efforts.<sup>1-7</sup>

The high energy density and relative ease of ignition of conventional propellants are liabilities during their manufacture, transportation, handling, and storage. Propellants are hazardous materials and must be treated with the utmost care lest they be accidentally ignited; once ignited the combustion reaction cannot be controlled.<sup>1-8</sup> The special manufacturing, storage, packaging, handling, and quality control requirements of propellant materials make them an expensive energy source.

### Military Applications

Electromagnetic launch technology is very attractive for advanced weapons systems; table 1-1 shows typical military

Mission Number	Mission Type	Flight Projectile Mass (kg)	Muzzle Velocity (km/s)	Nominal Kinetic Energy (MJ)	Allowable Accelerator ( $\times 10^5 \text{m/s}^2$ )	Launch Rate
1	Fire support	45	1.1	27	1.5	4 rounds in 15 s, 105 s between
2	Fire support	90	1.2	65	2.0	5 rounds in 120 s, 480 s between
3	Fire support	100	2.3	260	4.0	5 rounds in 120 s, 480 between
4	Counter armor	5.3	1.7	7.5	6.0	2 rounds in 5 s, 22.5 s between
5	Counter armor	3.2	2.5	10	7.0	2 rounds in 5 s, 22.5 s between
6	Counter armor	2.4	2.5	7.5	7.0	2 rounds in 5 s, 22.5 s between
7	Counter armor	1.7	3.0	7.5	12.0	2 rounds in 5 s, 22.5 s between
8	Counter armor	8.0	1.7	12	6.0	2 rounds in 5 s, 22.5 s between
9	Counter armor	3.7	2.5	12	10.0	2 rounds in 5 s, 22.5 s between
10	Counter armor	2.5	3.0	12	10.0	2 rounds in 5 s, 22.5 s between
11	Counter air and missile	0.45	3.0	2.0	7.0	100 rounds in 2 s, 13 s between
12	Counter air and missile	0.45	2.0	0.9	7.0	100 rounds in 2 s, 13 s between
13	Counter air and missile	7.45	2.0	15	5.0	10 rounds per min
14	Counter air and missile	14.5	2.5	45	5.0	8 rounds per min
15	Counter air and missile	4.5	3.6	29	10.0	8 rounds in 30 s, 90 s between
16	Counter air and missile	14.5	3.6	94	5.0	0.5 rounds per min
17	Special operations	0.36	2.5	1.1	7.0	10 rounds in 10 s, 20 s between
18	Special operations	2.0	2.2	5.0	7.0	10 rounds per min

Table 1-1 Electric energy gun missions<sup>1-9</sup>

applications proposed for electric guns. A key attraction of the technology is that the sonic limit upon launch velocity is eliminated; launch velocity is constrained only by material stress limits. Today, conventional tank guns launch their highest velocity projectiles (kinetic energy rounds) at 1500-1750 meters per second; air defense guns and artillery projectiles achieve launch velocities of 1100-1130 and 750-800 meters per second respectively. These launch velocities

may be improved by up to 50 percent using innovative propellant and projectile designs before the ultimate velocity limits are reached; but even these improvements fall short of the 3,000 meter per second and faster muzzle velocities desired for some counter armor and air defense weapon systems.<sup>1-10</sup>

Electromagnetic launch offers a number of benefits over conventional guns. Increased muzzle velocity provides improved target penetration, reduced time of flight, and increased range. Reduced time of flight is expected to reduce projectile dispersion on target -- consequently improving accuracy.<sup>1-11</sup> Military tactical EMLs would almost certainly derive their electrical energy from turbines or generators powered by common vehicle fuels; this is a distinct advantage since petroleum fuels are much less hazardous and cheaper than conventional propellants. Replacing conventional propellant with vehicle fuel would reduce some of the ammunition logistics burden.

### Space Applications

Today rockets are the only available means of placing payloads into space. Unfortunately, the cost of rocket launch is in the range of \$1,000 to \$40,000 per pound of payload. The rocket propellant constitutes as much as 90 percent of the total system weight. Electromagnetic launch systems offer several advantages over current rocket launch systems. A chief advantage is reduced cost. The large capital investment is in the launcher which stays on the ground and can be used repeatedly as opposed to the rocket that is typically single use. Much of the EML launch energy can be supplied by electrical energy sources which are safer and cheaper than rocket propellants. The projectile can be much smaller since a large fraction of the required launch kinetic energy is imparted by the launcher; although, a small rocket would still be required to boost the payload into its final

orbit. Since the launcher remains on the ground, the weight and volume constraints on it are less stringent than those on rockets.<sup>1-12</sup>

Electromagnetic launchers have the potential to make space operations economical and much more accessible. However, EMLs are useful only for those payloads that can be hardened to survive the extreme acceleration forces of launch. Possible payloads include a variety of small satellites and bulk materials. EMLs have been proposed as an economical means of disposing of nuclear waste in space.<sup>1-13</sup> EMLs may also be suitable as engines for propelling orbital vehicles.<sup>1-14</sup>

### Other Applications

Electromagnetic launch can also be applied to several other applications. EMLs have been proposed and used for the study high velocity flight and impact. The Center for Electromechanics (CEM) at the University of Texas at Austin has used a railgun to launch glass beads (simulating micro-meteorites) at velocities of up to 11 kilometers per second at a variety of materials intended for use in space. This provided important information about material survivability that could not have otherwise been determined on the ground.<sup>1-15</sup> CEM has also proposed using electromagnetic launchers to accelerate models of advanced aircraft to hypervelocities in flight chambers for design testing.<sup>1-16</sup>

Electromagnetic launch may be a means of generating power via nuclear fusion. Conceptually, one or several gram sized pellets of nuclear fuel are accelerated to 20-50 kilometers per second and impacted on a target. The impact converts the pellets into extremely hot plasmas under great pressures -- conditions under which fusion can occur. Fusion would occur for nanoseconds and release several

**gigajoules of energy more than required to accelerate the fuel pellets; the energy released would be captured and used to generate electrical power.<sup>1-17</sup>**

**High velocity electromagnetic launch may also be useful for a variety of materials processing and manufacturing applications. Metals launched at high velocity melt upon impact and if applied in thin layers are rapidly quenched; metal coatings could be sprayed on to surfaces very quickly. Amorphous metal materials have been formed by high velocity impact. Special micro-machining processes are possible using ion clusters accelerated to hyper velocities.<sup>1-18</sup>**

## Chapter 2

### ELECTROMAGNETIC GUN SYSTEMS

#### Energy Conversion

An electric gun is fundamentally a device that converts magnetic field energy to projectile kinetic energy. Unlike a conventional gun system which is a purely mechanical system, an electric gun is a hybrid electrical and mechanical system. The most convenient basis for linking the electrical and mechanical parts of the system is conservation of energy. In a general electromechanical system, the difference between the electrical energy input and the mechanical energy output can exist in several forms

$$\begin{array}{rcccccc} \text{Electric} & \text{Mechanical} & & \text{Electric} & \text{Magnetic} & \text{Potential} & \text{Thermal} \\ \text{Energy} & \text{Energy} & = & \text{Field} & \text{Field} & \text{Energy} & \text{Energy} \\ \text{Input} & \text{Output} & & \text{Energy} & \text{Energy} & & \end{array}$$

The electromagnetic launcher (EML) is a special case of the general system -- a magnetic field system. Energy stored in the electric field is insignificant relative to the magnetic field.<sup>2-1</sup> Potential energy from gravity or spring action is not a significant factor in EMLs. Finally, thermal energy, which results from dissipative processes such as Joule heating and friction, can be neglected without significantly changing the fundamental physics of the device -- the system may be assumed to be lossless.<sup>2-2</sup> Thus, the important physical aspects of the system are contained in the expression

$$\begin{array}{rcl} \text{Electric} & \text{Mechanical} & \text{Magnetic} \\ \text{Energy} & - \text{Energy} & = \text{Field} \\ \text{Input} & \text{Output} & \text{Energy} \end{array}$$

Since energy must be conserved, its time derivative must also be conserved. Thus, the difference between the electric input power and mechanical output power can be expressed

$$i \frac{d\lambda}{dt} - F^e \frac{dx}{dt} = \frac{dW_m}{dt}$$

where,

$$\begin{array}{l} W_m = W_m(\lambda, x), \text{ magnetic energy density} \\ \lambda = \text{flux linkage} \\ i = \text{electric terminal current} \\ F^e = \text{electric force} \\ x = \text{position} \\ t = \text{time} \end{array}$$

Using Faraday's law, the first derivative term on the left becomes electromotive force (emf)<sup>2-3</sup>, and the expression can be written in a more familiar form

$$i v - F^e \nu = \frac{dW_m}{dt}$$

where,

$$\begin{array}{l} v = \text{electrical terminal voltage} \\ \nu = \text{velocity} \end{array}$$

Electric power ( $i v$ ) is applied to the system and mechanical power ( $F^e \nu$ ) is output as indicated by the minus sign.<sup>2-4</sup>

The total system power is the sum of the mechanical and electrical powers. Multiplying both sides of the original equation by  $dt$  yields

$$(2-1) \quad dW_m = i d\lambda - F^e dx$$

Upon integration, this expression yields the system's magnetic energy. Further, it can be shown by mathematical manipulation that the force of electromagnetic origin is a function of the system's magnetic energy distribution

$$(2-2) \quad F^e = -\frac{\partial W_m(\lambda, x)}{\partial x}.$$

Thus, electromagnetic force results from magnetic energy gradients created in the system.<sup>2-5</sup>

Force can also be examined as a function of magnetic flux density. Magnetic energy can be expressed as<sup>2-6</sup>

$$W_m = \iiint_{vol} \frac{\mu H^2}{2} dv = \iiint_{vol} \frac{B^2}{2\mu} dv$$

where,

**H** = magnetic field intensity

**$\mu$**  = magnetic permeability

**B** =  $\mu H$  = magnetic flux density

Differentiating both sides and dividing by the differential element  $dv$  yields the energy density expression

$$(2-3) \quad \frac{dW}{dv} = \frac{B^2}{2\mu}.$$

The energy density can also be thought of as local stress which by definition is force per unit area (pressure).<sup>2-7</sup> When a uniform energy density exists along a surface, the force can be estimated as the product of energy density and surface area

$$(2-4) \quad F^e = \left( \frac{B^2}{2\mu} \right) A$$

where,

$$A = \text{area}$$

This is an alternate expression of equation (2-2) that is often useful in estimating forces in magnetic field systems.

The concept of force resulting from energy gradients is common to all electric guns. Notice that the magnetic energy density is a function of the independent variables  $\lambda$  and  $x$ . Determining the flux linkage and the associated magnetic energy distribution is not simple -- making this force expression difficult to use.

Fortunately in a linear, conservative system, a mathematical expression called coenergy can be constructed that is equivalent to energy but a function of the independent variables  $x$  and  $i$ . Coenergy is useful since both position and current are easily measured.<sup>2-8</sup> Coenergy is a mathematical expression and has no physical meaning. In a conservative system, magnetic energy is a single valued function of the independent variables  $\lambda$  and  $x$ ; this means that energy is independent of the path that brought the system to a particular energy

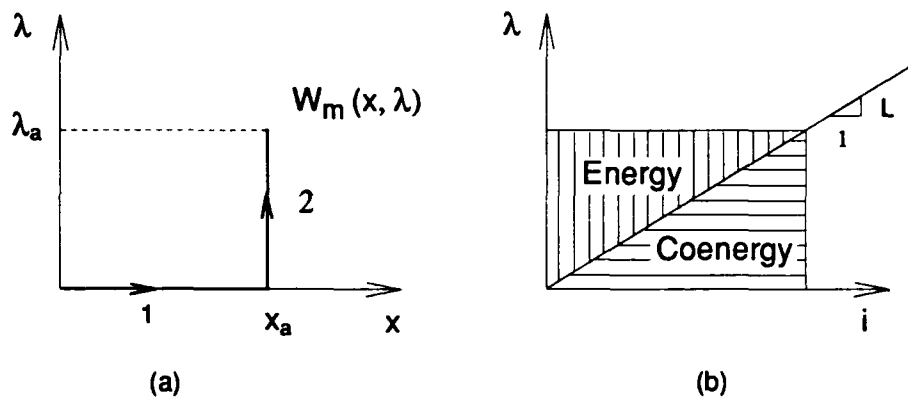


Figure 2.1 (a) A path of integration to determine the energy of a system.  
 (b) The relationship between energy and coenergy in a linear system.

state. The system's energy can be determined by integrating equation (2-1) along the path shown in figure 2.1(a)

$$W_m = \int i d\lambda - \int F^e dx.$$

Along the first leg of the path there is no electrical excitation ( $\therefore F^e = 0$ ) and  $\lambda$  is constant ( $\therefore d\lambda = 0$ ); integration along leg one makes no contribution to magnetic energy. Along the second leg of the path,  $x$  is constant ( $\therefore dx = 0$ ).<sup>2-9</sup> Thus, the system energy can be determined from the simplified expression

$$(2-5) \quad W_m = \int i d\lambda$$

For a linear system (non-magnetic materials), energy is numerically equal to coenergy as evident in figure 2.1(b).<sup>2-10</sup> The relationship between  $\lambda$  and  $i$  is

$$(2-6) \quad \lambda = Li$$

where,

$L =$  self inductance

Differentiating both sides yields

$$d\lambda = L di$$

Coenergy is obtained by substituting this expression into equation (2-5)

$$\begin{aligned} W'_m &= \int Li di \\ (2-7) \qquad &= \frac{1}{2} Li^2 \end{aligned}$$

Since  $W_m$  for a linear, conservative system is equal to  $W'_m$ , then

$$(2-8) \qquad W_m = \frac{1}{2} Li^2.$$

It can also be shown that force is a function of coenergy given by the expression<sup>2-11</sup>

$$(2-9) \qquad F^e = \frac{\partial W'_m(i, x)}{\partial x}.$$

In systems with two or more terminals, mutual inductance terms must be added to account for the energy stored in magnetic

fields between terminal elements. This results in the magnetic energy expression<sup>2-12</sup>

$$(2-10) \quad W_m = \sum_{i=1}^N \frac{1}{2} L_i I_i^2 + \sum_{i=1}^N \sum_{j=1}^N I_i I_j M_{ij}$$

where,

**M** = mutual inductance

**N** = number of terminal pairs.

The Lorentz force law, derived from Maxwell's equations, is also useful in determining electric forces<sup>2-13</sup>

$$\mathbf{f} = q\mathbf{E} + \mathbf{J} \times \mathbf{B}$$

where,

**f** = force density

**q** = charge

**E** = electric field intensity

**J** = current density

In a magnetic field system, the electric field does not make a significant contribution to force density reducing the expression to

$$(2-11) \quad \mathbf{f} = \mathbf{J} \times \mathbf{B}$$

Force is determined by integrating the resulting force density over the appropriate volume. This approach is particularly useful in determining force direction.

## The Railgun

The railgun is an energy conversion device consisting of two parallel conducting rails which are electrically connected by a sliding conductor (or armature); the armature is constrained to slide down the rails as illustrated in figure 2.2. When a current is applied to the rails as shown, a magnetic field is created according to the right-hand rule. The magnetic field interacts with the current flowing in the armature to push the projectile down the length of the barrel. The vector direction of the force can be determined using equation (2-11).

The fundamental principles of railgun operation can be understood by considering an idealized system as illustrated in figure 2.3(a). In this system, two very wide, perfectly conducting plates are shorted by a third perfectly conducting plate with the dimension  $h$  being much less than the dimension  $d$ .<sup>2-15</sup> The voltage source produces a sheet current in the upper plate given by

$$\mathbf{K} = \mathbf{a}_x K_x = \mathbf{a}_x \frac{I}{d}$$

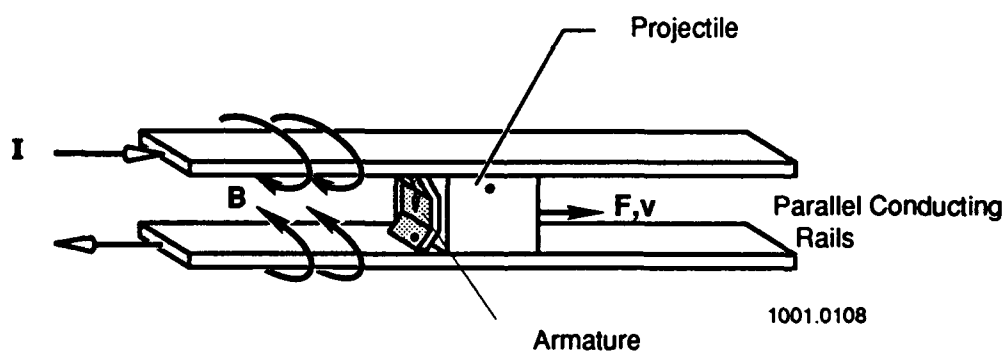


Figure 2.2 Railgun diagram<sup>2-14</sup>

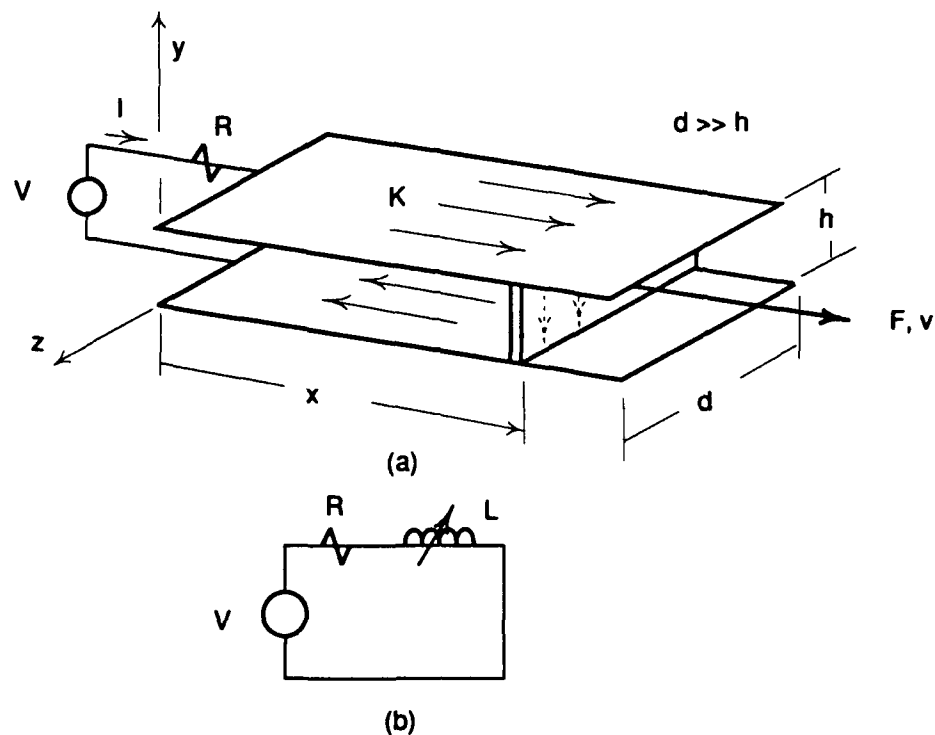


Figure 2.3 (a) Idealized railgun (b) Equivalent circuit model

Similar sheet currents exist in the other two plates with directions as indicated. Because  $h$  is much less than  $d$ , the magnetic field,  $\mathbf{H}$ , can be considered approximately uniform between the conducting sheets and can be expressed as the cross product of the surface current and the surface normal<sup>2-16</sup>

$$\mathbf{H} = \mathbf{K} \times \mathbf{n} = \mathbf{a}_x \frac{I}{d} \times -\mathbf{a}_y = -\mathbf{a}_z \frac{I}{d}.$$

This results in the magnetic flux density

$$\mathbf{B} = \mu \mathbf{H} = -\mathbf{a}_z \frac{\mu I}{d}$$

The flux linked by this circuit can be determined by integrating  $\mathbf{B}$  over the cross sectional area perpendicular to the vector direction of  $\mathbf{B}$

$$\begin{aligned}\lambda &= \int_s \mathbf{B} \cdot \mathbf{n} \, dA = \int_s -\mathbf{a}_z \frac{\mu I}{d} \cdot -\mathbf{a}_z \, dx \, dy \\ &= \frac{\mu h x I}{d}\end{aligned}$$

This results in the self inductance as defined in equation (2-6)

$$(2-12) \quad L = \frac{\mu h x}{d}$$

Note that the self inductance is a function of geometry and varies with the position of the armature. The system can also be considered as a lumped parameter electric circuit as shown in figure 2.3 (b).

Assuming that this is a conservative system, the force on the armature can be determined using magnetic coenergy; combining equations (2-7) and (2-9), the force is

$$\begin{aligned}(2-13) \quad F &= \frac{\partial W'_m(i, x)}{\partial x} = \frac{\partial}{\partial x} \left[ \frac{1}{2} L I^2 \right] = \frac{1}{2} I^2 \frac{\partial}{\partial x} \left[ \frac{\mu h x}{d} \right] \\ &= \frac{1}{2} \frac{\mu h I^2}{d}\end{aligned}$$

We see that the force is a function of geometry (but independent of  $x$ ) and the current. In this example, magnetic field exists to the left of the armature, but no magnetic field exists to the right of the armature;

thus, a magnetic energy gradient exists across the armature that produces a force in the  $x$  direction. Part of the railgun's elegance is that the position of the magnetic energy gradient is perfectly synchronized with the position of the armature. The armature can be thought of a switch that continuously switches the current to produce magnetic field behind the armature.

The direction of force on the armature can also be obtained using equation (2-11) where  $\mathbf{J}$  is the current flowing in the armature. The force on the armature can be found by integrating the force density over the volume of the armature, but this requires knowledge of the  $\mathbf{B}$  field distribution inside the armature. The Lorentz force law provides important insight into other forces acting upon the barrel. Lateral forces arise on both plates due to the interaction of the currents flowing in the plates and the magnetic field (figure 2.4). The railgun barrel must sustain lateral pressures in much the same way that a conventional gun barrel does. A significant difference is that the force in a railgun barrel is asymmetric about the barrel center line; whereas, the force in a conventional barrel is symmetric about the barrel center line.

The power required to drive the gun must be determined as a

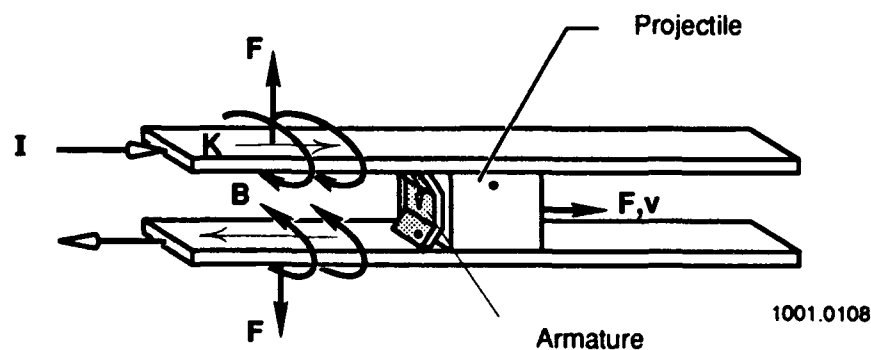


Figure 2.4 Railgun diagram<sup>2-14</sup>

function of the magnetic energy; the magnetic energy is given by

$$W_m = \frac{\mu}{2} \iiint_{vol} \frac{\mu \mathbf{H}^2}{2} dv = \frac{\mu}{2} \left( \frac{I^2}{d^2} \right) (x dh)$$

This is the same result that equation (2-8) produces using the expression for self inductance from equation (2-12). This leads to an expression for power

$$\begin{aligned} P &= \frac{\partial W_m}{\partial t} = \frac{\partial}{\partial t} \left[ \frac{1}{2} L I^2 \right] \\ &= \frac{1}{2} I^2 \frac{dL}{dx} \frac{dx}{dt} + I L \frac{dI}{dt} \end{aligned}$$

This is an interesting result. The first term is the product of force (equation (2-13)) and velocity -- or mechanical power. The second term is the product of current and an electromotive force (emf) resulting from the current changing in the inductor. Thus, the change of magnetic energy with time is manifested both electrically and mechanically -- indicating the energy conversion process that takes place.

The railgun is the simplest of the electric guns and has been successfully demonstrated. The Center for Electromechanics (CEM) at the University of Texas at Austin has launched two kilogram masses at velocities exceeding 2.3 kilometers per second.<sup>2-17</sup> A crucial obstacle, however, to a practical gun outside the laboratory is finding a way to prevent rail and insulator damage during launch.<sup>2-18, 2-19</sup> The sliding contacts between the armature and rails must be able to withstand the extreme mechanical and electrical stresses of launch

with little or no damage. The sliding contact problem has spurred research into contactless electric guns.

### The Coilgun

The coilgun is the principle alternative to the railgun and has the advantage of no electrical contact between the armature and stator. As illustrated in figure 2.5, the coilgun consists of a series of coaxial stator coils and an armature coil that travels along the stator coil axis. Unlike the railgun that has one electrical terminal pair, the coil gun may have an electrical terminal pair for the armature and each stator coil; this adds considerable complexity to the analysis of the coilgun.

Like the railgun, the driving force in the coilgun is created by the magnetic energy gradient along the axis of the barrel

$$(2-14) \quad F = - \frac{\partial W_m(\lambda, z)}{\partial z}$$

In a linear, conservative system, it is once again convenient to express the force as a function of magnetic coenergy

$$\begin{aligned} F &= \frac{\partial W'_m(i, z)}{\partial z} \\ &= \frac{\partial}{\partial z} \left[ \frac{1}{2} L_a I_a^2 + I_a I_s M + \frac{1}{2} L_s I_s^2 \right] \end{aligned}$$

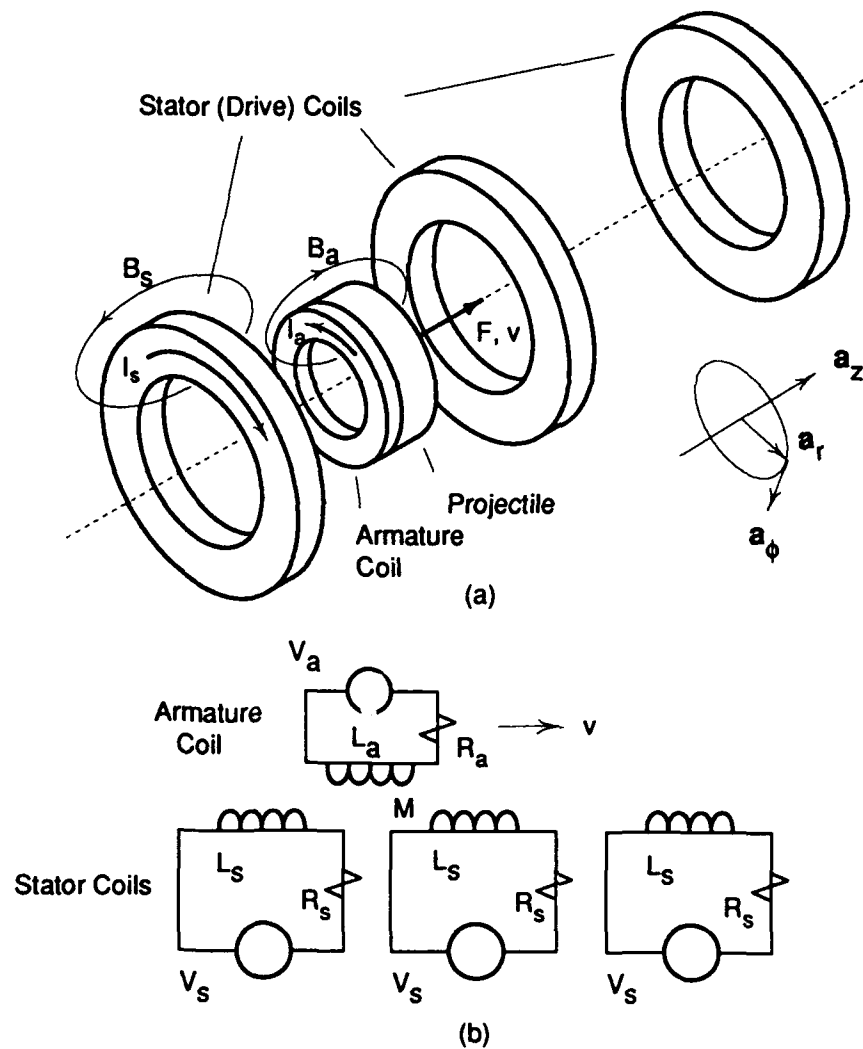


Figure 2.5 (a) Coilgun diagram. (b) Coilgun equivalent circuit.

In the coilgun, the self inductances of the armature and stator coils are independent of position; thus, the force is dependent only upon the term containing the mutual inductance which is a function of  $z$

$$(2-15) \quad F = I_a I_s \frac{\partial M}{\partial z}.$$

For coaxial coils, the mutual inductance is a complicated expression involving complete elliptic integrals of the first and second kind. The mutual inductance between filamentary coils is given by<sup>2-20</sup>

$$(2-16) \quad M = \frac{2\mu}{k} \sqrt{r_a r_s} \left[ \left( 1 - \frac{k^2}{2} \right) K(k) - E(k) \right]$$

where,

$$k = \sqrt{\frac{4r_a r_s}{(r_a + r_s)^2 + z^2}}$$

- $K(k)$  = complete elliptic integral of the first kind
- $E(k)$  = complete elliptic integral of the second kind
- $r_a$  = armature filament radius
- $r_s$  = stator filament radius
- $z$  = axial position.

Based upon the symmetry of the filaments, the mutual inductance is a function of the axial position of the filaments relative to each other and the radius of each of the filaments. This expression for filamentary elements can be used to construct the mutual inductance of finite coils by assuming that the coils are composed of multiple filamentary elements; the mutual inductance is the sum of the mutual inductances between each of the filaments (see Appendix A). The self-inductance of a coil is a special case of mutual inductance; the self inductance is the sum of the mutual inductances between each of the filamentary elements that make up a single coil.<sup>2-21</sup> A representative mutual inductance curve for a 10 cm radius stator filament and a range of armature filament sizes is shown in figure 2.6 (a).

The gradient of the mutual inductance in the  $z$  direction is also a function of complete elliptic integrals<sup>2-22</sup>

$$(2-17) \quad \frac{\partial M}{\partial z} = \frac{\mu k z}{4(1-k^2)\sqrt{r_a r_s}} \left[ 2(1-k^2)K(k) - (2-k^2)E(k) \right]$$

A representative mutual inductance gradient curve for a 10 cm radius stator filament and a range of armature filament sizes is shown in figure 2.6 (c). Notice that the mutual inductance gradient increases as the radius of the armature approaches the radius of the stator. Also note that the mutual inductance gradient is significant only within one coil diameter on either side of the stator coil. Again, the mutual inductance gradient of finite coils may be constructed assuming that the coils are composed of an array of filamentary elements.

Based upon equations (2-15) and (2-17), the direction of force on the armature depends upon the relative directions of the armature and stator currents regardless of the relative positions of the armature and stator. If the currents are in the same direction; the coils experience an attractive force; on the other hand, currents of opposite signs generate a repulsive force between the coils. The currents are in essence generating magnetic poles. Like magnetic poles repel and opposite magnetic poles attract. Thus, with the appropriate combinations of current directions, the coilgun can operate in one of three modes: push, pull, or a combination of the two.

Once again, the Lorentz force law provides useful insight into the forces at work. Figure 2.7 depicts the forces on a pair of coils operating in the push mode. The magnetic field generated by the stator interacts with the armature current to produce forces on the armature; likewise, force is produced on the stator by the interaction of the armature magnetic field and stator currents. In addition to the propulsive force, radial forces exist on both the armature and stator; the armature is acted upon by compressive forces while the stator must contain radially outward forces. These opposing radial forces act to

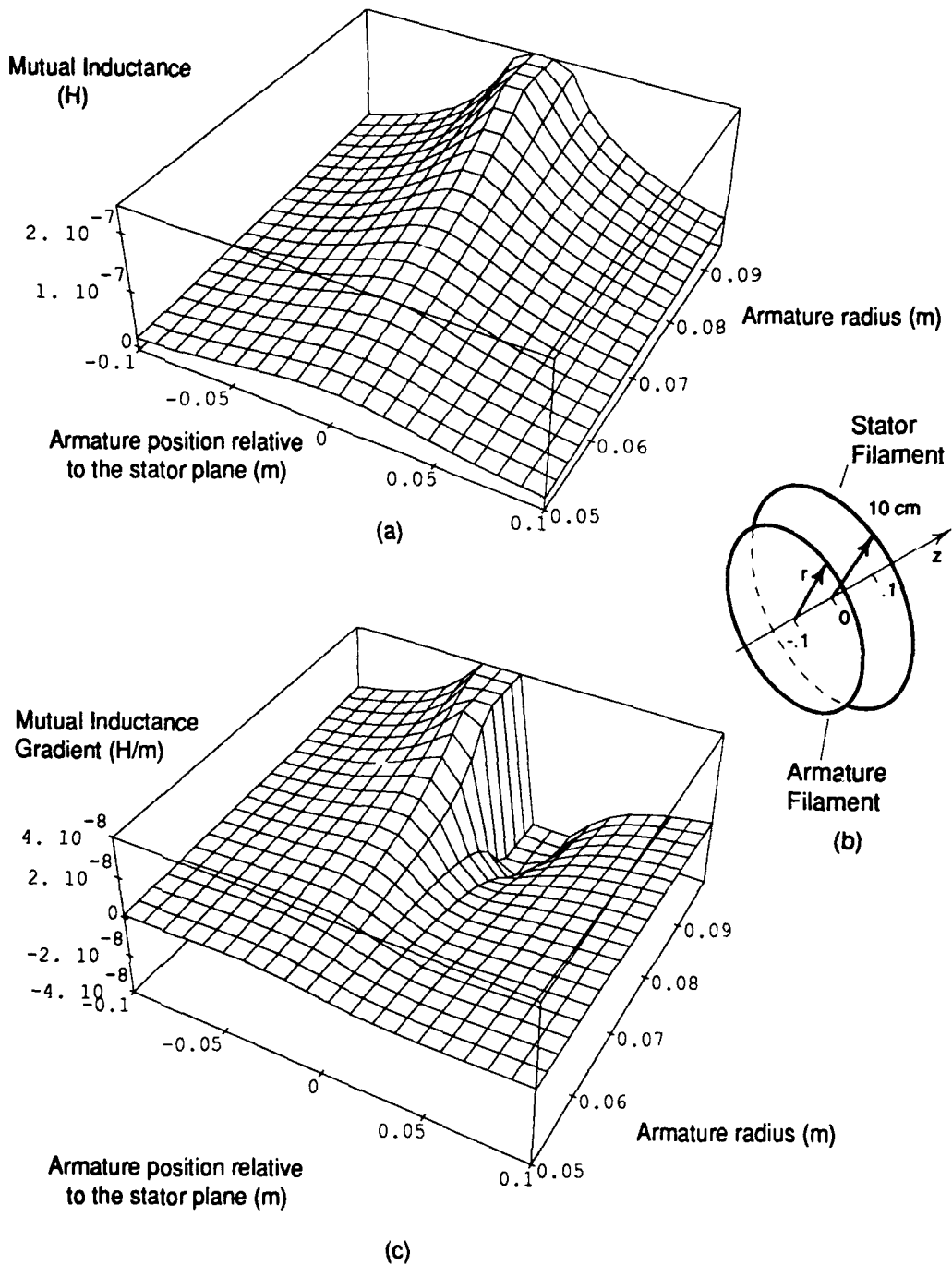
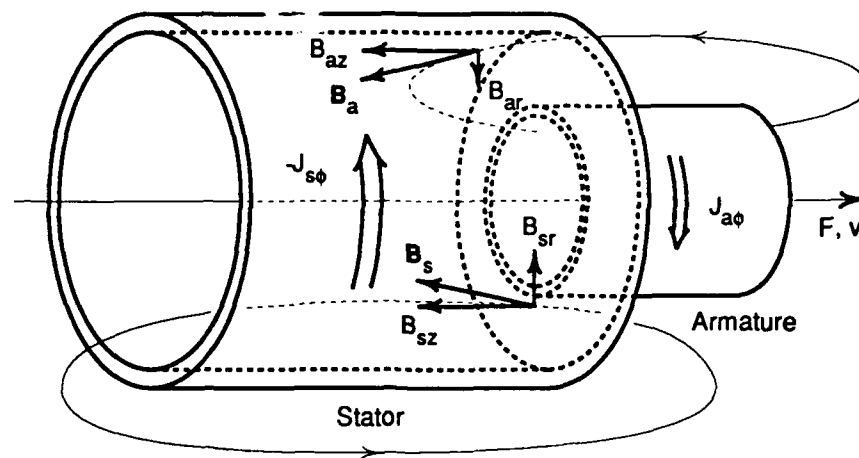


Figure 2.6 Mutual inductance relationships between a 10 cm radius stator filament and a range of armature filament radii plotted as a function of armature position with respect to the plane of the stator filament. (a) Mutual inductance. (b) Coaxial armature and stator filaments. (c) Mutual inductance gradient in the  $z$  direction.



Stator Force  
Density Components

$$-J_{s\phi} \times -B_{az} = f_{sr}$$

$$-J_{s\phi} \times -B_{ar} = -f_{sz}$$

Armature Force  
Density Components

$$J_{a\phi} \times -B_{sz} = -f_{ar}$$

$$J_{a\phi} \times -B_{sr} = f_{az}$$

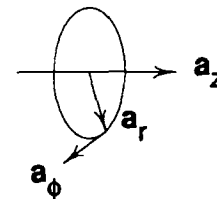


Figure 2.7 Forces that exist on stator and armature coaxial coils. Note that due to symmetry no net forces exist in the  $a_\phi$  direction.

center the armature inside the stator coil making contactless launch possible.

The coaxial coil accelerator was dramatically demonstrated by Bondaletov and Ivanov of the Soviet Union in the middle 70's. They succeeded in accelerating a one gram aluminum ring to 4.9 kilometers per second in a distance of less than one centimeter. Unfortunately, the stator coil self-destructed during launch.<sup>2-23</sup> This illustrates that the amount of energy that can be applied to a stator coil is limited by the thermal and mechanical stresses that the coil can withstand. In a practical sense, this implies that several or many stator coils are necessary to transfer a large amount of kinetic energy to the armature.

The temperature change of a conductor can be estimated using

the conservation of energy. The energy deposited in a conductor during a current pulse is

$$(2-18) \quad W_T = \left(\frac{\rho l}{A}\right) A^2 \int J^2 dt = \int RI^2 dt$$

where,

- $W_T$  = thermal energy
- $\rho$  = resistivity
- $l$  = conductor length
- $A$  = cross sectional area of the conductor
- $J$  = current density
- $R$  = conductor resistance

Determining the energy deposited is complicated somewhat because resistivity is a function of temperature. Fortunately, the change in resistivity is approximately linear and can be expressed <sup>2-24</sup>

$$\rho = \rho_0(1 + \alpha(T - T_0))$$

where,

- $\rho_0$  = resistivity at temperature  $T_0$
- $\alpha$  = temperature coefficient of resistivity
- $T$  = temperature

Assuming that none of the thermal energy deposited in the conductor is removed (an adiabatic process), then

$$(2-19) \quad W_T = \int_{T_1}^{T_2} C_v m dT$$

$$\Delta T = T_2 - T_1 = \frac{W_T}{C_v m}$$

where,

$$C_v = \text{specific heat of the material}$$

$$m = \text{mass.}$$

The model is valid up to the point the conductor melts.<sup>2-25</sup> The model also assumes that the current density is uniform across the cross section of the conductor; this assumption may not be valid in high frequency systems when the skin depth is small compared to the thickness of the conductor.

The radial mechanical stress on the armature and stator can be determined in several ways. In figure 2.7, note that the radial force densities arise from the interaction of azimuthal current densities and axial magnetic flux densities. The force on the armature can be determined by integrating equation (2-11) over the armature volume using the armature current density and stator axial magnetic flux density. Likewise, the force on the stator can be determined using the same method. The point stress on both components can be estimated using equation (2-3). Both of these methods require knowledge of the magnetic flux density.

Often times, the coilgun system is simulated using an equivalent circuit model; consequently, the magnetic flux densities are not directly known and must be approximated based upon the currents. The axial magnetic flux density can be estimated using the long solenoid approximation.<sup>2-26</sup> Inside a long solenoid, the magnetic flux density has only an axial direction; the value of  $B_z$  is uniform across the solenoid cross section and given by

$$(2-20) \quad B_z = n\mu I$$

where,

$$n = \text{turns per meter.}$$

Outside the long solenoid,  $B_z$  tends to zero.<sup>2-27</sup> Thus, the magnetic field density in air gap between the armature and stator coils is dominated by  $B_{zs}$ . The long solenoid approximation represents an upper bound on  $B_z$  in the air gap because it neglects fringing effects that significantly reduce  $B_z$  in coils with low length to diameter ratios. More precise solenoid approximations and numerical techniques are available when precise knowledge of the magnetic flux density is required. This upper bound is, however, useful for determining the maximum expected forces and stresses that the barrel and launch package must withstand.

Since a coilgun must have many stator coils and the effective range of force on either side of a single stator coil is small, the energy gradient created in the launcher must move down the barrel with the armature. The motion of the energy gradient can be thought of as a traveling wave of energy. In the railgun, the energy gradient is naturally synchronized with the position of the armature because the armature acts as its own continuous switch. In the coilgun, there is no inherent switching mechanism that creates a traveling wave; a traveling energy wave must be imposed on the system.

As with the railgun, the power required to drive the coilgun is a function of the magnetic energy as given by equation (2-10). Considering one armature and stator pair, the magnetic energy is

$$W_m = \frac{1}{2}L_a I_a^2 + I_a I_s M + \frac{1}{2}L_s I_s^2.$$

The power expression is

$$P = \frac{\partial W_m}{\partial t} = \frac{\partial}{\partial t} \left[ \frac{1}{2}L_a I_a^2 + I_a I_s M + \frac{1}{2}L_s I_s^2 \right].$$

In the coilgun, the self-inductances are constants, so the power expression reduces to

$$P = I_a L_a \frac{\partial I_a}{\partial t} + I_s M \frac{\partial I_a}{\partial t} + I_a M \frac{\partial I_s}{\partial t} + I_s L_s \frac{\partial I_s}{\partial t} + I_a I_s \frac{\partial M}{\partial x} \frac{\partial x}{\partial t}.$$

Like the railgun, power is manifested both electrically and mechanically. The first four terms are current and emf products (electric power); the last term is a force and velocity product (mechanical power). This expression describes how energy flows in one armature and stator pair. Only a portion of the electrical energy input to the system is converted to mechanical energy; the remainder of the flow in the system is magnetic energy necessary to drive the system. Note that this expression assumes a lossless system and does not include any energy converted to heat due to resistive losses. A similar power relationship exists between each of the armature and stator pairs that make up the gun.

Many clever concepts have been proposed in the race to build and demonstrate a practical coilgun. The ideas are so divergent that it is difficult to find common ground to classify and compare the concepts. One method of classifying the key features of electromagnetic launchers resulted from a 1987 workshop on non-railgun accelerators hosted by the U.S Army Armament Research, Development, and Engineering Center (ARDEC). A refined version of the resulting EML taxonomy is presented in table 2-1 to lend structure to the subsequent discussion of coilguns.<sup>2-28</sup>

### Armature Excitation

Exciting the coilgun armature is challenging since it must have a large magneto-motive force (mmf) but no contact with the launcher

<b>Coilgun Classification</b>			
<b><u>Armature Excitation</u></b>	<b><u>Stator Excitation</u></b>	<b><u>Stator Field Control</u></b>	<b><u>Mode of Operation</u></b>
1. Induction	1. Discrete coils (Individual, independently controlled coils)	1. Active	1. Advancing wave
2. Persistent Current	2. Continuous coils (Multiple connected coils -- a continuous coil in the limit)	2. Passive	2. Receding wave
3. On-Board Power Source			3. Combination of Advancing and Receding waves

Table 2-12-28

during launch. First, the armature current can be induced. In this case, the armature is a shorted coil in the stator magnetic field. As the stator magnetic field moves down the barrel, the armature coil experiences a time rate of change in the magnetic flux density which induces a voltage in the coil; the induced voltage causes a current to flow in the armature that opposes the change of the magnetic flux density. The armature current always flows in a direction opposite to the stator current; consequently, when the armature current is induced, the coilgun can operate only with a repulsive force. The stator traveling wave must accelerate at a rate matched to the acceleration of the armature. If the speed of the traveling wave is excessive, it may outrun the projectile and cease to induce voltage. Also, the rate of change in magnetic flux density must not produce a current that causes the armature to heat excessively.

A second approach to exciting the armature is to design the armature to have a long inductive time constant ( $L/R$ ) compared to the launch time. Immediately before launch, current is either induced or injected into the armature. Upon launch, the current begins to decay

but persists at a high level during launch. The armature must have very low resistance which implies a large conductor cross section; this leads to large, massive armature designs. Superconducting armatures are not presently practical because they do not remain superconducting in the high magnetic fields required for electromagnetic launch. Finally, the armature could in theory carry its own on-board power source. The challenge presented by this approach is finding a power supply that can deliver high currents during launch and satisfy armature weight limitations.

### Stator Excitation

A traveling wave can be created in several different ways depending upon stator and power supply design. The stator coils can be either be discrete coils (individual, independently controlled coils) or continuous coils (multiple coils connected in series or parallel). In a discrete stator coilgun, each stator coil is excited only when it can effectively exert a force on the armature; this is illustrated in figure 2.8. An accelerating magnetic wave is created by switching "on" successive coil stator coils in progressively shorter intervals. Each coil may be excited by its own power source or share a common power source. Regardless of the number of power supplies, control and switching mechanisms are necessary to excite each stator coil during the precise period that useful force can be applied to the armature.

One of the challenges of building a coilgun is to turn on or off the high currents required to drive the gun. In a discrete coil gun, each stator coil must change between high and low energy levels in times short compared to the transit time of the armature past the stator coil. The rate at which the current can change is limited by the voltage available to drive the change.

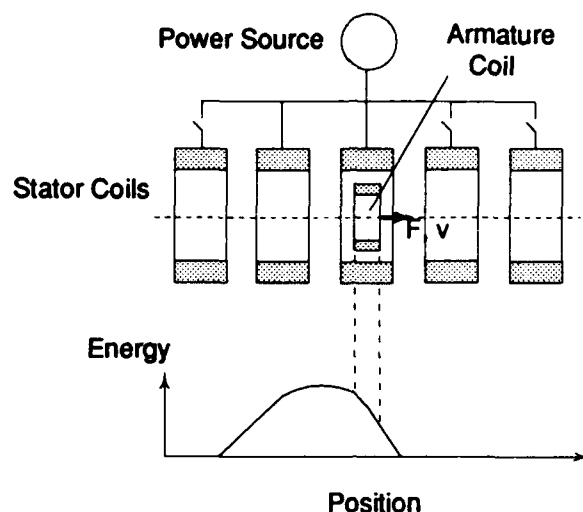


Figure 2.8 Traveling wave generated by sequenced closing of discrete coil switches

$$(2-21) \quad V = L_s \frac{dI_s}{dt}$$

The power supply can be either direct current or alternating current; designs using both types of supplies have been proposed. In the pull mode (illustrated in figure 2.9 (a)), the stator coil must have a large current as the armature approaches; the time to build that current to a high level can be relatively long except as limited by efficiency considerations. The current must remain high as long as possible to achieve maximum thrust; but by the time the armature reaches the point of zero mutual inductance gradient, the stator current must be off or change direction. The time required to turn off or reverse the stator current determines the amount of thrust that the stator can deliver to the armature. Thus, a very high power supply voltage is desirable, but the maximum voltage is technology limited. The voltage limitations of the power supply are most important near the end of the

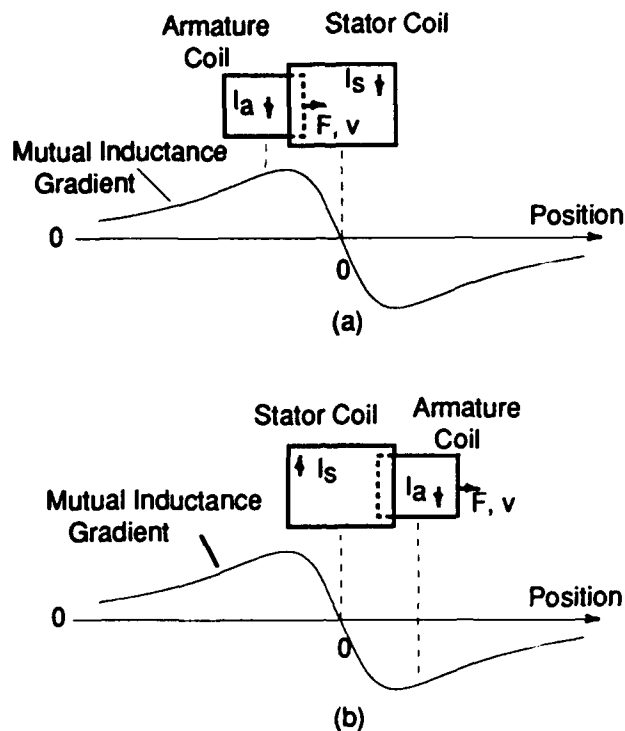


Figure 2.9 (a) Pull mode (b) Push mode

launch when the armature velocity is highest and the stator current must be turned off most quickly.

Similar requirements and limitations exist in the push mode (illustrated in figure 2.9 (b)). The stator current must be low when the armature is at the point of zero mutual inductance gradient and change very quickly as the armature passes that point. The rate of change of the stator current is determined by equation (2-21) and limited by the maximum voltage of the power supply. In both modes, the high stator current is useful only for a brief time while the armature is in the short zone in which the mutual inductance gradient is significant.

An accelerating magnetic wave can also be created using a multi-phase power supply to excite continuous coils. The apparent

speed of a traveling wave is given in the relation

$$(2-22) \quad v = 2\tau f$$

where,

$\tau$  = pole pitch of the winding (spacing between coils)

$f$  = frequency of the power supply

The speed of the traveling wave increases as the pole pitch and/or power supply frequency increase.<sup>2-29</sup> In the first case (figure 2.10), increasing the pole pitch means that the coils for each phase are spaced at increasing intervals down the length of the barrel; a constant frequency power supply can be used to excite each phase. In the limit, pole pitch may vary continuously resulting in a truly continuous

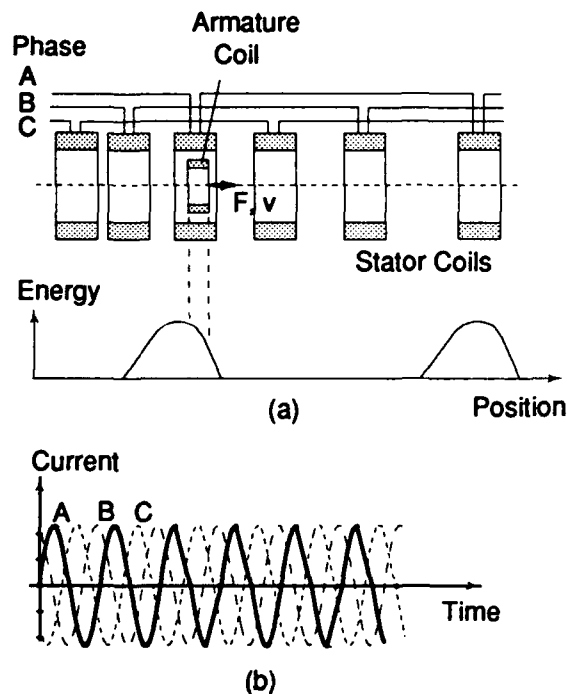


Figure 2.10 (a) Traveling wave generated by multi-phase excitation of series coils with increasing pitch. (b) 3 constant frequency phases that excite the stator.

coil.<sup>2-30</sup> Increasing the pole pitch has the obvious drawback of requiring a longer barrel which may not be acceptable in some applications; additionally, the acceleration profile will become less constant.

On the other hand, the spacing between coils may be kept constant and the power supply frequency may change with time during launch (figure 2.11). This approach requires a special power supply such as the rising frequency generator. One drawback to this approach is that as frequency increases the driving voltage must also increase.<sup>2-31</sup> The third permutation of the continuous coil stator excitation is to vary coil spacing down the barrel and vary power supply frequency during launch.<sup>2-32</sup> For all three variations of the continuous coil stator, the voltage and power requirements are higher than for the

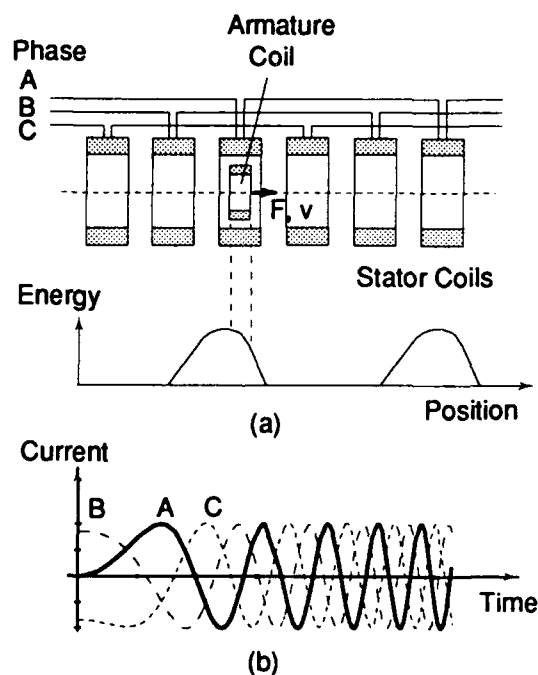


Figure 2.11 (a) Traveling wave generated by increasing frequency, multi-phase excitation of series coils. (b) 3 increasing frequency phases that excite the stator.

discrete coil stator. The power supply must drive all of the coils of each phase throughout the launch whereas the power supply in the discrete stator drives individual coils.

### Stator Field Control

Ultimately, the necessary traveling magnetic field is created by controlling the stator magnetic field. The stator field may be controlled either actively or passively. Active control means that armature position is sensed, and that information is used to change the state of the system to control the traveling wave. Passive control means that stator control and hence the traveling wave are independent of armature position.<sup>2-33</sup>

In theory, coilgun stator coils could be fired at pre-calculated times to launch a projectile. In practice, however, this proves to be very difficult; minor variations from ideal synchronization of stator coil energization with armature position would quickly compound over a large number of coils to significantly reduce the expected performance. This means that active control is necessary to insure that variations from ideal synchronization can be compensated and performance preserved. The disadvantage of active control is that switches are necessary for each coil; every switch in the system contributes to the probability that the system will fail.

The continuous stator coil gun has been suggested as a possible passively controlled system. The traveling wave is controlled by coil spacing and power supply frequency. Since the number of independent power systems is small, variations from pre-calculated armature position are less likely to cause significant degradation of launch performance. Moreover, multiple traveling waves are created, so if the armature drops behind the first wave, the next wave catches it. A chief

advantage of the passively controlled stator is the increased reliability of the system.

### Mode of Operation

There are three modes of operation: advancing wave front, receding wave front, and a combination of the two. These modes have already been alluded to in earlier discussions of the push and pull modes. The modes of operation are illustrated in figure 2.12. In an advancing wave front gun, the magnetic energy driving the system is concentrated behind the armature; energy must be injected into the system after the launch has begun. The advancing wave front pushes the armature down the barrel. The railgun is an advancing wave front device. Any launcher that relies upon induced armature currents must be an advancing wave front device; this makes sense in light of the earlier conclusion that an induction launcher could only work in the push mode.

In a receding wave front gun, the energy is concentrated in front of the armature. The traveling wave recedes in front of the armature as it moves down the barrel; the energy gradient pulls the armature down the barrel. This mode allows energy to be injected into the stator before launch over a relatively long time; this can be advantageous in terms of the voltage required to charge the stator. This mode requires that the armature currents be persistent or supplied by an internal armature power source since armature currents cannot be induced. Finally, a combination of traveling and receding waves can be imposed on the stator so that the armature is sandwiched between two energy gradients corresponding to a push/pull mode.

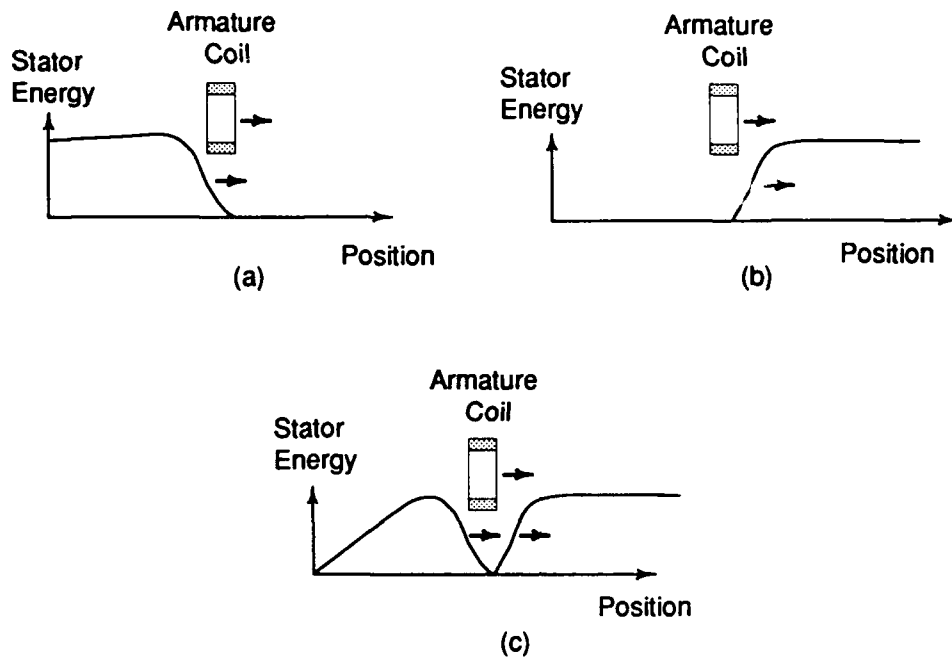


Figure 2.12 Coilgun modes of operation. (a) Advancing wave. (b) Receding wave. (c) Combination of advancing and receding waves.

This concludes the discussion of the principles that underlie coilgun operation. As mentioned earlier there are many proposed coilgun designs. Table 2-2 presents a summary of recent proposals and classifies them according to the presented methodology.

Summary of Proposed Coilguns						
Gun (Organization)	Armature Excitation	Stator Excitation (Power Supply)	Stator Field Control	Mode of Operation	Comments	
Multiple stage induction launcher <sup>2-34</sup> (Electromagnetic Launch Research Inc)	Induction	Discrete Coil (Capacitively driven)	Active	Advancing Wave	Demonstrated 150 m/s velocity of 40 -120 g projectiles	
Traveling wave induction launcher <sup>2-35</sup> (Jet Propulsion Laboratory)	Induction	Discrete Coil (Capacitively driven or Rising Frequency Gen)	Active	Advancing Wave	Conceptual only	
Linear Induction Launcher <sup>2-36</sup> (Polytechnic University)	Induction	Discrete Coil (Capacitively driven)	Active	Advancing Wave	Demonstrated 100 m/s velocity of 150 g projectile <sup>2-37</sup>	
Pulsed Induction Launcher <sup>2-38</sup> (UT Center for Electromechanics)	Induction	Discrete Coil (Capacitively Driven)	Active	Advancing Wave	Demonstrated 379 m/s velocity 31 g projectile <sup>2-39</sup>	

Table 2-2

Summary of Proposed Coilguns						
Gun (Organization)	Armature Excitation	Stator Excitation (Power Supply)	Stator Field Control	Mode of Operation	Comments	
Passive Coaxial Accelerator <sup>2-40</sup> (UT CEM)	Induction	Continuous Coil (Rising Frequency Gen)	Passive	Advancing Wave	Conceptual only	
DC Accelerator <sup>2-41</sup> (UT CEM)	Induction	Continuous Coil (Capacitively driven)	Passive	Advancing Wave	Explores a variety of methods for generating an accelerating wave using inductively/ capacitively graded coils	
Collapsing Field Accelerator <sup>2-42</sup> (UT CEM)	Persistent	Homopolar Generator	Active	Receding Wave	Conceptual only	

Table 2-2 (Cont)

## Chapter 3

### POWER CONDITIONING

The launcher constitutes only one-half of the engineering challenge presented by the electric gun; the second half of the challenge is to deliver the energy required for launch. The available power supply technologies determine to a great extent the launcher design that can be powered -- indeed many attractive launcher designs are not realizable because the pulsed power demands exceed the existing technologies. Two important yardsticks of energy supply and storage are energy density and power density. These two device characteristics determine to great extent the volume and mass of the power conditioning system which are often limited by the application.

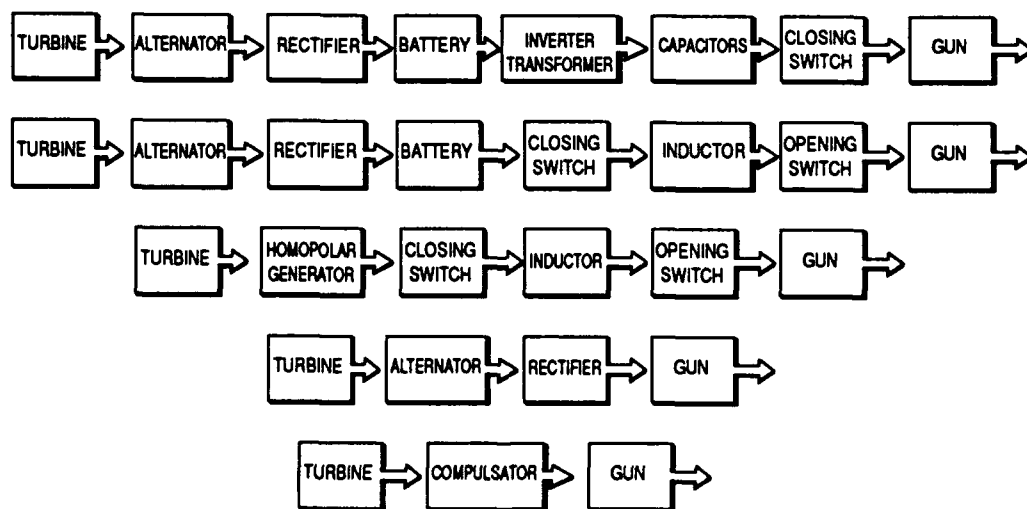
The energy and power requirements of an electromagnetic launcher can be estimated easily. The kinetic energy of the launch package (armature and projectile) as it leaves the muzzle is given by

$$KE = \frac{1}{2}mv^2$$

A reasonable and attainable efficiency goal for most electromagnetic launch energy conversion processes is about one-third;<sup>3-1 - 3-6</sup> thus, the total energy requirement of the gun is approximately three times the kinetic energy of the launch package as it leaves the muzzle. The average power requirement can be estimated by dividing the total energy requirement by the launch time. For example, a 2 kilogram projectile launched to 3 kilometers per second in 5 milliseconds has 9 megajoules of kinetic energy. The launcher's total energy requirement

is 27 megajoules applied in 5 milliseconds for an average power requirement of 5.4 gigawatts -- this is equivalent to the continuous power output of several generating plants. Fortunately, the electric gun's power requirement is of very short duration. This allows energy to be stored at low rates over an extended time and then discharged in a pulse with a duration comparable to or shorter than the launch time.

The power conditioning system consists of the energy supply, intermediate energy storage devices, and switches that are required to generate large power pulses. Figure 3.1 shows several typical power conditioning system options. The power conditioning system configuration is chosen based upon the launcher power requirement and EML system constraints. This chapter examines energy storage devices and switching devices that are or could be used to generate pulsed power for electromagnetic launchers. Finally, some important considerations relating to the electrical connections (buswork) between components will be addressed.



4701.0002

Figure 3.1<sup>3-7</sup> Typical Power Supply Options

## Energy Storage

Pulsed power discharge is realized by using combinations of staged energy storage devices. Energy storage devices used in pulsed power generation fall into four categories: electrochemical, magnetic field, electric field, and inertial. Typical characteristics of energy storage devices are shown in table 3-1.<sup>3-8</sup> The table shows that there is wide variation in the characteristics of the available energy storage devices; the optimum combination of energy storage components depends upon the application and specific type of launcher.

### Batteries

Batteries have the highest energy storage densities among the devices and store energy for very long periods of time. Batteries, however, cannot deliver their stored energy quickly as reflected in relatively low power densities. Batteries store energy electrochemically; when the electrical circuit is completed, current flows as the result of the interaction of the electrolyte and electrodes. Current

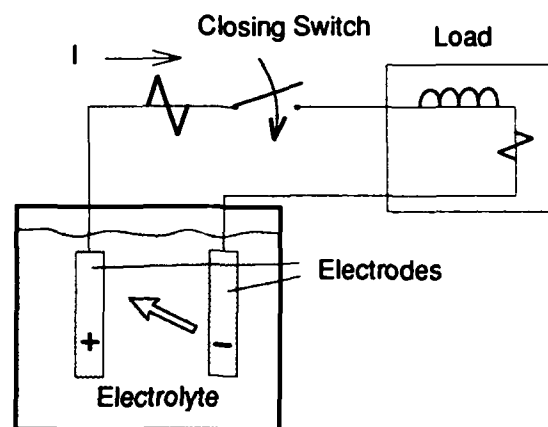


Figure 3.2 Schematic of a battery circuit.

Typical Characteristics of Pulsed Power Systems								
Storage technique and device	Storage capacity	Energy density (kJ/kg)	Power density (kW/kg)	Pulse width	Module voltage	Source impedance (ohms)	Short-circuit current (kA)	Storage time (seconds)
<b>Electric field</b>								
Capacitor	15 kJ	.2	8000	0.1-0.5 ms	10 000	0.212	50	1000
<b>Magnetic field</b>								
<b>Inductor</b>								
Room Temperature	5 MJ	1.2	324	1-5 ms	3000	0.002	1500	0.45
Cryogenic	3 MJ	3.1	1000	1-100 ms	5000	0.005	1000	1.2
Superconducting	500 kJ	2.2	50	1 ms	10 000	3142.	3	1012
<b>Inertial</b>								
<b>Flywheel</b>								
DC generator	0.8 MJ	0.32	0.3	1 sec	1800	0.0142	1	100
Homopolar generator	6 MJ	8.5	70	0.1-0.5 sec	100	10 <sup>-5</sup>	2000	415
Alternator	185 MJ	1.3	0.7	1 sec	6900	1.12	6	3000
Compulsator	200kJ	3.8	250	0.1-2 ms	6000	.084	71	254
<b>Electrochemical</b>								
<b>Battery</b>								
Lead Acid	5 MJ	200	0.3	1 sec	12	0.02	0.5	10 <sup>8</sup>

Table 3-13-8

flow is limited by the rate at which the electrolyte diffuses between the electrodes. Typically, the diffusion process is slow compared to electrical processes causing batteries to have high internal impedances; this characteristic can lead to thermal dissipation problems. A schematic of a battery circuit is shown in figure 3.2. Note that the battery requires a closing switch and depending upon the application may also require an opening switch. At present, two promising batteries for electromagnetic launch applications are bipolar lead acid and lithium metal sulfide batteries.<sup>3-9</sup> The characteristics of these batteries are presented in table 3-2.

The lead acid battery is familiar to us as the common car battery. Because the lead acid battery has a low power rating and cell voltage, electromagnetic launcher power (current and voltage) requirements can only be met by connecting many batteries in series

<b>Battery Technology Under Development</b>		
	<b>Bipolar Lead-Acid</b>	<b>Lithium Metal Sulfide</b>
<b>Power Density (20 s Goal)</b>	3.5 kW/kg	7.3 kW/kg
<b>Energy Density Goal</b>	80 kJ/kg	280 kJ/kg
<b>Available in Quantity</b>	1991	1994
<b>Recharge Time</b>	80 min.	1 min.
<b>Operation</b>	Sealed Unit	Heater/Cooling
<b>Temperature</b>	75°C	480 to 550°C
<b>1 MW Mass</b>	220 kg	137 kg
<b>50 MJ Mass</b>	1,000 kg	231 kg

Table 3-2.3-9

and parallel. The size and mass of the resulting battery array is unacceptable for many applications.<sup>3-10</sup> The lithium metal sulfide battery is a promising alternative having both improved power density and lower internal impedance.<sup>3-11</sup> At present and in the foreseeable future, neither of these batteries has the power density necessary to directly drive a launcher. These batteries are, however, candidate energy sources for charging other intermediate, high power density storage devices that can discharge energy quickly.

### Inductors

The inductor stores energy in a magnetic field created by current flow. Inductors are capable of storing energy at high densities (except compared to the battery) and discharging that energy in times attractive for electromagnetic launch applications. However, the inductor has several short comings as a high energy storage device: short energy storage time, large mass and volume, and difficult current switching requirements. The energy stored in the inductor is given by equation (2-8)

$$W_m = \frac{1}{2}LI^2$$

and is strongly dependent upon the magnitude of the current.

An electromagnetic launcher application using intermediate inductive energy storage is shown in figure 3.3. The current in the inductor (and corresponding magnetic energy) is built up over a relatively long period of time (seconds). Launch is initiated by opening switch one -- interrupting current flow in the inductor but leaving a large amount of energy stored in the inductor. Switch two closes at the

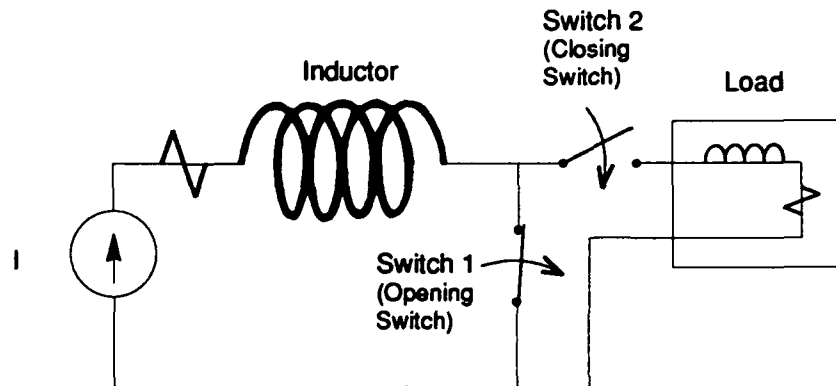


Figure 3.3 Typical use of an inductor as an intermediate energy storage device. The inductor is charged with the switch 1 closed and switch 2 open. When fully charged, switch 1 is opened and switch 2 is closed discharging the stored energy into the load.

same instant creating an alternate current path. The energy stored in the inductor dissipates very rapidly by causing current flow in the load. Switching (or commutating) the current out of switch one and forcing it into switch two is a difficult task that will be addressed further under opening switches. The rate at which the current changes in the inductor is determined by the inductive time constant ( $L/R$ ) of the circuit -- usually less than one second. After three time constants, the current (and stored energy) is effectively dissipated.

Whenever current flows in the inductor, magnetic energy is stored; but some system energy is simultaneously dissipated as heat due to conductor resistance. The large currents required for EML applications cause rapid temperature rise even in the best conductors -- imposing short inductor energy storage times. Prolonged current flow will raise the conductor temperature to the melting point and cause circuit failure. Energy storage time can be improved by reducing conductor resistance; this can be done by either increasing the conductor cross section or by cooling the conductor. Both of these solutions can dramatically increase the size and weight of the inductor.<sup>3-12, 3-13</sup>

In addition to the electrical characteristics of the inductor, the mechanical strength of the device must be considered. A goal in designing a pulsed power inductor is to achieve the highest possible energy density. This results in a steep energy gradient across the inductor structure. According to equation (2-2), the steeper the energy gradient is then the greater the force on the mechanical structure of the inductor. Storing very high energy densities requires a mechanically robust (and larger) inductor.

Today, the potential for substantially improving the inductor for pulsed power applications seems remote. Using ferromagnetic materials holds little promise because these materials are non-linear and lose their advantage of high permeability in very strong magnetic fields. One possibility for future improvement is the development of a high temperature superconducting material that remains superconducting in high magnetic fields. The dim prospects for substantially improving the inductor for pulsed power applications is evident in the lack of published research by the pulsed power community.

### Capacitors

Capacitors typically have power densities an order of magnitude higher than the inductor; on the other hand, today's capacitors have energy densities an order of magnitude lower than inductors. Capacitors store energy in an electric field created by static charge deposited and held on the electrode plates; the energy stored is determined by the equation

$$(3-1) \quad W = \frac{1}{2} C V^2$$

where,

$$C = \frac{\epsilon A}{d} \quad (\text{parallel plate capacitor})$$

$\epsilon$  = dielectric permittivity

$A$  = surface area of the capacitor plates

$d$  = separation between the capacitor plates.

and is strongly dependent upon the applied voltage. Because energy storage is the result of static charge, the capacitor does not have the severe heating problems of the inductor and can store energy for attractively long periods of time. A schematic of a typical capacitor circuit is shown in figure 3.4. Note that to charge the capacitor with an alternating current source, a rectifier is needed; for direct current sources, a closing switch is used. A closing switch is used to discharge the capacitor.

Capacitor designers hope to significantly improve energy densities by using advanced dielectric materials, but the improvements will require substantial research effort and investment. Increasing the applied voltage provides the greatest increase in energy density, but

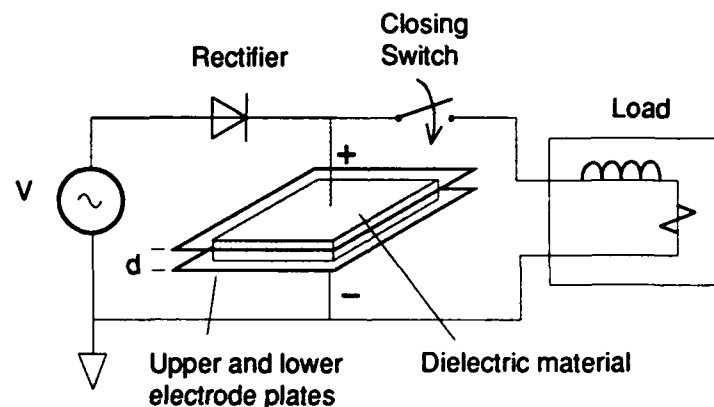


Figure 3.4 Capacitor circuit.<sup>3-14</sup> For an alternating current source, the capacitor is charged through the rectifier; if a direct current source is used, a closing switch can replace the rectifier. For launch, the closing switch is activated discharging the capacitor into the load.

this depends upon the availability of dielectric materials that are able to withstand the stresses imposed by large electric fields. Typically, increasing the applied voltage leads to early dielectric material failure. Increasing the dielectric permittivity typically causes greater dielectric loss and early thermal failure.<sup>3-15</sup> Today's state of the art pulsed power capacitor has an energy density of .6 kJ/kg in a 50 kJ package. Capacitors with energy densities of up to 3.0 kJ/kg are undergoing testing in the laboratory. Capacitor technology is projected to achieve 15-20 kJ/kg energy densities.<sup>3-16</sup>

### Inertial Storage Devices

The fourth class of energy storage device for pulsed power generation is the electric machine which stores energy kinetically in a spinning flywheel. The special machines suited for pulsed power generation include the homopolar generator, compulsator, and rising frequency generator. Inertial energy storage devices combine high energy density, high power density, and long storage time in a single storage device. These machines can all be driven directly by a motor or turbine. In some systems, these machines can directly drive the EML -- reducing the auxiliary power conditioning equipment. These are distinct advantages for mobile power requirements.<sup>3-17</sup>

The homopolar generator is the oldest electric machine having been invented by Michael Faraday in 1831.<sup>3-18</sup> The homopolar generator is illustrated in figure 3.5. It consists of a disk that spins in a uniform magnetic field with electrical connections made at the disk shaft and on the disk rim. When a uniform magnetic field is applied to the spinning disk, a voltage appears across the radius of the disk. In pulsed power applications, energy is stored in the system by accelerating the disk. The kinetic energy stored in the rotating disk is given by

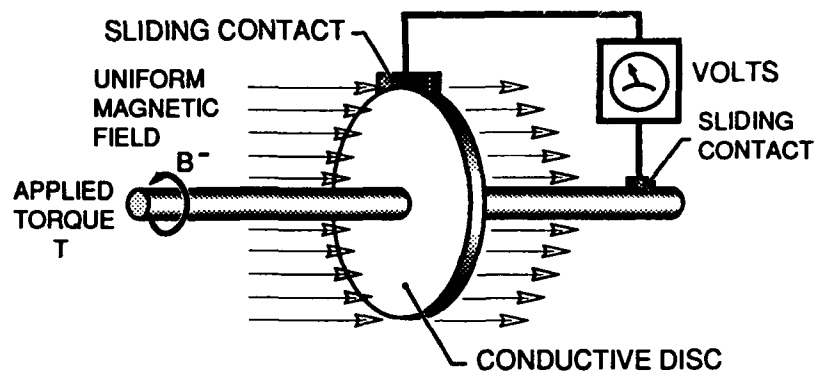


Figure 3.5 Homopolar Generator (Faraday disk) <sup>3-19</sup>

$$(3-2) \quad W = \frac{1}{2} J \omega^2$$

where,

$$J = \frac{\pi r^4 d \delta}{2} = \int_0^r \int_0^{2\pi} \int_0^d r'^3 \delta dz d\phi dr'$$

(polar moment of a disk)

$r$  = disk radius

$d$  = disk thickness

$\delta$  = mass density of the disk material

$\omega$  = radial velocity of the disk.

When a uniform magnetic field is applied to the disk, the induced voltage is given by<sup>3-20</sup>

$$(3-3) \quad V = (\pi B r^2) \frac{\omega}{2\pi}$$

The induced voltage causes a current to flow when the electric circuit is complete. The current interacts with the magnetic field according to the Lorentz force law to brake the disk's rotation; thus the disk's

kinetic energy is converted to electric energy. Since the total system energy is the sum of the electrical and mechanical energies and energy must be conserved, an equivalent mechanical capacitance can be derived by equating (3-1) and (3-2) and substituting for voltage using equation (3-3)<sup>3-21</sup>

$$C_{eq} = \frac{\pi d \delta}{B^2}.$$

The equivalent mechanical capacitance can range from ten to thousands of Farads.

As a one turn machine, the homopolar generator produces a low voltage and has significantly lower impedance than other electric machines. The homopolar generator's low impedance characteristic makes it well suited to drive low impedance loads. A disadvantage of the homopolar machine is that its long discharge time makes it unsuitable for driving electric guns directly; normally, the homopolar machine is used to charge an intermediate inductive store such as the inductor in figure 3.2.

The compensated pulsed alternator (compulsator) is a special alternator invented in 1978 at the Center for Electromechanics (CEM) at the University of Texas at Austin.<sup>3-22</sup> The conventional alternator, a many turn machine, has a high internal inductance which limits the time rate of change of current for a given voltage; this precludes the alternator from generating large current and power pulses. The compulsator is an alternator with compensating windings that reduce the effective inductance of the armature circuit to allow large current pulses. The compulsator has three variations: passive, selective passive, and active.<sup>3-23</sup>

First, consider the unmodified alternator, shown in figure 3.6. According to Faraday's law, the induced voltage that appears across

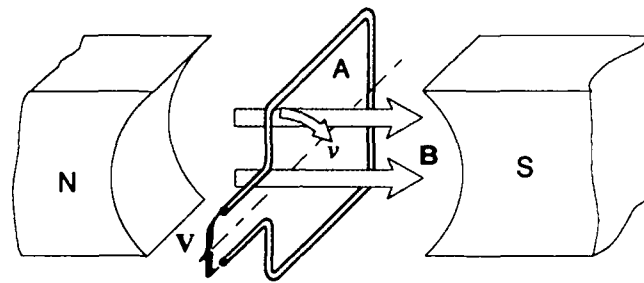


Figure 3.6 Alternator Representation.<sup>3-24</sup> The field excitation of the stator is represented by the static field of a magnet.

the armature terminals from a uniform  $\mathbf{B}$  field is

$$\begin{aligned}
 V &= \frac{d\lambda}{dt} = N \frac{d[\mathbf{B} \cdot \mathbf{a}_n A]}{dt} \\
 &= N \frac{d[|\mathbf{B}| |A| \cos\theta]}{dt} = -N |\mathbf{B}| |A| \sin\theta \frac{d\theta}{dt} \\
 &= -N |\mathbf{B}| l v \sin\theta
 \end{aligned}$$

where,

- $\lambda$  = magnetic flux linkage
- $\mathbf{B}$  = magnetic flux density
- $A$  = surface area enclosed by the loop of wire
- $\mathbf{a}_n$  = unit vector normal to  $A$
- $N$  = number of winding turns.
- $\theta$  = angle between  $\mathbf{a}_n$  and  $\mathbf{B}$ .
- $l$  = axial length of the winding.
- $v = r \frac{d\theta}{dt}$  = velocity of the winding

The dot product of the magnetic flux density and the unit vector normal to the area results in a sinusoidally varying voltage. Recall the relationship between flux linkage and current given by equation (2-6)

$$(3-4) \quad \lambda = LI.$$

When the self inductance is constant, the induced voltage becomes

$$V = L \frac{dI}{dt}.$$

The current is sinusoidal and 90 degrees out of phase with the voltage.

The definition of self inductance from equation (3-4) is

$$L = \frac{\lambda}{I}$$

or flux linkage per unit of current. Compensation results when the flux linkage per unit of current is reduced. Flux linkage is reduced by creating opposing fluxes that cancel; this is illustrated in figure 3.7. Since the exciting magnetic field is static, it diffuses through the shield

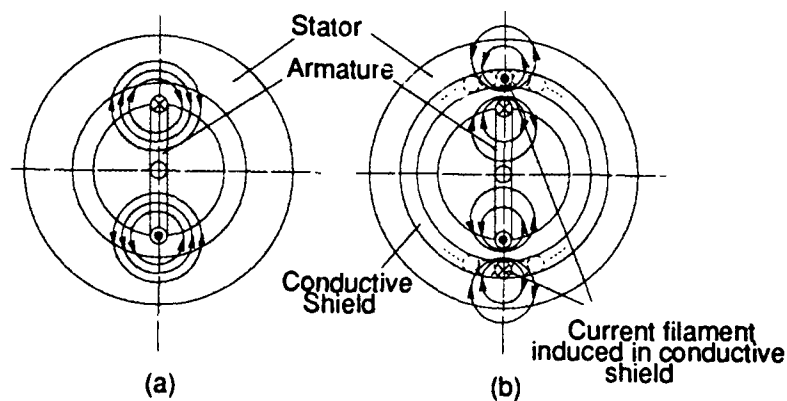


Figure 3.7 Compensation.<sup>3-25</sup> (a) Armature magnetic field in an uncompensated alternator. (b) Alternator with conductive compensating shield fixed to the stator. The armature magnetic field induces an opposing (eddy) current filament in the conductive shield which in turn creates an opposing magnetic field -- the two fields cancel reducing the inductance of the armature.

to induce a voltage in the moving armature. When the armature circuit is complete, the induced voltage causes a current that in turn generates an armature magnetic field. This magnetic field expands and begins to diffuse through the conducting shield and in doing so induces eddy currents in the shield. The eddy currents oppose magnetic diffusion and create a magnetic field that opposes the armature magnetic field. These two magnetic fields cancel reducing the flux that the armature circuit links per unit of current. This effectively reduces the inductance of the armature. This principle underlies the three compulsator variations.<sup>3-26</sup>

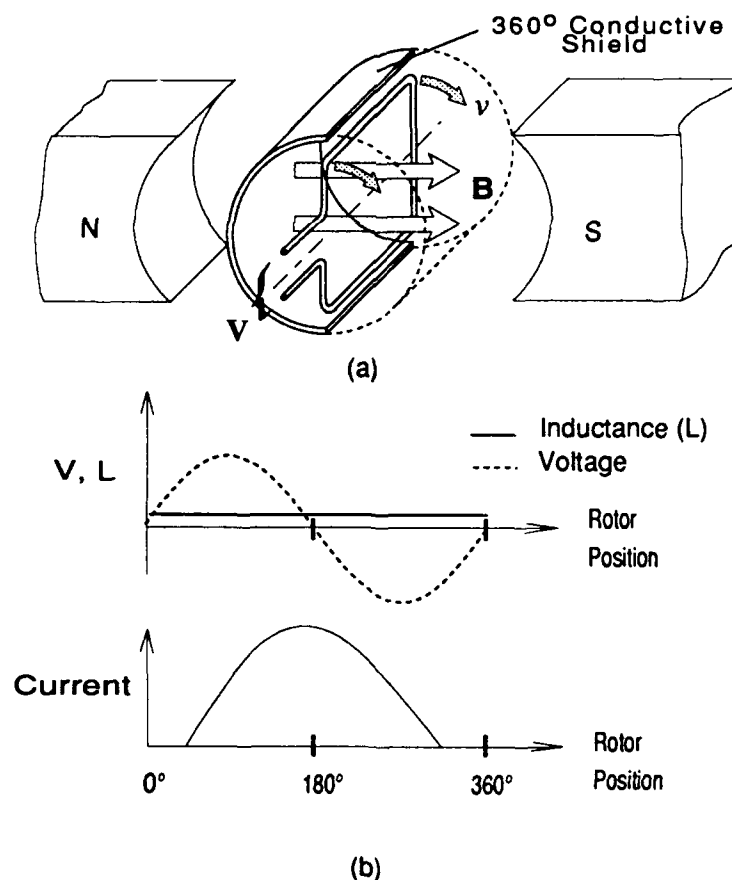


Figure 3.8 Passive compulsator.<sup>3-27</sup> (a) Machine representation. (b) Voltage, current, and inductance as a function of position.

The passive compulsator has a conductive shield fixed to the stator between the armature and stator windings as illustrated in figure 3.8. Compensation occurs at all points in the motion of the armature causing machine inductance to be uniformly reduced. The current output is sinusoidal as in the alternator. The selective passive compulsator operates in same way as the passive compulsator except that shorted conductors or a non-uniform conductive shield compensate only a portion of the armature's path; this is illustrated in figure 3.9. The shorted conductors are placed so that the effective inductance varies with position; the placement of compensating windings determines the output voltage and current waveforms.<sup>3-29</sup>

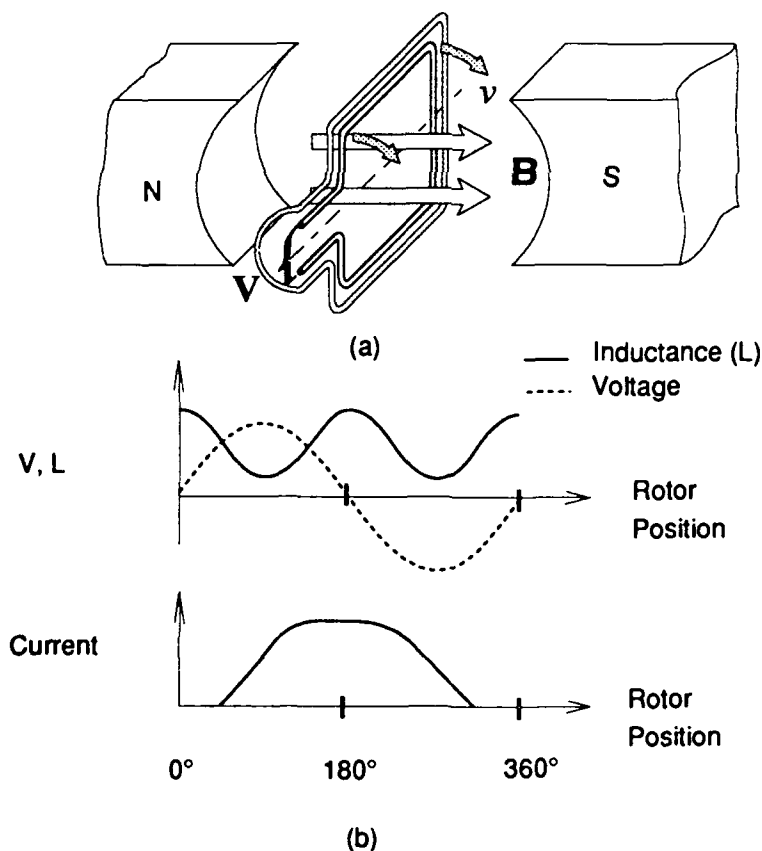


Figure 3.9 Selective passive compulsator.<sup>3-28</sup> (a) Machine representation. (b) Voltage, current, and Inductance as a function of position.

The active compulsator and its characteristic output waveforms are illustrated in figure 3.10. In the active compulsator, the armature and compensating winding are connected in series. This forces the armature and compensating winding currents to flow in specific directions relative to each other based upon armature position. In the rotor position shown in figure 3.11(a), the currents in the armature and stator winding flow in the same direction causing flux linkage and inductance to increase; in this position the flux density between the armature and compensation winding is negligible. When the armature is in the diametrically opposite position shown in figure 3.11(c), the currents flow in opposite directions causing flux to cancel -- reducing

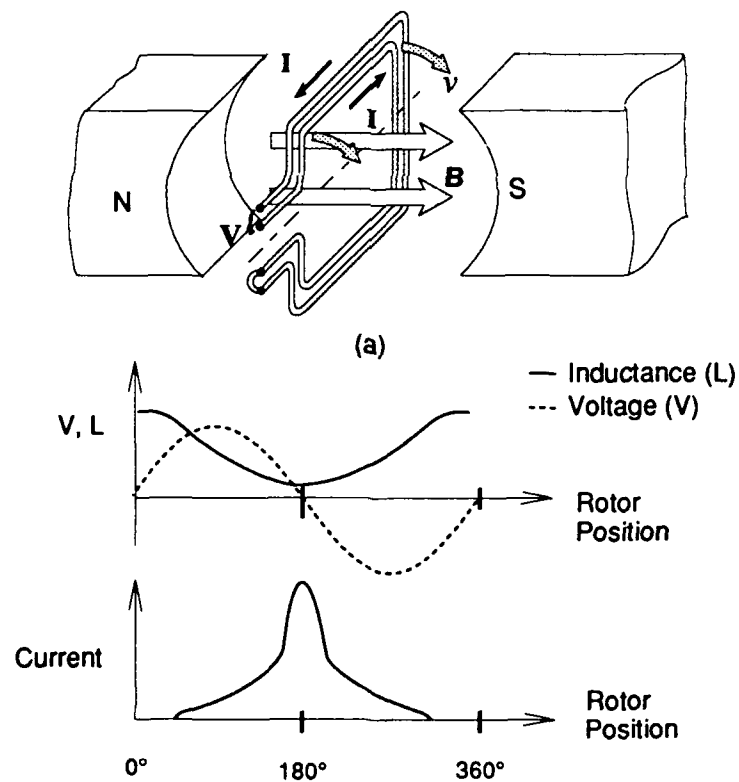


Figure 3.10 Active compulsator.<sup>3-30</sup> (a) Machine representation. (b) Voltage, current, and inductance as a function of position.

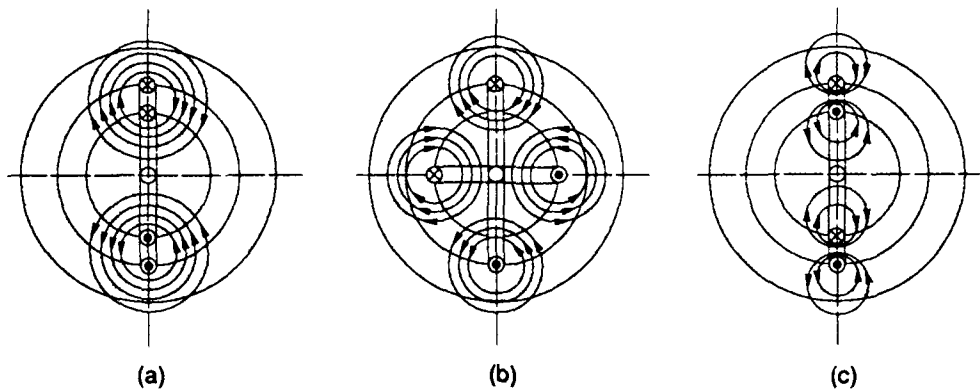


Figure 3.11 Active Compensation.<sup>3-31</sup> The armature and compensating windings are connected in series. (a) High inductance position. (b) Uncompensated Inductance position. (c) Low Inductance position.

flux linkage and inductance. In this position, the system flux is concentrated in the space between the armature and compensating winding -- resulting in high flux density.<sup>3-31</sup> The increase in flux density (and corresponding increase in magnetic energy density) between the armature and compensating windings in figures 3.11(b and c) is the result of flux compression; this phenomenon is not present in the passive compulsators.<sup>3-32</sup> Compressing flux requires energy. In this case, armature kinetic energy is converted into magnetic energy; thus as flux is compressed, the armature loses speed.

The compulsator has a number of advantages as an electromagnetic launcher power supply; a typical compulsator driven circuit is shown in figure 3.12. The compulsator acts as its own power conditioner; additionally, the current pulse shape and width can be adjusted to meet launcher requirements. The compulsator stores several times more energy than the energy delivered in one pulse; this means that the compulsator can deliver a series of power pulses in rapid succession.<sup>3-33</sup> The circuit uses a dual purpose closing and

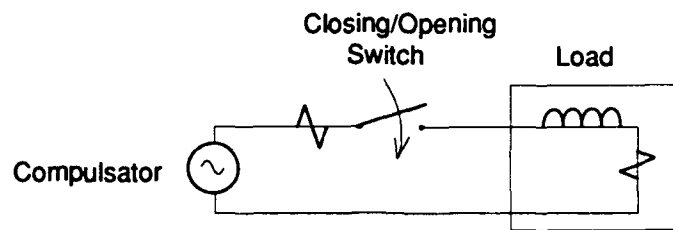


Figure 3.12 Compulsator circuit. The switch is closed when the gun is fired. The switch is reopened at the next current zero.

opening switch; the duty on the switch is minimized since it can be activated at a naturally occurring current zero.

The rising frequency generator (RFG) is a second special machine conceived at the Center for Electromechanics (CEM) to suit the particular power needs of electromagnetic launchers. The RFG, shown in one form in figure 3.13, is different from conventional machines in that both the armature and stator rotate. Just prior to discharge, the stator is rotating slightly faster than the armature.

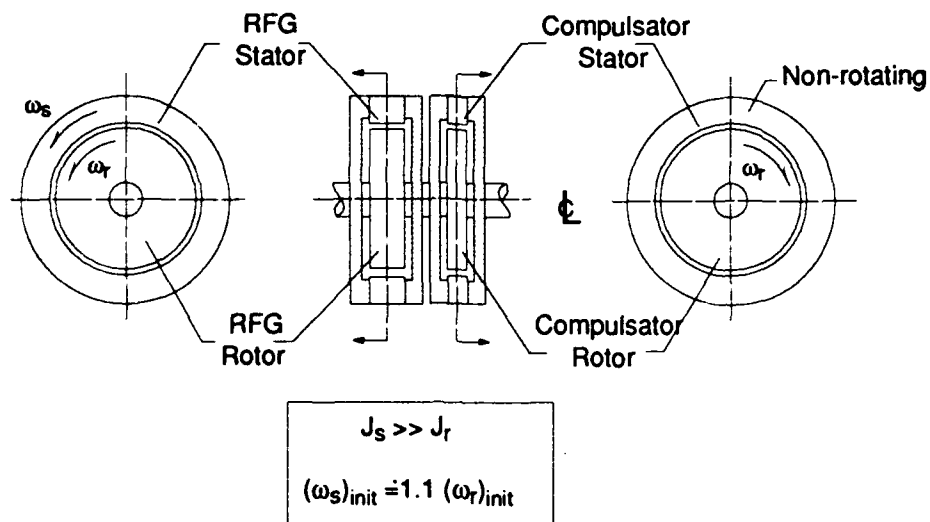


Figure 3.13 Rising Frequency Generator.3-34



today's power supply technologies are inadequate. Figure 3.14 shows device energy densities projected by the Electrical Energy Gun Study sponsored by the Defense Advanced Research Projects Agency (DARPA). The near term energy densities represent systems that were under development in 1989; far term energy densities represent values that can be substantiated by calculation.<sup>3-36</sup>

### Switches

Switches are vital components of an electromagnetic gun system that are often taken for granted -- until the system designer begins to seriously consider implementing a gun concept. The switching system constitutes a third major sub-system of the launcher. Typical switching requirements for EMLs are shown in table 3-3. Given today's technology, these current and voltage levels result in massive, voluminous switches; often switching requirements can only be met by connecting several switching elements in series and/or parallel arrays. Other important factors that affect switch selection include switch speed and expected switch life. Gun system volume and weight constraints demand that switching technology be pushed to the limit.

The purpose of a switch is to control current flow (and hence energy distribution) in the gun circuit. In the "off" state, the switch

Electromagnetic Launcher Switching Requirements				
Voltage (kV)	Current (MA)	Switch Cycles Per Second (Hz)	Load Type	Pulse Energy (MJ)
2 - 20	.1 - 5	1 - 50	R and L	5 - 500

Table 3-3<sup>3-37</sup>

must have very high impedance to prevent current flow; the impedance must be able to withstand (or hold off) electric potentials on the order of tens of kilovolts without breaking down. In the "on" state, the switch must conduct current with very low resistive losses; heat generated by ohmic losses must be dissipated before the switch is damaged. Finally, in pulsed power applications, the switch must transition from one state to another quickly and often at a high repetition rate. Switches are classified as either closing or opening -- the switch being designed to optimize one or the other function.

### Closing Switches

The closing switch starts from the "off" state and transitions to the "on" state -- completing the electric circuit. Initially, the switch must present a large impedance; on switching, the impedance must drop rapidly and allow a large current to flow. Typically, the switching process must be completed in much less than a millisecond since launch times are on the order of milliseconds. Typical closing switch applications for EMLs are shown in figures 3.3, 3.4, and 3.12. Switches that are considered suitable for EML applications include ignitrons, spark gaps, and solid state switches.<sup>3-38 -- 3-40</sup> Table 3-4 shows typical characteristics of these switches. The listed switches are representative and not necessarily inclusive of all closing switches that could be used. This spark gap and SCR have been specifically proposed for use in EML applications.

The ignitron, shown in figure 3.15(a), is designed to transfer a set amount of charge; hence, it is useful for discharging capacitors that store energy in static charge. In the "off" condition, the anode and cathode are separated by a distance sufficient to prevent breakdown under the applied voltage. Switching occurs when a trigger pulse is applied to the cathode -- vaporizing the mercury pool. The vaporized

Typical Closing Switch Characteristics					
	Peak Current (kA)	Peak Voltage (kV)	Dimensions (volume m <sup>3</sup> )	Weight (kg)	Comments
Ignitron <sup>3-43, 3-44</sup> NL-9000 Richardson Elect	500	10	15.75" x 8" dia (.013)	27.2	$\frac{dI}{dt} \cong 3.3 \frac{\text{kA}}{\mu\text{s}}$  Careful leveling required
Spark gap <sup>3-45</sup> ST 3000 Physics Int'l	280	55	11" x 9" dia* (.011)	9.7*	$\frac{dI}{dt} \cong 4.7 \frac{\text{MA}}{\mu\text{s}}$  Pulse width -- 160 ns
SCR <sup>3-48</sup> General Electric/ CEM	35.6	4.5	5.6mm x 79.4 mm dia** (2.7 x 10 <sup>-5</sup> )	.3**	$\frac{dI}{dt} \cong 100 \frac{\text{A}}{\mu\text{s}}$  Pulse width depends on action integral
*Does not include accompanying trigger generator (.038 m <sup>3</sup> and 13.6 kg per spark gap).					
**SCR alone -- does not include control circuitry or packaging.					

Table 3-4

mercury provides a conduction path between the anode and cathode allowing current to flow. Once triggered, the switch remains "on" until the charge is transferred to the load. Once the discharge is complete, the mercury condenses and re-pools on the cathode.<sup>3-41</sup> The ignitron is not suitable for many applications because it must have a specific orientation to keep the mercury pooled on the cathode.

The spark gap (figure 3.15(b)) consists of two electrodes separated by a dielectric; the dielectric may be vacuum, gas, liquid, or solid. The spark gap begins conducting when a trigger voltage signal

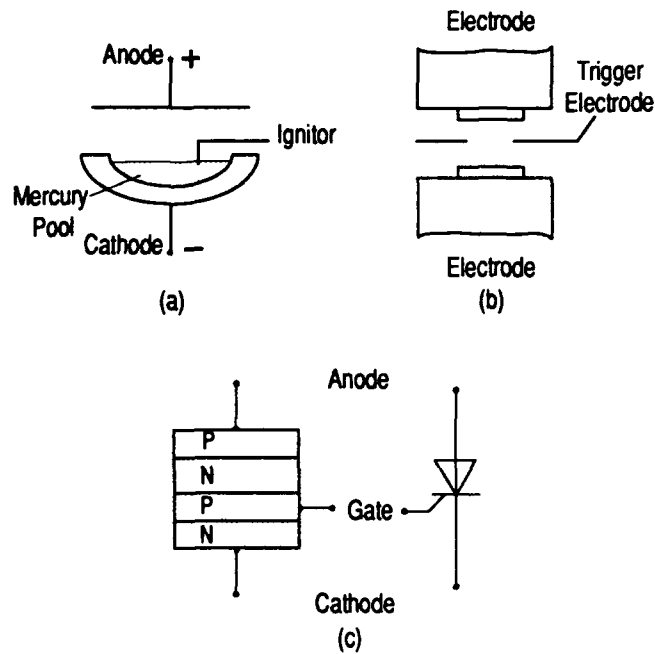


Figure 3.15 Closing Switches. (a) Ignitron.<sup>3-41</sup> (b) Sparkgap.<sup>3-42</sup>  
 (c) Thyristor (SCR or GTO).<sup>3-46</sup>

causes the dielectric to breakdown; the trigger voltage may be applied across the two electrodes or by a third electrode as illustrated. The spark gap continues to conduct until the voltage drops below the level necessary to sustain dielectric breakdown. Spark gaps are widely used for pulsed power applications and cover a wide range of currents, voltages, coulomb transfers, repetition rates, etc.<sup>3-42</sup>

The thyristor is a four layer solid state electronic device (figure 3.15 (c)). The thyristor becomes conducting when a trigger signal is applied to the gate; it remains conducting until a current zero occurs that sweeps carriers out of the junctions. Among the many thyristor variations, the silicon controlled rectifier (SCR) and gate turn off (GTO) thyristor are most suitable for pulsed power applications; the GTO has a faster turn-off time and can be turned off without a current zero. The thyristor offers the advantages of solid state construction

and long life when operated within device ratings.<sup>3-46</sup> The relatively low ratings of individual thyristors require that many of the devices be connected in series and parallel arrays to meet switch requirements. As an example, CEM assembled a switch to carry three million amps at 4.2 kV that consists of 288 thyristors; the switch's volume and weight are 1.6 cubic meters and 2,800 kilograms.<sup>3-47</sup>

### Opening Switches

Opening a switch is more demanding than closing the switch. Any current that is flowing must be interrupted, and the stored magnetic energy must be dissipated (commutated) as part of the switching process. Faraday's law (equation (3-4)) also applies to opening a switch

$$V = L \frac{di}{dt}$$

When the current changes, a voltage is induced across the switch; rapid switching induces a large voltage that can in turn cause dielectric breakdown -- and continued current flow. Opening switches are classified as either direct interruption or current-zero devices.<sup>3-49</sup>

A repetitive, direct opening switch for EMLs is elusive. The most successful direct interruption devices for EMLs are explosive switches and fuses.<sup>3-50</sup> In the explosive switch, the force of detonation mechanically disrupts the conductor and interrupts current flow; this switch offers rapid action and precise control.<sup>3-51</sup> A fuse opens the circuit when ohmic heating causes the fuse material to melt or vaporize.<sup>3-52</sup> Unfortunately, these switches are inherently one shot

devices; neither of these switches is likely to be useful in systems with repetitive firing requirements. A mechanical switch capable of repetitively switching 750 kiloamps has been developed but it weighs 1,000 kilograms;<sup>3-53</sup> the weight of this switch is unappealing since a single device is not rated to carry the current for projected electric guns.

A current-zero switch is a device that switches when the current is either forced or naturally goes to zero. When the current is zero, energy need not be commutated out of the switch. The duration of the current zero must be long enough for the switch to transition to a high impedance state. The current can be forced to zero by counterpulsing the switch with an equal and opposite current. The equal and opposite current can be created by discharging a capacitor, but this technique increases system size and energy requirements. Naturally occurring zeros occur in alternating current power supplies such as the compulsator and capacitively driven systems which ring. Typical current zero devices are the vacuum gap switch and the thyristor which has already been described.<sup>3-54</sup>

The vacuum gap switch is similar to the spark gap closing switch. A trigger pulse is applied across the switch electrodes. The voltage causes an arc that conducts current; the arc is sustained by metal vapor that evaporates from the electrode surfaces. When the current goes to zero for a few microseconds, the metal vapor condenses on the electrodes -- interrupting the current flow mechanism. Experiments have shown that vacuum gap switches are capable of carrying 100 kA and holding off 100 kilovolts.<sup>3-55</sup>

### Buswork

The buswork consists of the high power electrical connections between system components. Buswork receives the least attention of all aspects of EML design but is none the less critical to efficient system operation. From an electrical standpoint, the buswork must carry extremely large currents between components; buswork insulation must also sustain extremely high voltages without breaking down. The buswork must have the lowest possible inductance and resistance. Low inductance translates into small magnetic flux (and stored energy) associated with the buswork -- which means greater system efficiency. Low buswork inductance also contributes to the efficiency of switching processes. Mutual inductances between adjacent conductors are also an important consideration since they can significantly alter system performance. Low buswork resistance is important to minimize dissipative losses and thermal management problems. Resistance is minimized by increasing the conductor cross section; the buswork designer must consider the current frequency (and resulting skin depth) in determining conductor geometry.

From a mechanical standpoint, the buswork must be able to withstand the magnetic forces caused by the interactions of currents and magnetic fields. Magnetic stresses are not limited to the launcher but exist anywhere current flows in the system. Large currents can cause conductor movement; this in turn places stresses upon electric connections and insulating materials. As a consequence, the physical routing of the buswork is an important consideration. As a rule, the length of the buswork should be kept as short as possible.<sup>3-56, 3-57</sup>

## Chapter 4

### ELECTROMAGNETIC GUN SELECTION METHODOLOGY

This chapter proposes a methodology for selecting an electromagnetic launcher; the method is depicted in figure 4.1. The description of launchers, power supplies, and switches in chapters two and three is indicative of the fact that EMLs are complex systems. The EML system and its component subsystems are shown in figure 4.2. Clearly, the designer is challenged to select the combination of components that will perform the launch mission and meet launcher design constraints. The system selected will depend upon the mission requirement and the available technology. As technology evolves, the EML that is best suited for a particular mission is likely to change; accordingly, this methodology is intended to be independent of the present state of technology so that a gun appropriate for the existing technology at any point in the future will be selected.

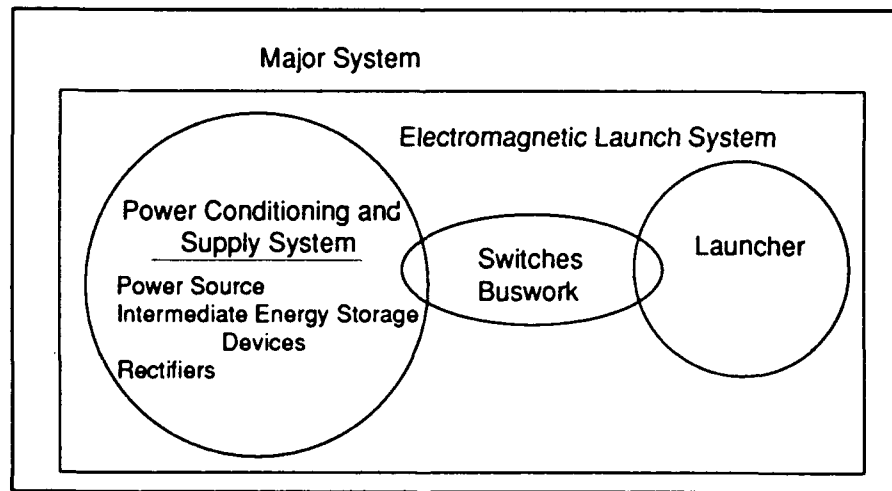


Figure 4.2 Electromagnetic launch system diagram.

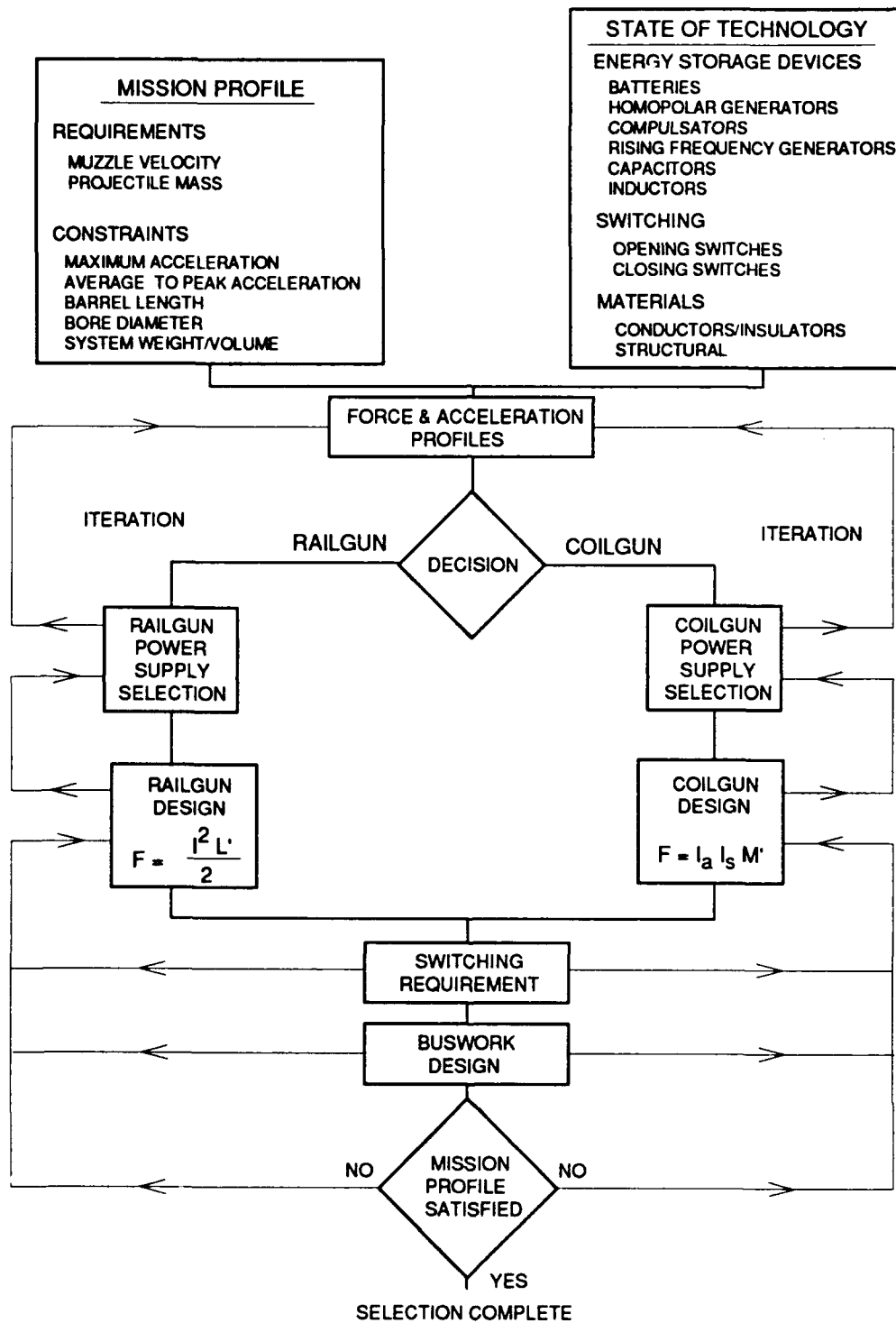


Figure 4.1 Electromagnetic launcher selection methodology.

### Mission Profile

The process of selecting an electromagnetic gun begins with the mission profile and knowledge of the state of existing technology. In general, the goal of EML design is to build the smallest, lightest, and most efficient launcher that will meet mission requirements -- to stretch technology to the limit. A thorough knowledge of the capabilities of each launcher component is essential to understanding how those components interrelate to form the EML system. The technologies incorporated into an EML span many disciplines and must be carefully blended to obtain the best possible launcher. The engineer must make the most of the available technology -- and recognize opportunities for improving existing designs. Selecting an EML system will almost certainly be an iterative process meshing electrical and mechanical design; hopefully, the process will converge to an acceptable system design.

The mission profile specifies the performance requirements and constraints that the system must satisfy (table 4-1). Fundamentally, the purpose of an EML is to accelerate a given mass to a desired muzzle velocity -- these requirements must be specified. Performance

<b>Mission Profile</b>	
<u>Performance Requirements</u>	
Muzzle velocity	Projectile mass
<u>System Constraints</u>	
Maximum allowable acceleration	Barrel length
Average to peak acceleration ratio	Bore diameter
Projectile design	System mass
System volume	

Table 4-1

requirements should be specified over a reasonable range of values, so the selected launcher is capable of firing more than one specific projectile. Often times, a launcher must be able to fire several types of projectiles for different terminal effects. At the very least, this allows projectile design to evolve.

System constraints on the other hand may or may not be explicitly specified depending upon the overall system. If the system constraints are not explicitly stated, the designer has some degree of freedom -- but is limited to system configurations that can realistically be implemented. Typical system constraints are listed in table 4-1, but other constraints may also be specified. The purposes of the listed constraints are briefly summarized as follows. The maximum allowable acceleration and average to peak acceleration ratio are specified to limit mechanical and thermal stresses on the launcher and projectile. The high velocity projectile is optimized for flight characteristics and terminal affect; more often than not, the designer will be provided a projectile to launch. A minimum bore diameter may be specified to accommodate a particular projectile design. The barrel size and mass may have upper bounds so that the barrel can be moved and aimed quickly. Barrel length is restricted by the distance the barrel can extend unsupported and not droop under its own weight. Any EML that must be mobile or transportable will have mass and volume restrictions.

### Barrel Length and Average Acceleration

Given the specific mission profile of the gun, the first step in selecting a gun is to determine the barrel length and average acceleration for the most demanding projectile and velocity

combination. In the initial selection process, two assumptions are helpful:

- 1) The armature weight is equal to projectile weight; together, the armature and projectile constitute the launch package. The weight of the armature must be minimized so that the maximum energy is transferred to the projectile.
- 2) A constant force is applied to the launch package.

The selection process is iterative so as design decisions are made these assumptions can be modified.

Launch package position and acceleration are related by the equation

$$\frac{d^2x}{dt^2} = a$$

where,

$a$  = average acceleration

$x$  = launch package position.

The velocity of the launch package is determined by integrating acceleration over time

$$\begin{aligned} v &= \frac{dx}{dt} = a \int dt ; (a = \text{constant}) \\ &= at + v_0 \end{aligned}$$

where,

$v_0$  = initial launch package velocity

Launch package position is determined by integrating velocity over time

$$\begin{aligned} x &= \int (at + v_o) dt \\ &= \frac{1}{2}at^2 + v_o t + x_o \end{aligned}$$

where,

$$x_o = \text{initial launch package position.}$$

Defining the initial launch package position and velocity to be zero yields the relationships

$$(4-1) \quad v = at$$

and

$$(4-2) \quad x = \frac{1}{2}at^2.$$

Combining these equations to eliminate t leads to the expression

$$(4-3) \quad x_b = \frac{1}{2} \frac{v_m^2}{a}$$

where,

$$x_b = \text{barrel length}$$

$$v_m = \text{muzzle velocity}$$

This expression, the mission profile, and engineering judgment are

used to determine an acceptable combination of barrel length and average acceleration. As a rule, longer barrels mean lower average acceleration and applied force -- and less stress on the launcher and projectile. A longer barrel also reduces the peak power requirement for the power supply though the energy requirement remains unchanged.

Once target values for barrel length and average acceleration are determined other useful information follows. The average force that must be applied to the launch package is also known from Newton's second law

$$(4-4) \quad F = m_{lp} a.$$

where,

$$m_{lp} = \text{launch package mass}$$

The launch time can be determined from the expression

$$(4-5) \quad t_l = \sqrt{\frac{2x_b}{a}}$$

where,

$$t_l = \text{launch time.}$$

The kinetic energy of the projectile is

$$(4-6) \quad KE = \frac{1}{2} m_{lp} v_m^2$$

which by using equations (4-1) and (4-2) can also be expressed

$$(4-7) \quad KE = \frac{2m_{lp} x_b^2}{t_i^2}.$$

The instantaneous mechanical power required to drive the projectile at the end of the launch is

$$(4-8) \quad P = F v_m = m_{lp} a v_m$$

which by using equations (4-1) and (4-2) can be expressed

$$(4-9) \quad P = \left[ \frac{2m_{lp} x_b^2}{t_i^2} \right] \frac{2}{t_i} = [KE] \frac{2}{t_i}.$$

#### Decision: Railgun or Coilgun?

At this point, the engineer must decide to pursue either a railgun or a coilgun. As discussed in chapter two, railguns are fundamentally simpler than coilguns but are plagued by rail damage during launch. Low barrel wear rates are important for consistent launch performance and achieving barrel life expectancies of thousands of launches. If the sliding electric contact problems can be solved, the railgun should be given serious initial consideration as the launcher of choice -- simplicity is a virtue. If on the other hand the sliding contact problem cannot be solved, the complexity of the coilgun may become a necessary evil. While a major consideration, the acceptability of the sliding contact is certainly not the only consideration; for some very large scale launchers, the railgun may not

be suitable. The engineer must consider the mission requirement and level of available technology against the technology requirements for each of the candidate gun types.

### Power Supply Selection

Once either a railgun or coilgun is selected, there is a natural tendency to focus upon designing the launcher. In fact, the next step must be to identify a power supply and conditioning system that is suitable to drive the desired EML. Attempting to design the launcher without having done this can lead to the embarrassing situation of having a spectacular launcher concept that cannot be driven by any existing power supply. Once selected, the power supply and conditioning system constrains launcher design. The power supply system selected determines the types of switches that must be employed. Given current and projected switch technology, closing and current-zero opening switches are preferable over opening switches.

The railgun has a relatively straight forward power supply system requirement since it is a one terminal device. The power supply system does not affect the fundamental design of the railgun. Coilgun design on the other hand is greatly influenced by the capabilities of available power supplies. The candidate power supply determines the types of coilgun launchers that can be built. If for example capacitors are chosen as the final intermediate energy storage device, then a discrete coil launcher must be built. If a rising frequency generator is chosen, then a continuous coil launcher will probably result. Often times, the engineer may have a particular gun concept in mind when selecting the power supply system. An example of this is the collapsing field accelerator; the stator coils serve as energy storage inductors.<sup>4-1</sup>

The energy that the power supply and conditioning system must store can be estimated from the muzzle kinetic energy of the projectile. Likewise, the peak power can be estimated from the muzzle kinetic energy and launch time. A review of the technical literature on EMLs indicates that 30 percent overall system energy conversion rate is typical.<sup>3-1 -- 3-6</sup> Assuming a 33 percent efficiency for converting of stored energy to launch package kinetic energy is therefore reasonable and convenient for initial calculations; this assumption can be changed as experience with EMLs becomes broader. Thus, the power supply and conditioning system must be sized so that the energy delivered by the energy storage device is three times the projectile kinetic energy as determined by equation (4-7)

$$(4-10) \quad W_s = 3 KE = (3) \frac{2m_{lp} x_b^2}{t_l^2}$$

where,

$W_s$  = Stored energy delivered by the power supply.

The peak power requirement can be estimated by considering the instantaneous mechanical power requirement as developed in equation (4-9) and carrying forward the assumption that determined  $W_s$

$$(4-11) \quad P_s = \left[ (3) \frac{2m_{lp} x_b^2}{t_l^2} \right] \frac{2}{t_l} = [(3) KE] \frac{2}{t_l}$$

where,

$P_s$  = Peak instantaneous power.

The power supply energy and the peak instantaneous power requirements determine the size of the power supply and power conditioning components. In practice, the power supply system capabilities must exceed launcher requirements to provide a margin for reliable and safe operation. The designer uses energy and power density factors (such as those found table 3-1) to size the candidate power supply system components. The size of power supply and power conditioning system components is determined by the larger of the two requirements; ideally, the selected components will strike a balance between energy and power density so that neither dominates component sizing. For example, the battery has outstanding energy density but poor power density; the low power density would require an excessively large battery to meet peak power requirements. At the other extreme, the capacitor has excellent power density but low energy density; the energy density dictates a capacitor bank much larger than necessary to deliver the required power.

At this point, the power supply system selected is tentative. Once the launcher is designed, the designer must perform further analysis to further define the power supply system design.

### Railgun Design

Having established a baseline power supply, the designer can now turn his attention to designing the launcher. Recall that for the railgun, force is given by the expression

$$(4-12) \quad F = \frac{1}{2} I^2 \frac{\partial}{\partial x} [L] = \frac{1}{2} I^2 L'.$$

The current is determined by the interaction of the power supply and launcher impedance -- determined by launcher design. In a railgun with a circular bore, the inductance and inductance gradient are more complicated than the simplified railgun discussed in chapter two and must be solved using numerical methods. The simplified railgun is, however, illustrative; recall that the inductance, equation (2-8), and inductance gradient, equation (2-9) are

$$L = \frac{\mu h x}{d}$$

and

$$L' = \frac{\mu h}{d}$$

The distance between the rails and the width of the rails are the important factors for the designer to consider; though this particular model is limited by the assumption that the rail separation distance is much less than the width of the plates.

Designing the barrel and armature is an interdisciplinary mechanical and electrical engineering problem. The rail geometry must be designed in conjunction with the armature to obtain the optimum combination of the two components. The rails must be able to carry megaamp currents and have an attractive inductance gradient; the rails must also be able to dissipate the thermal energy deposited for the rated number of repetitive launches. The barrel must be robust enough to withstand the launch forces exerted upon the rails. At the same time, the volume and mass of the barrel must meet system constraints. The armature must be highly conductive, maintain contact with the rails, and withstand the mechanical stresses of launch; armature mass must be minimized to maximize the kinetic

energy imparted to the projectile. Once the armature is designed, the assumption regarding the armature mass must be updated.

The next step in the selection methodology is to determine whether the power supply will generate the current waveform necessary to drive the launcher. The current waveform can be determined by mathematically modeling the launcher. The first equation is based upon the equivalent model shown in figure 2.3(b) is

$$\begin{aligned}
 (4-13) \quad V_s &= IR + \frac{d\lambda}{dt} \\
 &= IR + L \frac{dI}{dt} + I \frac{dx}{dt} \frac{dL}{dx}
 \end{aligned}$$

where,

$$V_s = \text{power supply voltage.}$$

This equation has three time dependent variables and therefore requires an equal number of equations to determine a unique solution. The inductance and inductance gradient are dependent only upon system geometry and can be calculated independently of the system of equations. Equation (4-12) provides the second required equation

$$F = m \frac{d^2x}{dt^2} = \frac{1}{2} I^2 L'$$

The final equation is determined by the relationship between the power supply voltage and current; the relationship is dependent upon the specific power supply chosen. The solution to this set of coupled differential equations models the system. If the system does not meet

specified performance requirements, the design must be iterated until this condition is satisfied.

### Coilgun Design

Recall from table 2-1 that there are several coilgun classifications based upon armature excitation, stator excitation, stator field control, and mode of operation. The classes of coilgun that can be built are largely determined by the power supply and conditioning system already selected -- the power supply system selected will reduce the number of possible systems to one or two. In the event that there is a choice, the engineer must use his knowledge and judgment to select a specific class of launcher. Once a specific class of launcher is selected, the engineer is left with the complicated task of designing the launcher. The number of interrelated factors that must be considered and optimized is large.

The expression for force in a coilgun given by equation (2-15) is

$$(4-14) \quad F(z,t) = \sum_{i=1}^N I_{ai}(z,t) I_{si}(z,t) \frac{\partial M_i(z)}{\partial z}$$

where,

N = number stator coils.

The mutual inductance, equation (2-16), and its gradient, equation (2-17), are functions of armature position. The armature and stator currents are functions of time and armature position and must be determined from the system of differential equations that model the

equivalent circuit for one armature and stator coil pair shown in figure 2.5(b).

$$\begin{aligned}
 V_s &= I_s R_s + L_s \frac{dI_s}{dt} + M \frac{dI_a}{dt} + I_a v \frac{dM}{dz} \\
 (4-15) \quad V_a &= I_a R_a + L_a \frac{dI_a}{dt} + M \frac{dI_s}{dt} + I_s v \frac{dM}{dz}
 \end{aligned}$$

These equations have five independent variables requiring five independent equations to specify a unique solution. Equation (4-14) can be rewritten to form a third equation

$$m \frac{dv}{dt} = I_a I_s \frac{dM}{dz}.$$

The remaining equations which relate the power supply voltages  $V_s$  and  $V_a$  to the currents  $I_s$  and  $I_a$  are dependent upon the selected power supply system. A similar set of differential equations must be solved for each armature and stator coil pair. The solutions to the  $N$  sets of differential equation systems model the behavior of the complete launcher system. This simple coilgun model does not account for the mutual inductance between adjacent stator coils or resistance changes as the conductor temperature rises; both affect overall system performance.

The differential equations that model system behavior reflect only part of the complexity of the coilgun. Many electrical and mechanical parameters interact to determine self and mutual inductances. The system must carry the desired currents and be able to withstand the mechanical stresses. Table 4-2 lists major coilgun

parameters that must be optimized to produce an interesting launcher; this list does not include many parameters of lesser importance. Due to its complexity, the design process does not lend itself well to intuitive design decisions. Coilgun designers at CEM have resorted to computer optimization to find favorable combinations of coilgun parameters. Optimization works best when a favorable range of key parameter values that will produce interesting coilguns is known.<sup>4-2</sup>

Coil geometry is a determining factor in gun performance.

<b>Major Coilgun Parameters</b>	
<b>Dimensional</b>	
1.	Gun bore or stator coil inside diameter.
2.	Armature outside diameter or air gap.
3.	Stator and armature lengths.
<b>Electrical</b>	
1.	Turns in the stator and armature coils.
2.	Stored energy in the power supply.
3.	Power supply impedance.
<b>Operational</b>	
1.	Offset of the armature at stator turn-on.
<b>Initial Conditions</b>	
1.	Armature and stator initial currents.
2.	Armature velocity.
3.	Armature and stator initial temperatures
<b>Materials</b>	
1.	Armature and stator coil conductor materials
2.	Allowable stresses.
3.	Allowable temperature rise.

Table 4-2.<sup>4-2</sup>

Consider the effects of bore diameter. Force is a function of magnetic flux density and area, equation (2-4); the force down the length of the bore is

$$F = \left( \frac{B^2}{2\mu} \right) A = \left( \frac{B^2}{2\mu} \right) \pi r^2$$

For a desired force, the required magnetic flux density decreases as bore radius increases. The larger the bore, the less the mechanical stress in all directions. From an electrical standpoint, a larger bore allows the mean armature radius to be closer to the mean stator radius; this means a larger mutual inductance and mutual inductance gradient (see figure 2.6). Increased bore size provides both electrical and mechanical advantages. But increased bore size must be balanced against the consequent increase in armature mass. Armature mass increases as a cubic function of armature radius; as radius increases, armature length must also increase for stability reasons.

One approach to determining bore size is to use armature mass as the design constraint. Armature mass can be determined using the expression

$$m_a = \pi k (r_o^3 - r_i^3) \delta$$

where,

$m_a$  = desired armature mass

$k$  = proportionality factor between armature length and bore radius

$\delta$  = armature mass density

$r_o, r_i$  = outer and inner armature radius.

The proportionality factor  $k$  is determined by armature launch stability and or the required contact area between the armature and projectile. The armature mass density is a weighted average of the mass density and quantity of each material used to build the armature. This equation can be solved for the armature outer radius that results in the desired armature weight

$$(4-16) \quad r_o = \sqrt[3]{\frac{m_a + \pi k r_i^3 \delta}{\pi k \delta}}$$

The gun bore will then be set slightly larger than the armature radius.

A stated system constraint is the average to peak acceleration ratio which is specified to minimize projectile and launcher stress; the ratio is a measure of the constancy of the applied force. Applying a nearly constant force throughout the launch is a difficult undertaking because of the time variations of the currents and the position variation of the mutual inductance gradient. One measure to help achieve constant force is to design armature and stator coils so that the mutual inductance gradient of adjacent coils overlap. The concept is illustrated in figure 4.3. With mutual inductance gradient overlap from stator coil to stator coil down the length of the bore, it becomes possible to approach constant force by controlling current switching. With careful design, force can be exerted on the armature simultaneously by adjacent stator coils.

The selection of the stator coil length must balance among other factors the number of stator coils in the barrel, the energy that will be discharged through each coil, and the overlap of mutual inductance gradient curves from coil to coil. Assuming that the power supply energy will be evenly distributed to the stator coils, a large number of stator coils keeps the energy discharged through each coil small. A

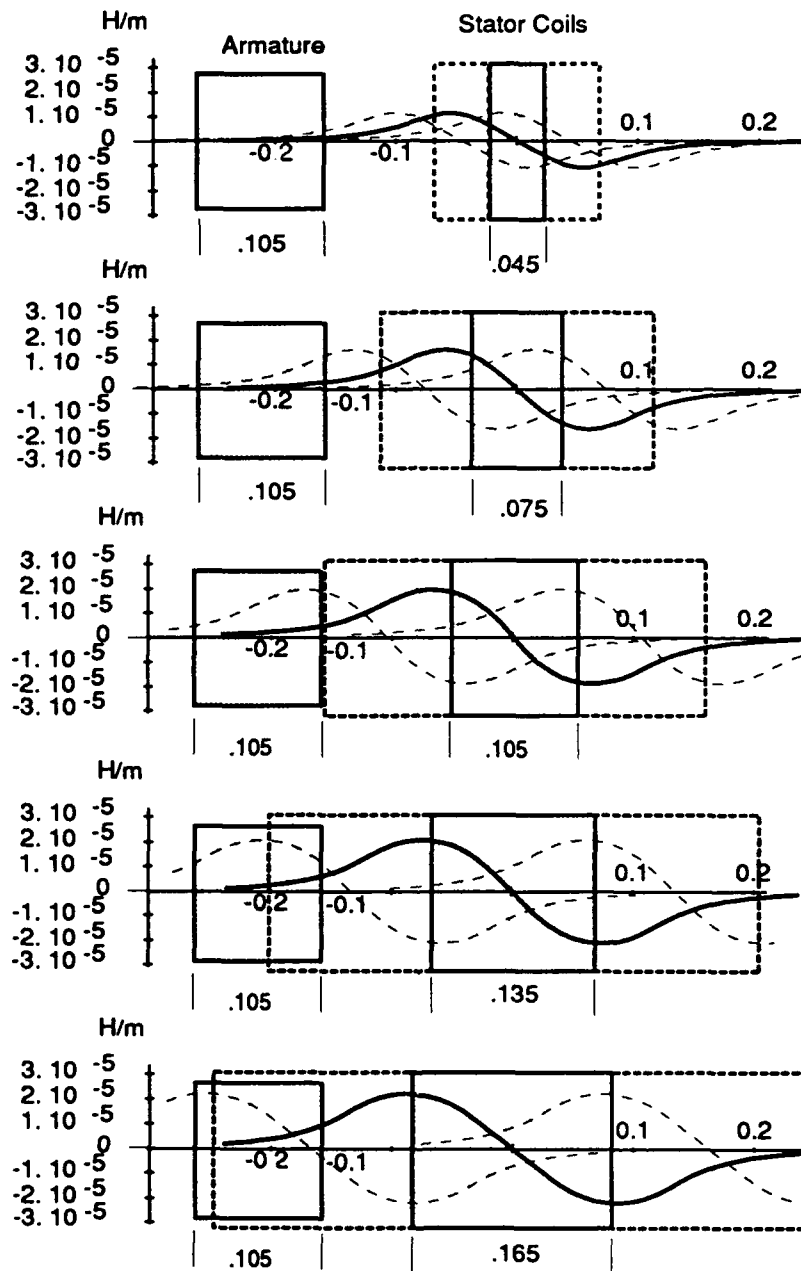


Figure 4.3 Mutual Inductance gradient curves for a specified armature length and various stator lengths. These curves were prepared in accordance with the procedure in Appendix A with the number of turns on each coil proportional to axial coil length.

large number of stator coils also increases the degree of mutual inductance gradient overlap. But, a large number of stator coils also increases the number of switches and electrical connections (buswork). A small number of coils has the opposite affect upon these parameters.

The factors that determine mutual inductance gradient also determine the coil self inductance; the self inductance in turn determines the rate of change of current in the coil. The rate of change must be fast compared to the transit time of the armature through the coil. The coil geometry and number of turns must be selected to give acceptable values of self and mutual inductance. If the coilgun is to have a persistent armature current, then special consideration must be given to insure that the  $L/R$  time constant of the coil is long compared to the launch time of the projectile. Likewise, the stator coils for the collapsing field gun must also have time constants long compared to the launch time.

Mechanical design considerations are as important as electrical design considerations. The launcher and armature must be designed to withstand severe thermal and mechanical launch stresses. The barrel must contain the magnetic pressures without destructive deformation. Armature design is particularly important due to the severe size and mass constraints that must be imposed. Once the armature is designed the assumptions regarding launch package mass must be updated.

Once the system is initially designed, it must be simulated to insure that the performance requirements are satisfied. If the requirements are not satisfied, the design procedure must be iterated until the system satisfies the mission requirements and constraints.

### Switches and Buswork

The final steps in the selection methodology are to select switches and buswork. Although these elements are considered last, their importance to the overall system function cannot be overemphasized. At this point in the EML selection process, the characteristics of the current and voltage waveforms required to drive the launcher are known. The goal is to select switches and design buswork that will allow the desired waveforms to be applied to the launcher and meet imposed weight and volume constraints. Unfortunately, no existing switch technology is ideally suited for EML applications; so finding appropriate switches can be a significant obstacle to building the desired launcher.

When the power supply system was selected, the types of switching operations (closing, current-zero opening, and opening) required to drive the EML were implicitly determined. At this point, the designer selects specific switching devices to perform these switching functions. As with other design decisions, the most appropriate switch must be selected by balancing the capabilities of the available switches against launcher and power supply requirements. The capabilities of the selected switch must exceed the demands of the driving current and voltage waveforms; this provides a margin for safe and reliable operation.

A switch may consist of a single switching device or a group of connected switching devices that meet the desired switching requirements. The switching system includes all of the switches required for the EML to function; as a rule, there will be at least one switch per terminal pair. Important switch characteristics that must be considered include voltage standoff, maximum rate of current change, maximum current, current pulse width, repeatability of the switching operation, and switch life.

In the "off" state, the switch must be able to standoff a voltage exceeding the power supply voltage; otherwise, the switch will breakdown and allow undesired current flow. If the driving voltage is greater than a the rated standoff voltage, then several devices can be connected in series to attain the desired capability.

In the "on" state, the switch must be rated to conduct currents exceeding the peak current. If necessary, several switching devices can be connected in parallel to attain the desired current rating. For pulsed power switches, the length of time that the switch is able to conduct must exceed the pulse width of the current waveform; some pulsed power switches will have pulse widths that are shorter than the desired current pulse width. The selected switch must also withstand the thermal stresses caused by current flow. The thermal stresses are dependent upon the current magnitude and pulse width; the deposited thermal energy, or action, is determined by equation (2-18). The switch packaging must quickly dissipate extreme thermal energy levels before the switch is damaged; thermal packaging requirements increase switch weight and volume significantly.

Switching time is a critical EML switch characteristic. For a closing switch, the switching time is determined by the achievable rate of current change,  $\left(\frac{di}{dt}\right)$ . The maximum current rate of change for the switch must exceed the desired current waveform rate of change. For a current-zero opening switch, the current switching time is determined by the length of the current zero required for the device to transition to the "off" state. Switching times are a limiting factor on EML muzzle velocities -- especially for the coilgun.

Other considerations in selecting a switch include the permissible repetition rate, reliability, jitter, and expected life of the switch. When the mission requires repeated launches in short periods of time, the selected switch must recover for the next launch in a time

that will satisfy the required launch repetition rate. The selected switches must be very reliable; each time a switch fails, launcher performance changes which may have dire consequences. Since precise switch timing is critical to EML performance, the statistical variations in the time required for conduction to begin, referred to as jitter, must be very small compared to the pulse width. The switch must be able to cycle hundreds or thousands of times without replacement.

The buswork that links the EML system components must be designed for the specific system. As mentioned in chapter 3, the buswork must have inductance and resistance low compared to other system components in order to minimize its effect upon electrical system performance. It must be able to withstand extreme mechanical and thermal stresses and meet weight and volume constraints. Buswork routing must be carefully designed to minimize unwanted electrical and mechanical interaction between adjacent conductors.

The final step in the methodology is to examine the system as a whole to insure that the performance requirements are satisfied and that system constraints are met. If the system passes this critical examination, the EML selection is complete. If the system fails to meet any criteria, the selection process must be iterated until a satisfactory system is selected, or the determination is made that the system cannot be built given existing technology and the imposed constraints.

## Chapter 5

### METHODOLOGY APPLICATION

In this chapter, the selection methodology is applied to mission 7 from table 1-1 considering existing and projected technology. This mission is interesting since the desired muzzle velocity is twice the velocity attainable from a conventional chemical propellant gun. Such a leap in capability helps to justify the transition from conventional propellant weapon systems to electromagnetic launch systems. The mission profile is summarized in table 5-1. Table 5-2 shows characteristics of the M1A1 Abrams main battle tank; this information is the basis for the EML system constraints imposed for this example.

The EML system volume includes the power supply, intermediate energy storage devices, switches, and buswork. The EML system weight must include the power supply, intermediate energy storage devices, switches, buswork, and the barrel.

#### Force and Acceleration Profiles

To begin the process of selecting an electromagnetic launcher, assume that

- 1) A constant force is applied to the launch package.
- 2) The launch package mass (armature and projectile) is 3.4 kg.
- 3) The average acceleration will be one-half the maximum allowable acceleration ( $6 \times 10^5 \text{ m/s}^2$ ).

Mission 7 Profile: Tank Main Gun			
Flight projectile mass (kg)	1.7	Muzzle velocity (km/s)	3.0
Flight projectile diameter (mm)	14	Allowable acceleration (m/s <sup>2</sup> )	12 x 10 <sup>5</sup>
Flight projectile length (mm)	570	Launch rate	2 rounds in 5 s, 22.5 s between

Table 5-15-1

M1A1 Main Battle Tank Characteristics			
Approximate hull volume (m <sup>3</sup> )	Weight (kg)	Gun bore diameter (mm)	Gun barrel length (m)
42.7 (length 7.9 m, width 3.6 m, height 1.5 m)	57,154	120	9.8

Table 5-25-2

Proposed EML System Constraints				
EML volume* (m <sup>3</sup> )	EML weight** (kg)	Gun bore diameter (mm)	Gun length (m)	Maximum system voltage (kV)
8.54 (excluding barrel)	14,290	120	10.0	20
* 20% of M1A1 hull volume		** 25% of M1A1 weight		
These percentages are intended to place reasonable bounds on the EML system.				

Table 5-3

Using Equation (4-3), the required barrel length is

$$\begin{aligned} z_b &= \frac{1}{2} \frac{v_m^2}{a} = \frac{1}{2} \frac{(3000)^2}{6 \times 10^5} \\ &= 7.5 \text{ m} \end{aligned}$$

The required force is known using Newton's second law, equation (4-4),

$$\begin{aligned} F &= m_{lp} a = 3.4 (6 \times 10^5) \\ &= 2.04 \times 10^6 \text{ N} \end{aligned}$$

The launch time is known from equation (4-5)

$$\begin{aligned} t_l &= \sqrt{\frac{2z_b}{a}} = \sqrt{\frac{2(7.5)}{6 \times 10^5}} \\ &= 5.0 \text{ ms} \end{aligned}$$

The launch package kinetic energy is

$$\begin{aligned} KE &= \frac{1}{2} m_{lp} v_m^2 = \frac{1}{2} (3.4) (3000)^2 \\ &= 15.3 \text{ MJ} \end{aligned}$$

### Select a Coilgun

At this point, either a railgun or a coilgun must be selected. For this example, a coilgun launcher is selected. This is based partially upon the assumption that the railgun sliding contact problem has not been solved. Additionally, selecting a coilgun provides greater insight into the complexities of EML selection.

### Power Supply Selection

The weight and volume restrictions imposed by the mission dictate a single electric power generation device. A rising frequency generator is attractive for powering a continuous coil launcher but is still only a conceptual power supply. A second option is to use a homopolar generator to power a collapsing field accelerator; this launcher is currently conceptual only. A third option that has been demonstrated, and the one chosen for this example, is to use capacitors as intermediate energy storage devices to drive the launcher.

Using capacitors as the intermediate energy storage device dictates that a discrete coil launcher be built. Each stator coil has a bank of capacitors charged by batteries, alternator, or compulsator prior to launch. Batteries are attractive because of their very high energy density, but connecting enough batteries in series to make very high capacitor charging voltages is not realistic. The alternator and compulsator are both capable of generating high voltages but also require intermediate rectification devices to hold the charge on the capacitors. All three power supply options require substantial switching networks. Table 5-4 shows the proposed allocation of the mass and volume constraints in table 5-3 to the EML sub components.

The overall energy storage requirement is estimated to be three

Proposed EML Component Masses and Volumes*					
	Alternator Rectifiers	Switches	Capacitors	Buswork	Barrel
Mass (kg)	3000	4000	4000	1000	2290
Volume (m <sup>3</sup> ) Interior to hull	2	2	3	1.5	--
* Note these are initial estimates intended to impose constraints on sub-system components and would be revised as the system design evolves.					

Table 5-4

times the launch package kinetic energy according to equation (4-10)

$$W_s = 3 KE = 45.9 MJ$$

and the peak instantaneous power requirement is determined using equation (4-11)

$$P_s = [(3) KE] \frac{2}{t_l} = [(3) (45.9)] \frac{2}{(5 \times 10^{-3})}$$

$$= 55.36 GW$$

State of the Art Capacitor			
Capacitance (μF)	840	Stored Energy (kJ)	50
Rated Voltage (kVDC)	11.0	Energy Density (kJ/kg)	.77
Volume (m <sup>3</sup> )	.047 (.046x.177x.655)	Energy Density (MJ/m <sup>3</sup> )	1.03
Weight (kg)	68		

Table 5-5-3

Table 5-5 shows typical characteristics of today's high energy density, state of the art capacitor. These values are typical; there are other capacitors available with a range of rated voltages and capacitances that have similar energy densities.<sup>5-3</sup> In the case of the capacitor, energy density is the factor that drives the size of the required capacitor bank. For this example, the volume and mass of the capacitor bank would be

$$\text{Capacitor bank mass} = \frac{45.9 \text{ (MJ)}}{.77 \text{ (kJ / kg)}} = 59,610 \text{ kg}$$

$$\text{Capacitor bank volume} = \frac{45.9 \text{ (MJ)}}{1.03 \text{ (MJ / m}^3\text{)}} = 44.6 \text{ m}^3$$

Clearly, this gun is impossible to build given today's technology since the required capacitor bank is as large and weighs as much as the tank itself. Capacitor energy storage density (mass and volume) must improve by a factor of 15 before the capacitor bank is of reasonable size and weight. For the sake of continued discussion, assume that capacitors become available with a 15 fold improvement in energy density; this is within the realm of possibility based upon figure 3.13. This results in capacitor weight and volume

$$\text{Capacitor bank mass} = \frac{45.9 \text{ (MJ)}}{11.5 \text{ (kJ / kg)}} = 3,974 \text{ kg}$$

$$\text{Capacitor bank volume} = \frac{45.9 \text{ (MJ)}}{15.45 \text{ (MJ / m}^3\text{)}} = 2.97 \text{ m}^3$$

This combination of mass and volume is plausible given the imposed constraints. The specific characteristics of the capacitor bank will be determined in the next section as the coilgun design emerges.

### Coilgun Design

The first step in designing the coilgun must be to determine the bore size. In this case, the projectile diameter (14 mm) is quite small; a bore of this size would result in poor coupling between armature and stator coils. The maximum armature radius was determined using equation (4-16) assuming the following parameter values:

- 1)  $k = 2$ . This factor is chosen based upon the intuitive judgment that armature stability as it travels down the barrel will be satisfactory when the length equals the diameter.
  
- 2)  $\delta = 2.6 \text{ (g/cm}^3\text{)}$ . This is the mass density of carbon which would allow the use of a variety of composite structural materials (mass densities in the range of  $2.0 \text{ g/cm}^3$ )<sup>5-4</sup> and conductors for armature construction. Table 5-6 compares the characteristics of several possible conductors; beryllium is quite attractive as an armature conductor due to its relative mass density, conductivity, specific heat capacity, and high melting point.

Conductor Properties				
	Density (g/cm <sup>3</sup> )	Conductivity (10 <sup>6</sup> /Ω cm)	Specific Heat (J/g°K)	Melting Point (°K)
Copper	8.96	.596	.38	1357
Aluminum	2.70	.377	.90	933
Beryllium	1.85	.313	1.82	1560

Table 5-6<sup>5-5</sup>

The armature radius should be approximately

$$r_o = \sqrt[3]{\frac{m_a + \pi k r_i^3 \delta}{\pi k \delta}} = \sqrt[3]{\frac{1,700 + \pi 2 (.7)^3 (2.6)}{\pi 2 (2.6)}} \\ = 4.71 \text{ cm}$$

The armature outer radius was set at 4.9 centimeters. The bore diameter was set at 100 millimeters; this allows a one millimeter air gap between the armature and stator.<sup>5-6</sup> Based upon the assumption that the armature length be the same as the armature diameter, the armature length was set at 9.75 centimeters.

The next step is to select a stator coil length. Stator coil length must balance the number of coils, energy discharged through each coil, and the constancy of the mutual inductance gradient down the length of the barrel. On one hand, a smaller number of stator coils means fewer switches and accompanying buswork. On the other hand, a small number of stator coils increases the current in each coil and decreases the overlap of the mutual inductance curves from stator coil to stator coil. A large number of coils has the opposite affect on these parameters. For the purpose of this example, five stator coil sizes were evaluated with an incremental change in length of 1.5 centimeters. The various coil lengths are compared in table 5-7 and figure 5.1 In figure 5.1, the mutual inductance gradients are calculated based upon the assumption that the conductor thickness of both the armature and stator coils is 7.5 millimeters. The best balance of the factors discussed is in the 8.25 and 9.75 centimeter long stator coils. The 8.25 cm stator coil was selected because the energy discharged through each coil was smaller -- which implies smaller currents in each stator coil.

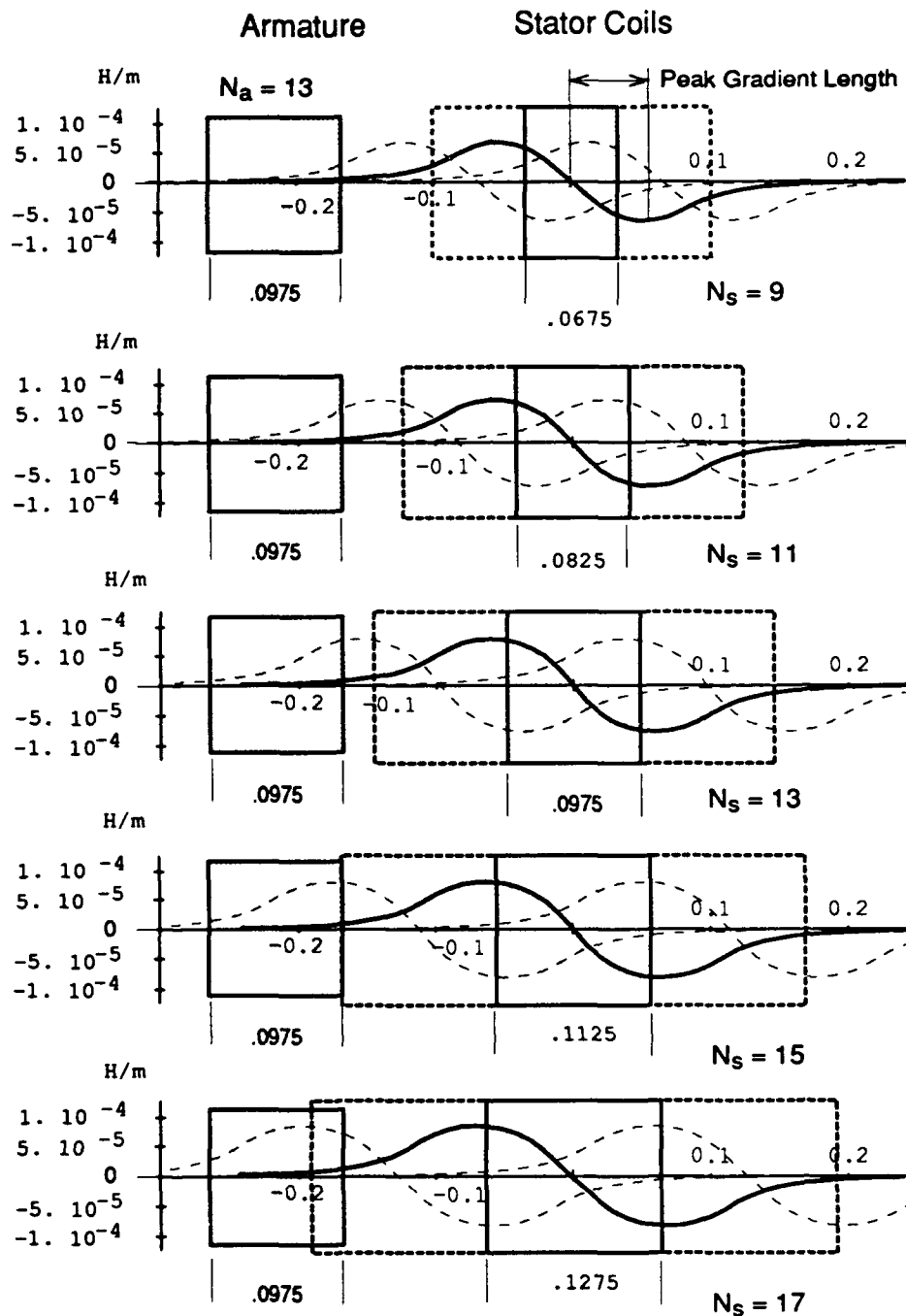


**Figure 5.1** Mutual inductance gradient curves for the desired armature length and various stator lengths. The degree of mutual inductance gradient overlap from coil to coil is an indication of the constancy of the force that can be applied to the armature as it moves down the barrel. These curves were prepared according to the procedure discussed in Appendix A with the number of turns indicated and a coil thickness of 7.5 millimeters.

Comparison of Stator Coil Lengths					
	Stator Coil Lengths (cm)				
	6.75	8.25	9.75	11.25	12.75
Number of Coils*	111	91	77	67	59
Energy per coil** (MJ)	.408	.497	.588	.676	.767
*7.5 meter long barrel		** 45.9 MJ total launch energy			

Table 5-7

Having selected the stator coil length and the energy to be discharged through each stator coil, the electrical parameters of the system must now be determined. There are several unspecified variables that determine the electrical parameters: the capacitance and applied voltage of the capacitor bank and the number of turns on the armature and stator coils. A critical factor in designing the system electrically is that the current rise from zero to peak in the time that the armature moves from the point of zero mutual inductance gradient to the point of maximum mutual inductance gradient (hereafter referred to as the peak gradient length). Using equation (4-5), the time required for the armature to transit the peak gradient length is

$$\Delta t = t_p - t_z = \sqrt{\frac{2z_p}{a}} - \sqrt{\frac{2z_z}{a}}$$

where,

$t_p, t_z$  = time that armature is at peak,  
zero mutual inductance gradient

$z_p, z_z$  = armature position at peak, zero  
mutual inductance gradient.

For this armature and stator geometry, the peak gradient length is 6 centimeters. Using this information, the armature peak gradient length transit time for each stator coil is shown in figure 5.2. The armature peak gradient length transit time drops very rapidly in the first meter of the gun; after the first meter, the change in armature transit time becomes relatively small.

The system of equations, (4-15), that describes the behavior of the coilgun does not lend itself to direct analytical evaluation of the electrical circuit parameters that will result in the desired current rise times. However, the simple LC circuit, figure 5.3(c), with the capacitor initially charged is a useful model for estimating the desired electrical parameters. The current waveform of the circuit is sinusoidal and

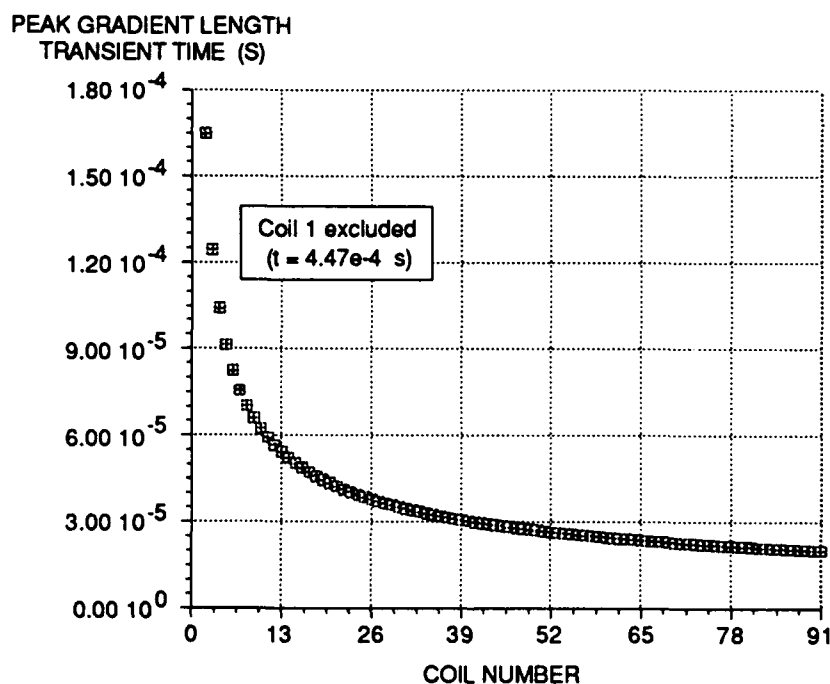


Figure 5.2 Armature transit time through the peak gradient length. Calculated assuming constant acceleration and a 6 centimeter peak gradient length.

has a natural frequency given by the expression

$$f = \frac{1}{2\pi} \frac{1}{\sqrt{L_{eq}C}}$$

The time for the current to rise from zero to peak is equal to one-quarter of the period

$$(5-1) \quad t_r = \frac{1}{4f} = \frac{2\pi \sqrt{L_{eq}C}}{4}$$

where,

$t_r$  = current rise time.

The capacitor bank must be charged to .497 megajoules where the energy is determined by equation (3-1)

$$W = \frac{1}{2} C V^2$$

The required rise time is short, so the product of C and  $L_{eq}$  must also be a small number. Therefore, select the smallest capacitance possible. Set the capacitor voltage to the allowable limit (20 kilovolts) and determine the required capacitance

$$C = \frac{2W}{V^2} = \frac{2(.497 \times 10^6)}{(400 \times 10^6)} = 2.5 \text{ mF}$$

As the system is designed, each stator coil provides useful energy to the armature when the two are in close proximity -- approximately one-half a current cycle. Therefore, a current zero opening switch will be placed in the circuit to interrupt the current flow. This will prevent the dissipation of the remaining energy as heat in the stator coil; the energy could with additional circuitry be reused.

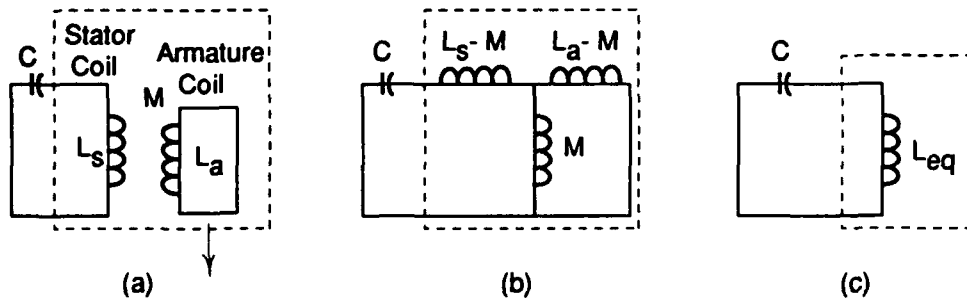


Figure 5.3 (a) Coilgun equivalent Circuit (b) T equivalent model of coilgun circuit.  $M$  is taken to be the median of the range of mutual inductance values. (c) LC equivalent circuit model of (b).

The next step is to determine the appropriate combination of inductances. The T equivalent of the lossless coilgun circuit model, figure 5-3(a), is shown in figure 5-3(b).<sup>5-7</sup> The T equivalent circuit provides an estimate of the equivalent self inductance for the circuit.

$$\begin{aligned}
 L_{eq} &= L_s - M + \frac{(L_a - M)M}{(L_a - M) + M} \\
 (5-2) \qquad &= L_s - \frac{M^2}{L_a} = L_s \left( 1 - \frac{M^2}{L_s L_a} \right)
 \end{aligned}$$

For the purpose of selecting the number of armature and stator turns, the mutual inductance is the median of the occurring values.

The self inductance of the armature and stator coils can be determined using formulas derived by Grover<sup>5-8</sup>

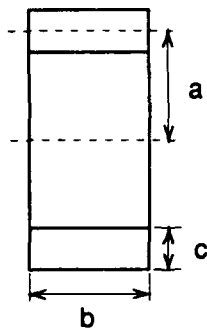


Figure 5.4 Dimensions for determining Coil Self Inductance<sup>5-8</sup>

$$(5-3) \quad L = .019739 \left( \frac{2a}{b} \right) N^2 a K' = L_o N^2$$

where,

$a$  = mean radius of the turns in cm

$b$  = axial dimension of the cross section

$c$  = radial dimension of the cross section

$N$  = number of turns

$K' = K - k$

$K$  is determined from table 36 (Grover)

$k$  is determined from tables 22 and 23 (Grover)

$L_o$  = self inductance for  $N = 1$ .

From Appendix A, the mutual inductance is

$$M = N_a N_s M_o$$

where,

$$M_o = \text{mutual inductance for } N_a, N_s = 1.$$

This yields the equivalent inductance

$$L_{eq} = N_s^2 L_{so} \left( 1 - \frac{(N_a N_s M_o)^2}{N_s^2 L_{so} N_a^2 L_{ao}} \right)$$

This expression shows that the armature reduces (or compensates) the stator coil self inductance. This results in a faster current rise time than would normally be expected of the stator self inductance in a LC circuit.

The minimum winding size that could tolerate the expected peak currents and ohmic heating for both the armature and stator windings was assumed to be 7.5 millimeters in diameter; therefore, the maximum number of armature windings was 13. To keep the armature current as low as possible (and minimize armature temperature rise), the number of armature turns was set to 13. This reduces the number of electrical variables affecting the rise time to one -- the number of stator turns. Equation (5-1) can now be used to predict the stator current rise times for various numbers of stator coil turns. Figure 5.5 shows the predicted current rise times of the equivalent circuit model for 1 to 11 stator coil turns.

The coilgun design can now be finalized. The utility of the design methodology will be put to the test by simulating the performance of the first, middle, and last stator coils. For the first stator coil, the number of turns was set at 11. The initial position of the armature center was offset 4.125 centimeters down the barrel from the stator coil center to match the estimated current rise time and the peak gradient length transit time from figures 5.2 and 5.5.

For stator coil 46, the number of turns was set to 3; this results in an estimated current rise time that is slower than the armature peak gradient length transit time, but the higher number of turns was intended to lower the stator current. The slower rise time was

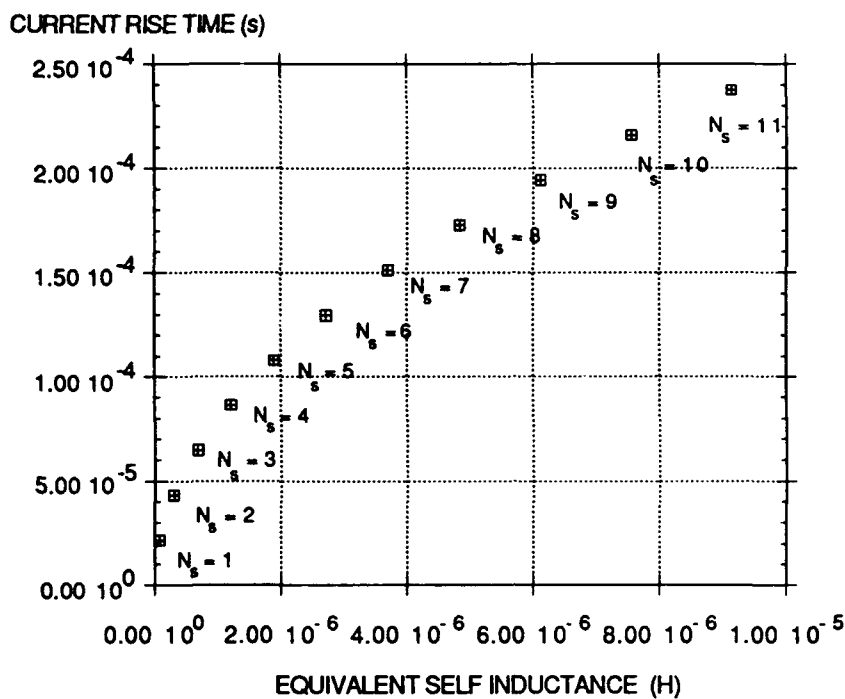


Figure 5.5 Equivalent circuit current rise time as a function of stator coil turns. Armature turns set to 13.

compensated by activating the stator coil when the armature center was offset 3.35 centimeters from the stator coil center toward the breech.

The armature peak gradient transit time for stator coil 91 is only slightly faster than that of stator coil 46; therefore, coil 91 was also set to have 3 turns. The stator coil is activated when the armature coil center is offset 5 centimeters from the stator coil center in the direction of the breech. The assumption is made that any force opposing the motion of the launch package will be small compared to the useful force gained by the large offset. The coilgun design is summarized in table 5-8 and depicted in figure 5.6

Coilgun Design Summary		
<b>Capacitor Bank</b>	<b>Armature</b>	<b>Stator</b>
Each Stator Coil 2.5 mF 20,000 V	4.9 cm outer radius 9.75 cm length 13 turns 7.5 mm thick conductor	5.0 cm inner radius 8.25 cm length 7.5 mm thick conductor coil 1 11 turns coils 46, 91 3 turns
Complete launcher 3.0 m <sup>3</sup> 4000 kg		

Table 5-8

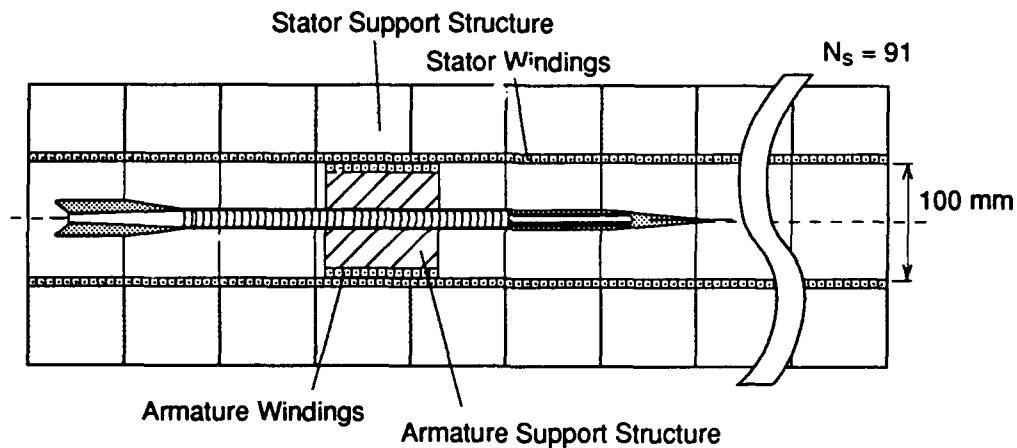


Figure 5.6 Coilgun Design. Armature, stator coils, and projectile are shown in correct proportions.

### Computer Simulation

The computer program written to evaluate the performance of the launcher solves the following system of differential equations for one armature-stator pair as illustrated in figure 5.7.

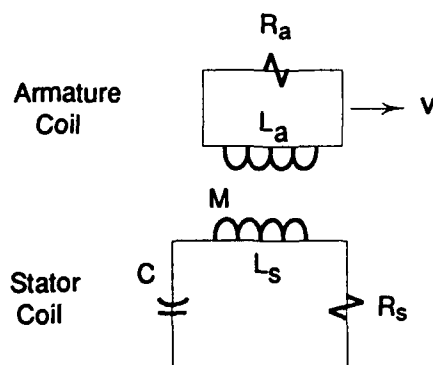


Figure 5.7 Coilgun circuit model to be evaluated.

$$V_s = I_s R_s + L_s \frac{dI_s}{dt} + M \frac{dI_a}{dt} + I_a v \frac{dM}{dz}$$

$$V_a = I_a R_a + L_a \frac{dI_a}{dt} + M \frac{dI_s}{dt} + I_s v \frac{dM}{dz}$$

$$m \frac{dv}{dt} = I_a I_s \frac{dM}{dz}$$

$$C \frac{dV_s}{dt} = I_s$$

$$V_a = 0$$

The computer code written to solve this system of equations is at Appendix B. The first, middle, and last armature-stator coil pairs were evaluated by varying the initial velocity of the armature. The initial armature velocity conditions used to simulate coils 46 and 91 were determined by rearranging equation (4-3); the initial conditions are summarized in table 5-9.

$$v = \sqrt{2az}.$$

Initial Armature Velocity		
	Position (m)	Initial Velocity (m/s)
Stator 1	0	0
Stator 46	3.7125	2111
Stator 91	7.425	2985

Table 5-9

The armature and stator coil self inductances were calculated using equation (5-3) and are summarized in table 5-10.

Armature and Stator Coil Self Inductances					
	a (cm)	b (cm)	c (cm)	N	L (μH)
Armature	4.525	9.75	.75	13	9.23
Stator 1	5.375	8.25	.75	11	9.836
Stator 46, 91	5.375	8.25	.75	3	.731

Table 5-10

The resistance of the armature and stator coil windings was determined using the expression

$$(5-6) \quad R = \frac{l}{\sigma A}$$

where,

$l$  = conductor length

$\sigma$  = conductivity

$A$  = conductor cross sectional area.

An appropriate stranded conductor would be used to minimize the affects of skin depth. The conductor length was determined using the mathematical expression for the length of a helix<sup>5-9</sup>

$$(5-7) \quad l = 2\pi N\sqrt{r^2 + \tau^2}$$

where,

$r$  = mean radius of the conductor winding

$\tau$  = coil pitch

The conductor was assumed to fill 70 percent of the cross sectional area occupied by the windings; the remaining 30 percent is occupied by insulating and structural materials. Combining equations (5-6) and (5-7), the calculated resistances are summarized in table 5-11. Based upon Grover, the insulation was assumed to have negligible affect upon the calculated inductances.<sup>5-10</sup>

Mutual inductances and mutual inductance gradients were calculated by the simulation using the method described in Appendix A. The curves are depicted in figures 5.8 and 5.12. Note that the peak

Coil Conductor Resistances					
	Mean radius (cm)	Pitch (cm)	Length (cm)	Cross sectional area +(cm <sup>2</sup> )	Resistance (mΩ)
Armature*	4.525	.75	374	.393	3.04
Stator 1**	5.375	.75	375	.393	1.59
Stator 46, 91**	5.375	2.75	113.8	1.44	.13
*Copper conductor **Beryllium conductor +Accounts for packing factor					

Table 5-11

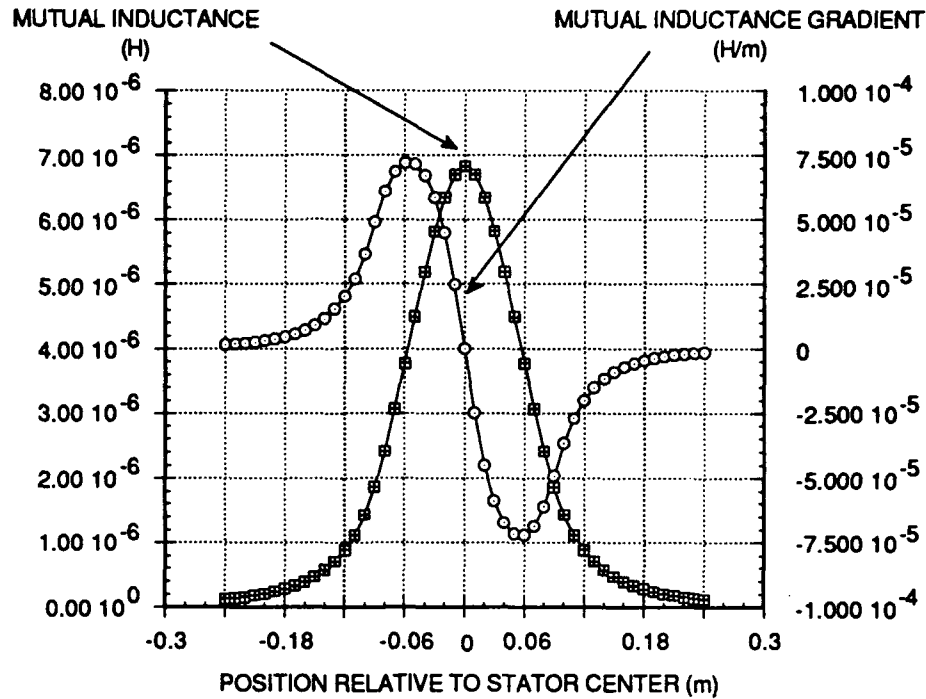


Figure 5.8 Mutual inductance and mutual inductance gradient curves for stator coil 1. ( $N_a = 13$ ,  $N_s = 11$ )

gradient length is very close to the 6 centimeter value used to calculate the armature peak gradient length transit time.

### Simulation Results Stator Coil 1

In figure 5.9, the peak force is noted to be twice the average force that was required in the initial assumptions; this indicates that the desired average force can be achieved. The peak acceleration is less than the maximum that the projectile is designed to withstand. The launch package gains substantial velocity in the first two centimeters of flight. The stator current rise time, figure 5.11, is very close to that predicted by the equivalent circuit model. The currents

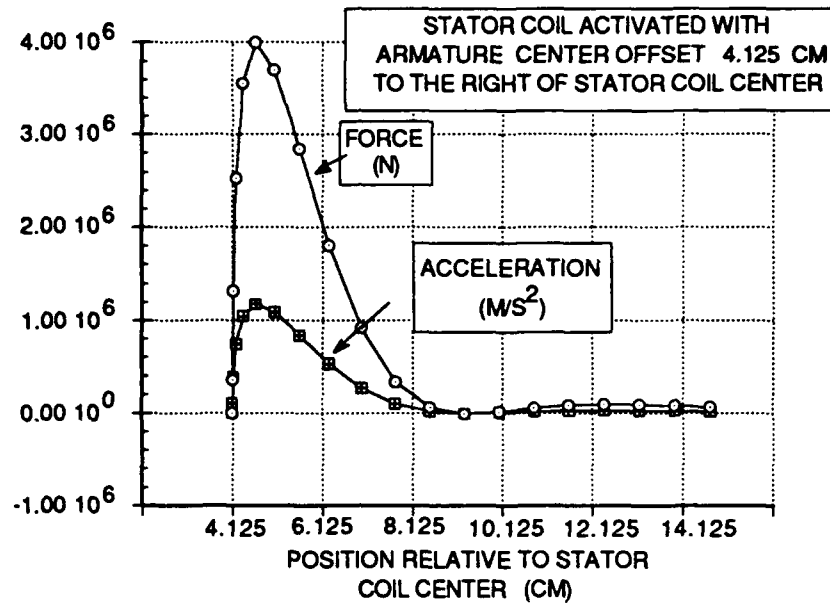


Figure 5.9 Force and acceleration stator coil 1.

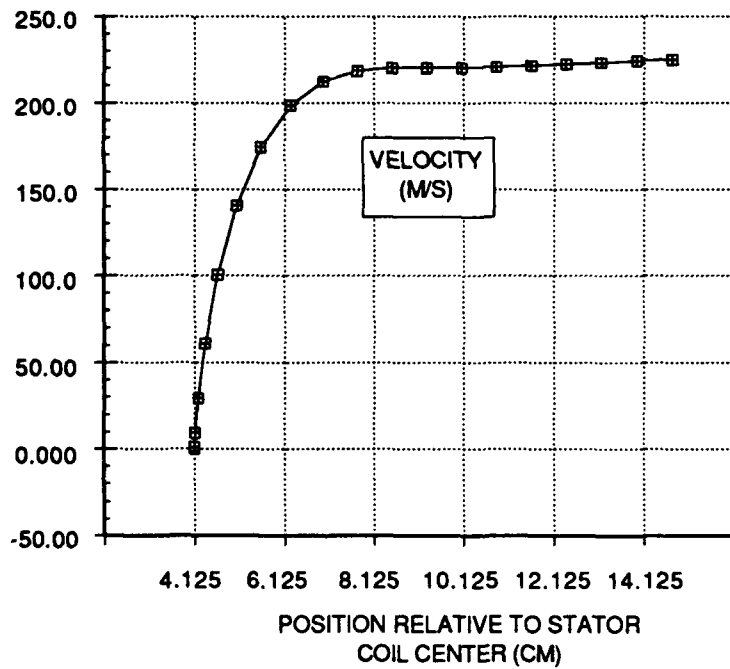


Figure 5.10 Armature velocity through stator coil 1.

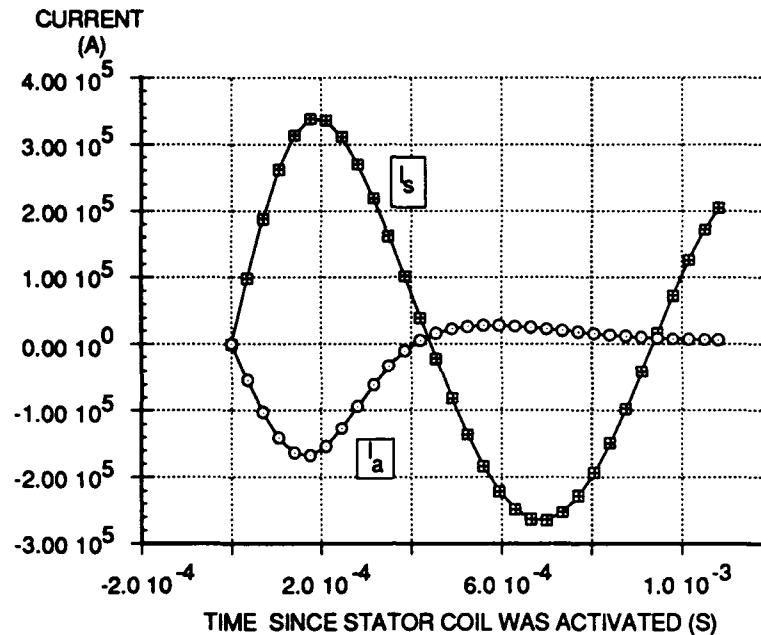


Figure 5.11 Stator and armature currents stator coil 1.

behave in the expected fashion. The current induced in the armature has the direction opposite the stator current; as expected, the induced armature current drops as the armature moves away from the stator. Although, figure 5.11 shows the current oscillating, a switch would have interrupted the current flow after the first half cycle.

#### Simulation Results Stator Coil 46

Figure 5.12 shows the mutual inductance and mutual inductance gradient for stator coils 46 and 91. The peak force on the armature as it passes through coil 46 (figure 5.13) again exceeds the required average force. The figure also shows a small negative force resulting from the offset position of the armature when the stator coil was activated. The change in armature velocity, figure 5.14, is much

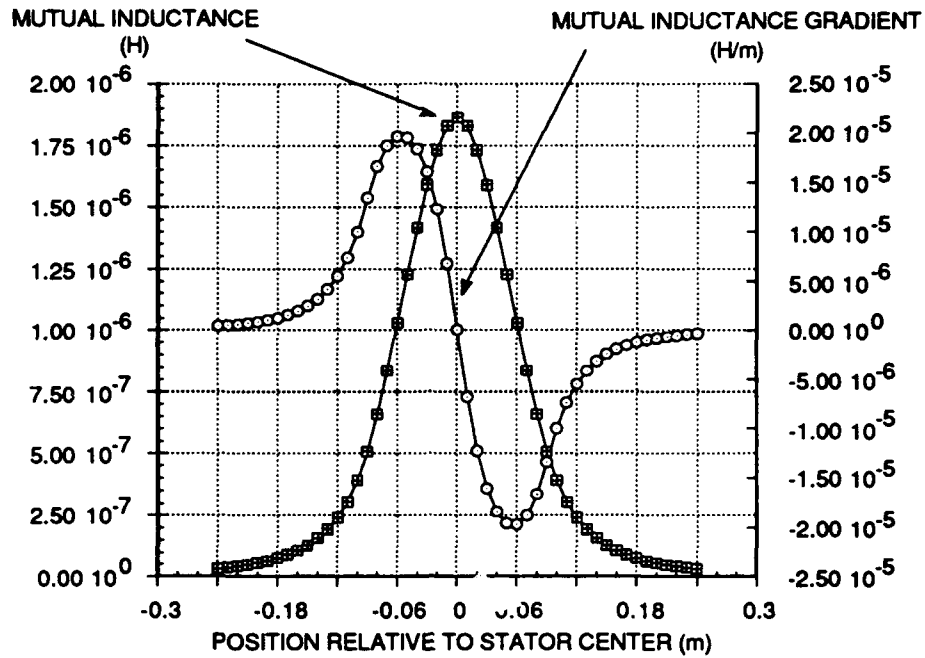


Figure 5.12 Mutual inductance and mutual inductance gradient curves for stator coils 46 and 91. ( $N_a = 13, N_s = 3$ )

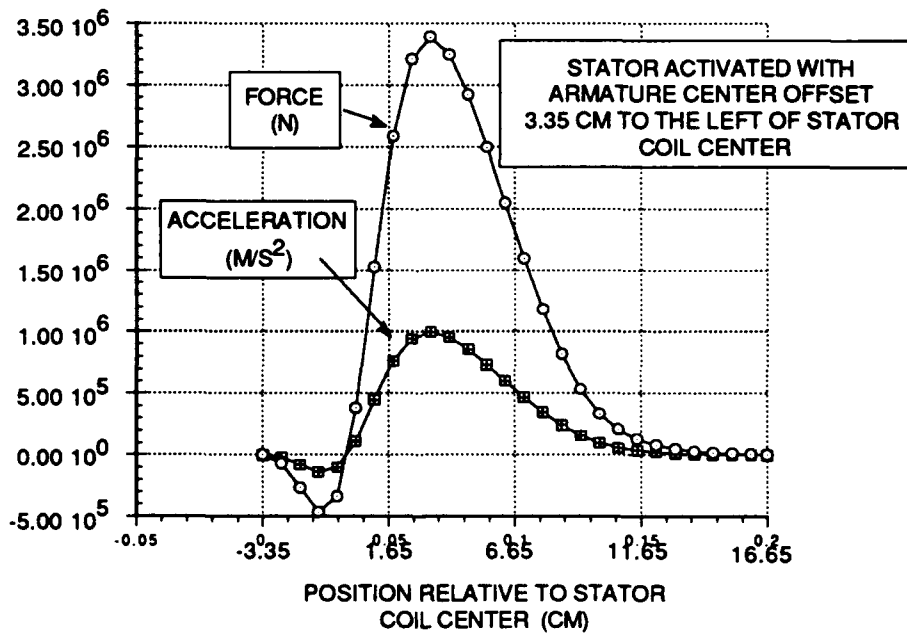


Figure 5.13 Force and acceleration stator coil 46.

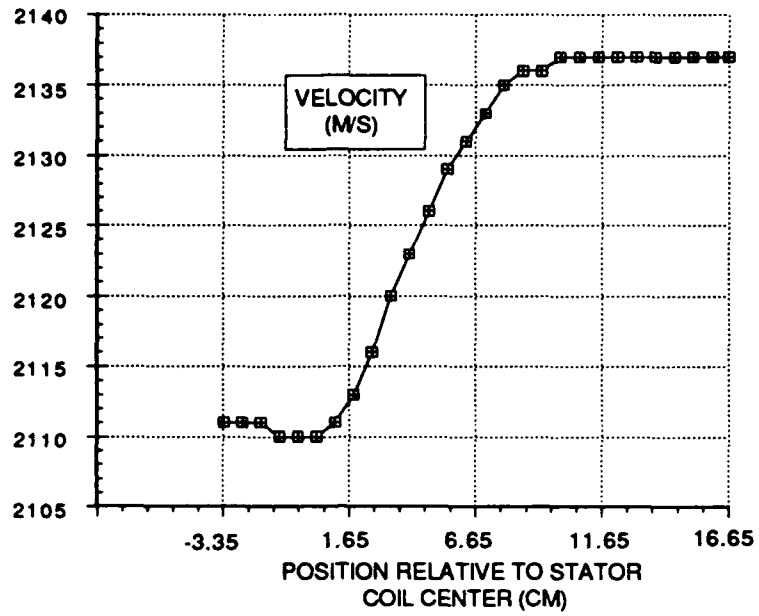


Figure 5.14 Armature velocity through stator coil 46.

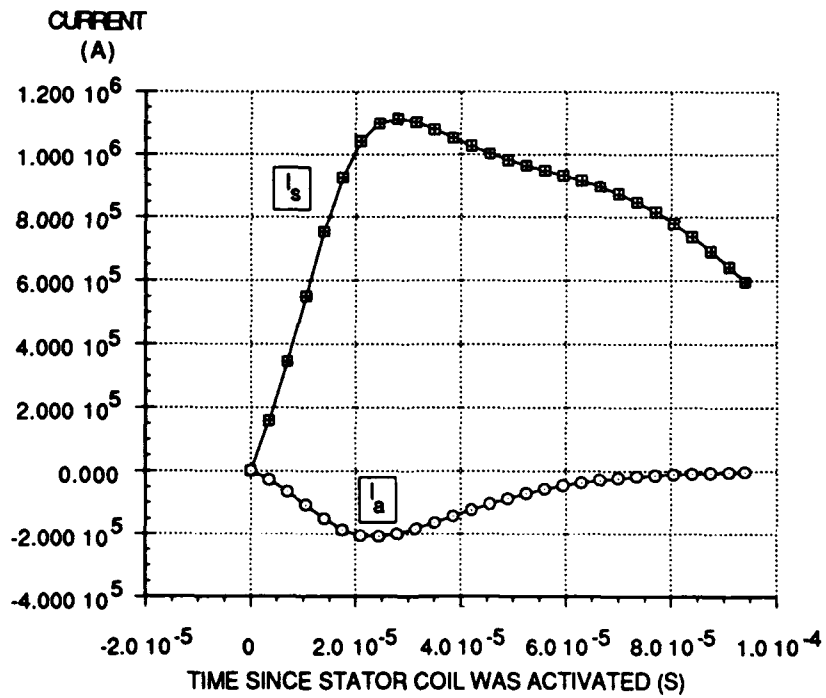


Figure 5.15 Stator and armature currents stator coil 46.

less dramatic than in the first stator coil.

The armature current in figure 5.15 is about the same magnitude and shape as the armature current in figure 5.11. The stator current magnitude on the other hand increases three fold due to the lower stator coil self inductance; this is of concern with regard to the circuit switching and buswork requirements. The stator current rise time is faster than predicted because the equivalent inductance seen by the stator is lower than predicted. Due to the armature offset when the stator is activated, the mutual inductance is greater than the median value which results in increased compensation by the armature. As the armature moves rapidly away from stator coil 46, the equivalent inductance seen by the stator rapidly rises; this increases the circuit inductive time constant ( $L/R$ ) much more quickly than the current falls. The larger time constant causes the current to fall slowly compared to the rise time.

#### Simulation Results Stator Coil 91

The simulation results for stator coil 91 follow the same trend as in stator coil 46. The peak force and acceleration both exceed the required values. Again, a small negative force initially appears due the armature offset toward the breech when the stator coil is activated; the decelerating force causes the launch package to initially lose velocity. Despite this, the launch package reaches the desired velocity of 3,000 meters per second. Despite the large force, the velocity gain through this stage is only 15 meters per second.

The armature and stator currents are nearly identical to those of stator coil 46. With this coil, however, the slow drop in the stator coil current is much more pronounced. This occurs because the armature is moving away from the stator coil faster causing the equivalent

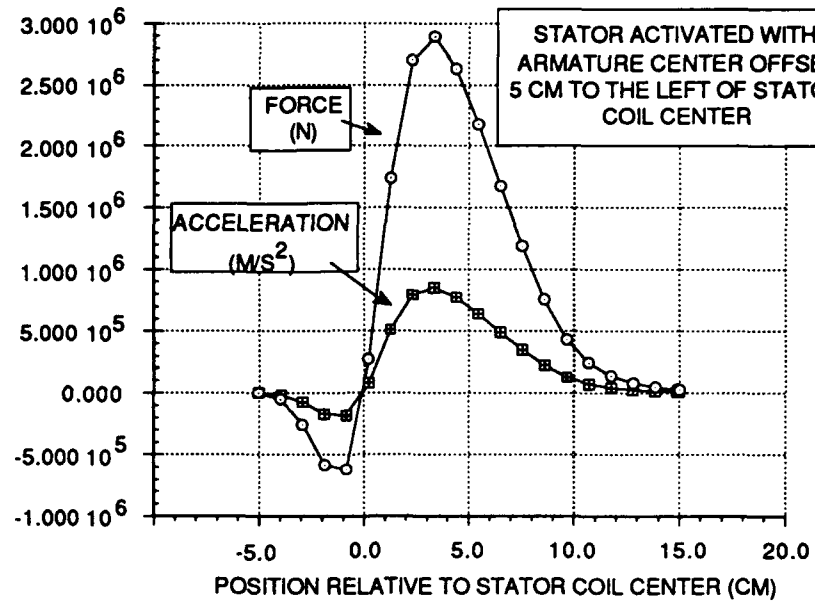


Figure 5.16 Force and acceleration stator coil 91.

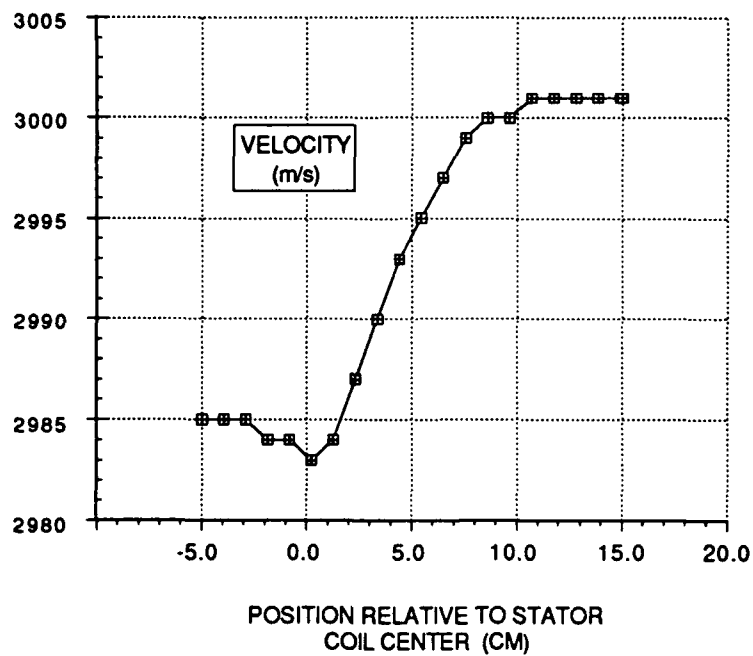


Figure 5.17 Armature velocity through stator coil 91.

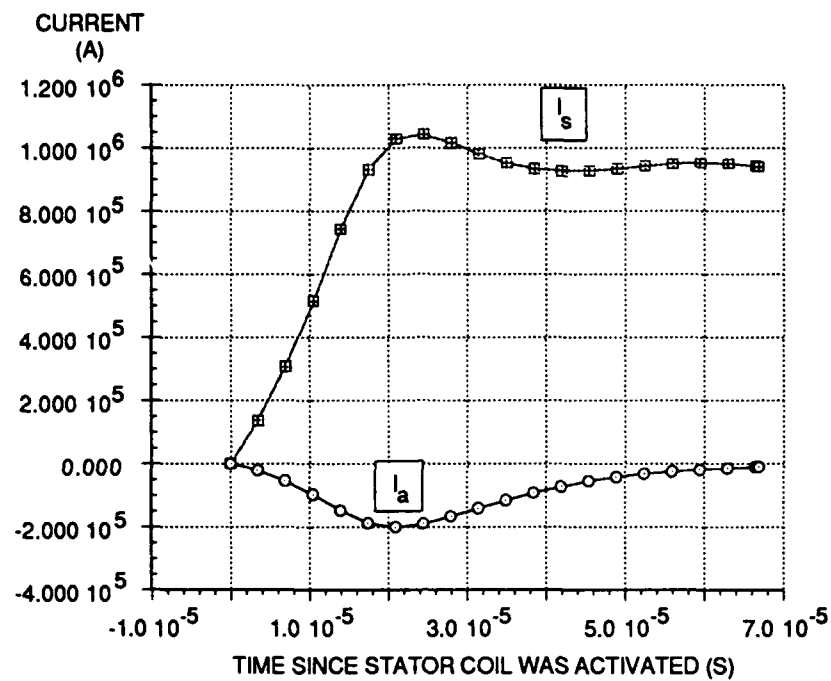


Figure 5.18 Stator and armature currents stator coil 91.

inductance seen by the stator coil to increase faster.

Conductor temperature rise can be estimated from figure 5.19. Due to the very short duration of the current pulses, the heating process is assumed to be adiabatic. The temperature change can be estimated using equations (2-18) and (2-19)

$$W_T = \int RI^2 dt$$

$$\Delta T = \frac{W_T}{C_v m}$$

Conductor masses are summarized in table 5-12. For example,

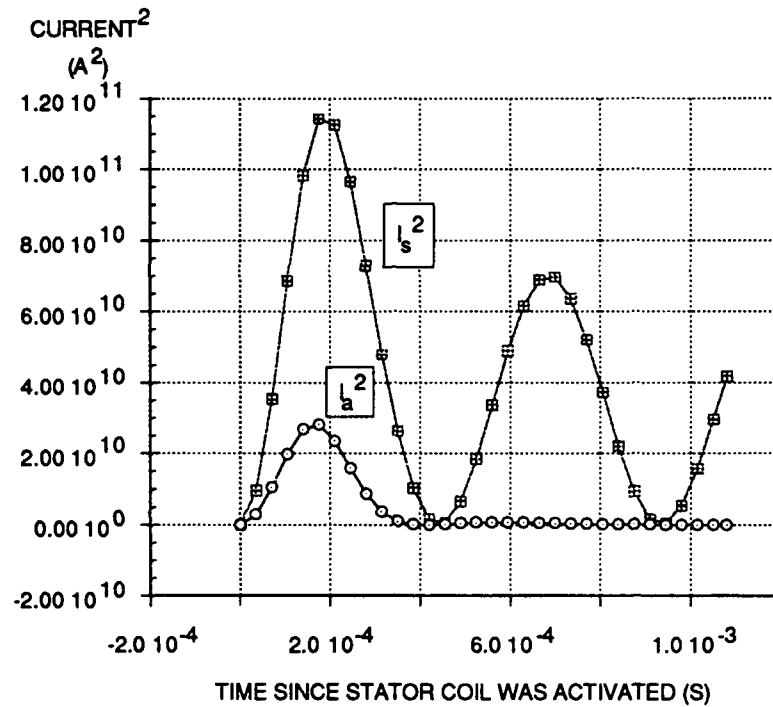


Figure 5.19 Stator and armature currents squared -- stator coil 1.

consider the temperature rise in the armature as it leaves stator coil 1

$$\begin{aligned}
 W_T &= R_a \int I_a^2 dt \cong (3.039 \times 10^{-3}) \left[ \frac{1}{2} (2.36 \times 10^{10}) (3.84 \times 10^{-4}) \right] \\
 &= 13.84 \text{ kJ}
 \end{aligned}$$

$$\begin{aligned}
 \Delta T &= \frac{W_T}{C_v m} = \frac{13.84 \text{ kJ}}{(1.8)(277.9)} \\
 &= 28.2 \text{ } ^\circ K
 \end{aligned}$$

The temperature changes of the coils are summarized in table 5-13. The temperature changes in the stator coils are quite reasonable; it

appears that several projectiles can be launched in a brief period without overheating the stator coils. The armature temperature rise is small enough that the armature will probably exit the muzzle without melting.

Coil Conductor Masses				
	Length (cm)	Cross Section (cm <sup>2</sup> )	Density (g/cm <sup>3</sup> )	Mass (g)
Armature*	374	.393	1.85	272
Stator 1**	375	.393	8.96	1,320
Stator 46, 91**	113.8	1.44	8.96	1,468
*Beryllium    **Copper				

Table 5-12

Conductor Temperature Change				
	$R \int I^2 dt$ (kJ)	$C_v$ (J/g <sup>o</sup> K)	Mass (g)	$\Delta T$ ( <sup>o</sup> K)
Armature*				
coil 1	13.8	1.8	272	28.2
coil 2	3.8	1.8	272	7.7
coil 3	3.06	1.8	272	6.2
Stator**				
coil 1	38.1	.32	1,320	75.88
coil 46	9.8	.32	1,468	17.6
*Beryllium    **Copper				

Table 5-13

At this point, the mechanical stresses on the armature and stator coils must be evaluated. A detailed evaluation of the stresses has not been performed for this example; but, an upper bound on the stress can be estimated using the long solenoid approximation discussed in chapter two. Using equation (2-20), the upper bound on the axial magnetic flux density interior to the stator coil is

$$\begin{aligned} B_{zs} &= \mu n_s I_s = (4\pi \times 10^{-7}) \left( \frac{11}{.0825} \right) (3.4 \times 10^5) \\ &= 56.9 \text{ Tesla} \end{aligned}$$

Outside the solenoid,  $B$  is non-uniform and has a much smaller value than inside the solenoid. Thus by using equation (2-3), an upper bound on the magnetic stress in the air gap between the armature and stator is

$$\begin{aligned} P &= \frac{B_{zs}^2}{2\mu} = \frac{56.9}{2(4\pi \times 10^{-7})} \\ &= 1.29 \text{ gigapascals} \\ &= 1.87 \times 10^5 \text{ pounds per square inch} \end{aligned}$$

This initial peak pressure estimate is somewhat higher than the pressures in conventional guns ( $10^5$  pounds per square inch); therefore, a more detailed analysis is needed to determine whether the barrel can sustain the launch stresses as designed. The magnetic flux densities and stresses would be analyzed using precise numerical techniques; the launcher design would be modified as necessary. Table 5-14 summarizes the estimated upper bound magnetic flux densities and stresses.

Two comments are in order with regard to the high currents. First, the gun may be overpowered. This could be determined with a more detailed computer simulation that modeled the interaction of all 91 stator coils. Such a detailed analysis might reveal that the energy discharged through each stator coil could be reduced. If the gun is not overpowered, the currents could be reduced by increasing the launcher length while retaining the same armature and stator coil design. In this way, the currents in each coil could be reduced to acceptable levels. One disadvantage of increasing the launcher length is that both the number of switches and amount of buswork are increased.

Upper Bound Radial Stress Estimates				
	n (turns per meter)	$I_s$ (A)	$B_z$ (Tesla)	$P = \frac{B^2}{2\mu}$ (psi)
Stator Coil 1	133.3	$3.4 \times 10^5$	56.9	$1.87 \times 10^5$
Stator Coil 46	36.3	$1.1 \times 10^6$	50.2	$1.45 \times 10^5$
Stator Coil 91	36.3	$1.0 \times 10^6$	45.6	$1.20 \times 10^5$

Table 5-14

The next step is to select suitable switches. The switches must conduct mega-amp currents for 40-100 microseconds, allow for current rates of change of 50 kiloamps per microsecond, and standoff 20 kilovolts. Consider the three switching devices listed in table 3-5. The ignitron is unsuitable because the mercury in the switches may not remain pooled on the cathode in all of the attitudes that a tank might have to shoot from.

The SCR is also unsuitable for this particular application. The SCR listed allows a maximum current rate of change of 100 amps per microsecond; for the switch to carry the desired current pulse, 500

parallel current paths would be required. Additionally, each current path would require four SCRs connected in series to meet the voltage standoff requirement. Given the weight and volume of the switch CEM developed using 288 SCRs, it is clear that 91 switches each consisting of 2,000 SCRs is out of the question.

The spark gap switch listed exceeds the current rate of change and voltage standoff requirements for the switch; although, four spark gaps in parallel would be required for each switch to meet the peak current requirement. However, the pulse width of this spark gap is more than two orders of magnitude lower than the pulse width of the waveform. Spark gaps have a reputation for having a wide range of parameter values, so this problem may be solvable. Table 5-15 shows that although the spark gap has several attractive characteristics, it does not meet weight and volume constraints.

We see that switching is indeed a critical EML task that cannot be taken lightly. The switching requirements for this launcher exceed existing technology. As with capacitor technology, switch technology must improve by at least an order of magnitude to bring this system to reality. Thus, the launcher must either be redesigned to use existing technology or shelved until technology advances.

Estimated Switch Requirements					
	Spark gaps per switch	Volume per switch (m <sup>3</sup> )	Weight per switch (kg)	Total volume 91 switches (m <sup>3</sup> )	Total weight 91 switches (kg)
Sparkgap	4	.196*	23.2*	17.9	8,500
*Sparkgap plus trigger device.					

Table 5-15

Next, the engineer must consider buswork design; in this case, the designer faces several challenges. The conducting cables must have a large conductor cross-section to safely carry mega-amp peak currents and substantial insulation to standoff 20 kilovolt potentials. Due to its size, the switching system must be mounted on the tank chassis; therefore, the buswork must be routed along the barrel to each of the stator coils. By necessity, many of the cables will be close to 10 meters long; this conflicts with the ideal situation in which the cables are short to minimize resistance and self inductance. The mutual inductance between adjacent conductors routed along the length of the barrel must be designed to minimize its affects on launcher performance. Finally, the buswork must meet the imposed weight and volume constraints.

The final step in the methodology is to perform an overall analysis of the system design to insure that the mission profile and constraints are met. If the criteria are satisfied, the engineer can begin detailed system design. If they are not met, the selection process must be iterated until a satisfactory design is attained.

The application of the EML selection methodology to mission 7 demonstrates the usefulness of the methodology. First, the methodology produced an EML that according to simulation meets the system requirement of launching a 1.7 kilogram projectile at a 3 kilometer per second muzzle velocity. Second, this example demonstrated that the methodology is useful for evaluating the technology requirements for a particular mission and EML system design. In this particular instance, critical power supply and switching technology deficiencies were identified.

## Chapter 6

### CONCLUSIONS AND RECOMMENDATIONS

This thesis has proposed a methodology for selecting an electromagnetic launcher based upon mission requirement and available technology. The intent of the study was twofold. First, it reviewed EML applications, the principles of electromagnetic launch, and major EML system components. The review revealed a wide range of potential EML applications and many divergent system concepts. Second, the study sought to outline a systematic procedure for selecting an EML system appropriate for a given mission. The resulting methodology can be used either to select the best launcher given existing technology or to project system technology requirements for future launch systems. The methodology is a flexible tool because it provides a general thought process; the designer must supplement it with his engineering judgment and ingenuity to select a credible EML system. The specific details of component and system analysis are left to the engineer; he is best able to select appropriate analytical techniques for his particular problem.

In chapter 5, the methodology was applied to the problem of selecting a high performance tank gun. The example showed that the selected coilgun system could not be implemented with present technology. Current capacitor and switch technologies fell short of the system requirements; this illustrates the importance of power supply and switch technology to high performance electromagnetic launchers. The methodology was then used to project the technology levels necessary to implement the launcher. Having assumed that the

projected technology levels were achievable, computer simulation showed that the required acceleration and muzzle velocity could be achieved.

The example also demonstrated the flexibility of the methodology which provided a general procedure for approaching the problem while specific techniques to determine component parameters were left to the designer. Thus, the designer was able to select the analytical techniques appropriate for the launcher concept under consideration. Thus, the usefulness of the methodology is not affected by the specific state of current or future technology.

The simulation of the selected EML system is a critical and often times difficult aspect of applying the methodology. The exact form of the simulation depends strongly upon the power supply selected to drive the system, so the simulation must be tailored to the system being investigated. The simulation conducted as part of the example showed that a simple first order simulation can provide useful information about EML system behavior; although, more detailed simulations will be required for detailed design.

Several aspects of the methodology warrant further investigation or refinement. First, the effects of launcher scale on railgun and coilgun performance merits study. This was one of two criteria proposed for determining whether a railgun or a coilgun should be chosen as the launcher; the other criteria being whether barrel wear was negligible so that consistent launcher performance and long barrel life could be achieved. Guidelines addressing the tradeoffs between launcher scale and performance would be a helpful in selecting the appropriate launcher; this is especially important if there is a range of launcher sizes for which one or the other launcher is clearly superior.

The methodology can be also be improved with the inclusion of guidelines for optimizing armature design to launcher performance. There are many trade-offs that must be considered in armature design.

In the example application, the optimum relationship between armature diameter and length was unknown; this will affect armature stability in the bore. Other uncertainties include the appropriate size for the armature interface with the projectile and aerodynamic shape of the armature. General guidelines for resolving these and similar unknowns of armature design would be helpful in launcher design.

This study showed the importance of switches to EML performance and identified several important criteria for selecting switches. But the review of switch technology did not reveal a clearly superior switch or group of switches for EML applications. The problem of selecting appropriate switches warrants further study so that the capabilities and limitations of the various switch technologies are more clearly understood. The results of such a study may also reveal critical technology shortfalls that need to be systematically addressed.

Electromagnetic launchers are extremely complex systems; consequently, the process of selecting and designing them is also complex. Hopefully, this methodology will be a useful tool for systematically considering the complexities of EML system selection.

## Appendix A

### MUTUAL INDUCTANCE OF FINITE COAXIAL COILS

As discussed in chapter 2, the mutual inductance and mutual inductance gradient can be computed using multiple filamentary elements. The method is described in Grover's Inductance Calculations. Consider the coil shown in figure A.1(a). A first order approximation of the mutual inductance can be obtained by computing mutual inductance of the central filaments of the two coils using equation (2-15)

$$M_{ij} = \frac{2\mu}{k} \sqrt{r_a r_s} \left[ \left( 1 - \frac{k^2}{2} \right) K(k) - E(k) \right]$$

where,

$$k = \sqrt{\frac{4r_a r_s}{(r_a + r_s)^2 + z^2}}$$

- $K(k)$  = complete elliptic integral of the first kind
- $E(k)$  = complete elliptic integral of the second kind
- $r_a$  = armature filament radius
- $r_s$  = stator filament radius. <sup>2-20</sup>

The mutual inductance is

$$M = N_a N_s M_{12}$$

where,

$$M_{12} = \text{mutual inductance between filaments 1 and 2.}$$

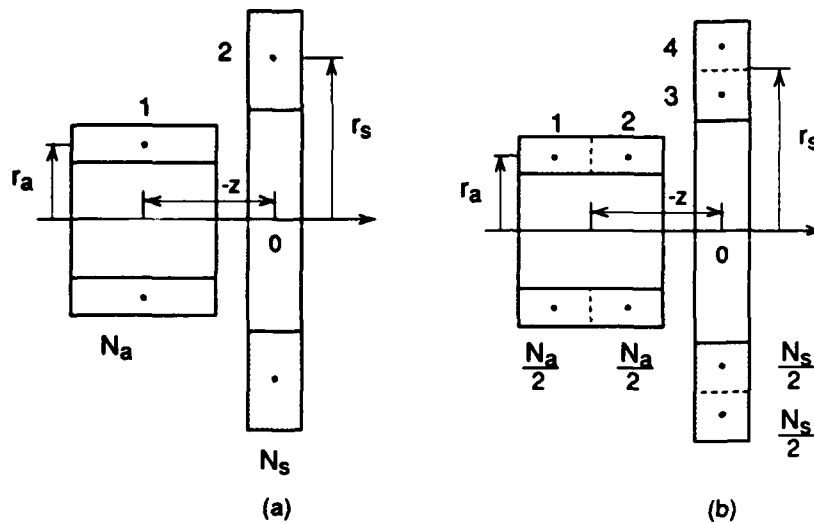


Figure A.1A-1 (a) Coil geometry showing central filaments used for a first order estimate of mutual inductance and mutual inductance gradient. (b) Diagram showing additional filaments being used to increase the computational accuracy.

The accuracy of the computed mutual inductance can be improved by increasing the number of filaments in the coil geometry; the filaments are imaginary and do not necessarily correspond to physical wires. The same computational procedure can be applied to the mutual inductance gradient using equation (2-16).

$$\frac{\partial M_{ij}}{\partial z} = \frac{\mu k z}{4(1-k^2)\sqrt{r_a r_s}} \left[ 2(1-k^2)K(k) - (2-k^2)E(k) \right]$$

In figure A.1(b), the cross section of each coil is split in half and assigned a filament; half of the coil turns are assigned to each filament. The mutual inductance is<sup>A-1</sup>

$$\begin{aligned}
 M &= \frac{N_a}{2} \frac{N_s}{2} (M_{13} + M_{14}) + \frac{N_a}{2} \frac{N_s}{2} (M_{23} + M_{24}) \\
 &= N_a N_s \frac{(M_{13} + M_{14} + M_{23} + M_{24})}{4} = N_a N_s M_o
 \end{aligned}$$

where,

$M_o$  = average of the mutual inductances between each filaments in the two coils.

The coil can be sub-divided as many times as desired to provide the desired accuracy. The mutual inductance in general is computed using the expression

$$M = N_a N_s \frac{\sum_{i=1}^{N_{fs}} \sum_{j=1}^{N_{fa}} M_{ij}}{N_{fs} N_{fa}} = N_a N_s M_o$$

where,

$N_{fs}, N_{fa}$  = number of filaments assigned to the armature, stator

In the example in chapter 5, the number of filaments to be assigned was determined by examining the behavior of the mutual inductance and mutual inductance gradient curves as the number of filaments was increased. Figure A.2 shows the coil geometry of the armature and stator coil 1. The coil geometry was divided into 7.5 millimeter square cross sections with at least one filament assigned to each cross section. The mutual inductance and mutual inductance gradients were calculated with the number of filaments assigned to each square cross section varying from  $1^2$  to  $7^2$ . The resulting curves are shown in figures A.3 and A.4. The number of filaments in each

cross section was chosen to be  $3^2$  to balance accurate computational values and the computational demands of larger numbers of filaments.

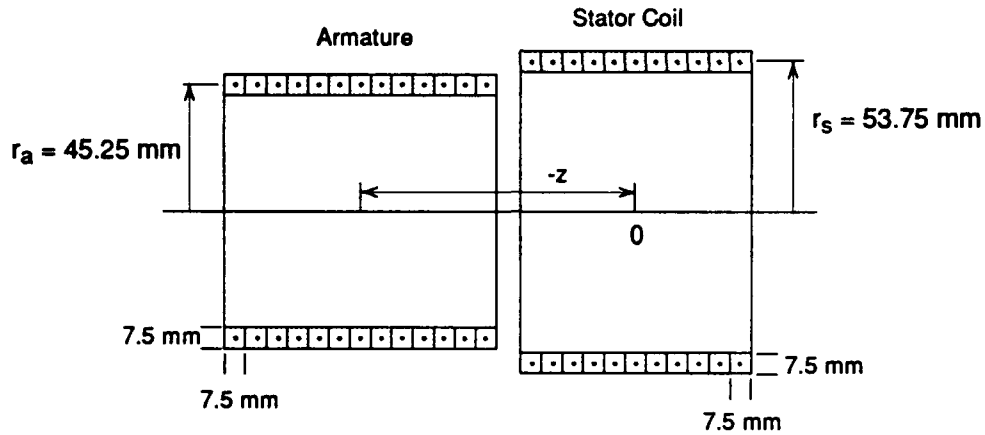


Figure A.2 Coil geometry for stator coil 1 of example in chapter 5. This figure shows 1 filament per square cross sectional area.

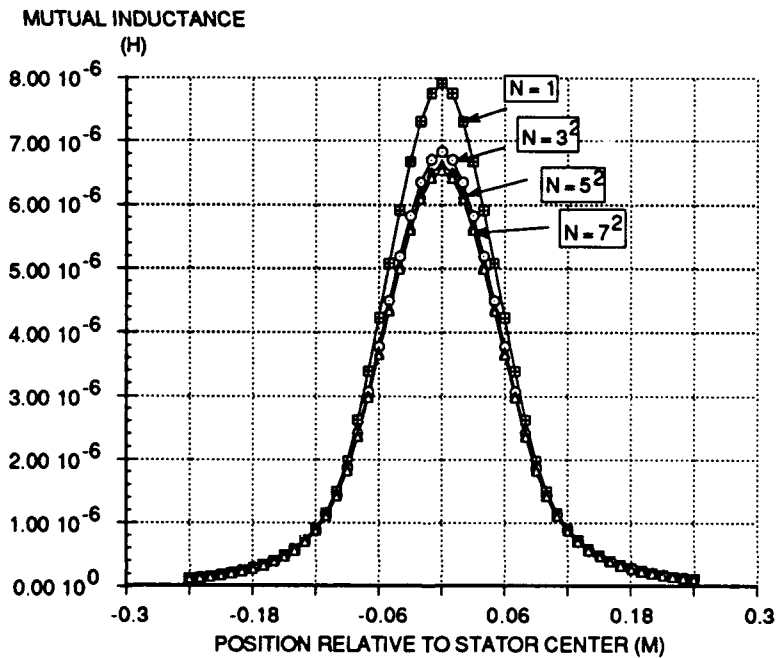


Figure A.3 Mutual Inductance computed with different numbers of filaments assigned to each square cross section. For the simulation the number of filaments per square cross section was set at 9.

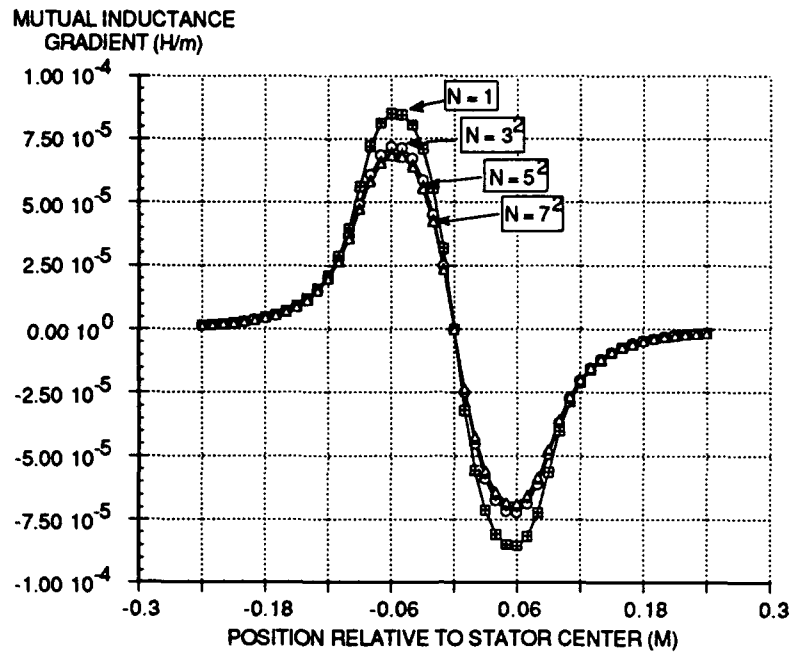


Figure A.4 Mutual inductance gradient computed with the indicated numbers of filaments assigned to each square cross section. For the simulation the number of filaments per square cross section was set at 9.

## Appendix B

### COILGUN COMPUTER SIMULATION

This appendix contains all of the computer code written to simulate the coilgun in chapter 5. The code was run on the University of Texas at Austin Cray computer. B-1, B-2, B-3

```
PROGRAM COILGUN
DIMENSION X(20),F(20)
COMMON/BLK1/RS,RA,AL,ALARM,AMUTL,CAP,AMASS,
*      DMDX,V0
COMMON/BLK2/W0,WMAG1,WMAG2,WCAP,WMV2,
*      WMAMU,PACC,VI
COMMON/MISC/TF,DT,DTMAX,IP,N
COMMON/BLK3/RADA,RADS,STATR,STATC,ARMR,ARMC,
*      INCRA,INCRS,NUM1,N2,COILCTR
REAL INCRA,INCRS,NUM1,N2

C***** START INPUT PARAMETERS *****
C   RS      is stator coil resistance
C   RA      is armature wdg resistance
C   AL      is stator coil self inductance
C   ALARM   is armature wdg self inductance
C   CAP     is capacitor connected to stator coil
C   AMASS   is mass of projectile
C   AMUTL   is the mutual between armature & stator
C   DMDX    is the mutual gradient
C   V0     is the initial voltage on capacitor
C   VI     is the initial velocity of armature
C*****
```

C\*\*\*\*\* VARIABLE DEFINITIONS \*\*\*\*\*

C X(1) is the current in the stator wdg  
 C X(2) the current in the armature wdg  
 C X(3) is the cap voltage  
 C WCAP is the 'current' capacitor energy  
 C W0 is initial stored enegy  
 C WMAG1 is mag.energy stored in stator coil  
 C WMAG2 s mag.energy stored in armature coil  
 C X(4) is the resisitive loss in the stator  
 C X(5) is the resisitive loss in the armature  
 C X(6) is velocity of the armature  
 C X(7) is the distance travelled by armature  
 C PACC is the acceleration of the armature  
 C WMV2 is the kinetic energy of armature

C\*\*\*\*\*

C STAT is the number of stator columns  
 C ARM is the number of armature columns  
 C N1 is the number of armature turns  
 C N2 is the number of stator turns  
 C COILCTR is the initial offset position of the armature  
 C RADA is the radius to the outer filament row of armature  
 C RADS is the radius to the inner filament row of the stator  
 C STATR is the number of stator filament rows  
 C STATC is the number of stator filament columns  
 C ARMR is the number of armature filament rows  
 C ARMC is the number of armature filament columns  
 C INCRA is the increment between armature filaments  
 C INCRS is the increment between stator filaments

C\*\*\*\*\*

```
C*****  
OPEN(UNIT=10,FILE='SCROUT',FORM='FORMATTED')  
OPEN(UNIT=8,FILE='MUTUAL',FORM='FORMATTED')
```

```
C***** INPUT PARAMETERS *****
```

```
VI=0.  
RS= 1.598E-3  
AL=9.836E-6  
RA=3.0390E-3  
ALARM=9.23E-6  
CAP=2.50E-3  
V0=20.0E3  
AMASS=3.4  
  
STAT = 11.  
ARM = 13.  
COILCTR = -.04125  
RADA = .04525  
RADS = .05375  
STATR = 3.  
STATC = 3. * STAT  
ARMR = 3.  
ARMC = 3. * ARM  
INCRA = .0025  
INCRS = .0025  
NUM1 = STAT  
N2 = ARM
```

C\*\*\* DO NOT INCLUDE INPUT PARAMETERS BELOW THIS LINE\*\*

```
      DO 10 KK=1,20
      X(KK)=0.0
      F(KK)=0.0
10    CONTINUE
      X(6)=VI
      X(3)=V0
      W0=0.5*CAP*X(3)*X(3)
      WCAP=0.0
      WMAG1=0.0
      WMAG2=0.0
      WMV2=0.0
```

```
      N=20
      T=0.0
      DT=5.0E-6
      IP=7
      DTMAX=1.0*DT
      DTT=DT
```

C\*\*\*\*\* TF IS THE TIME LIMIT ON THE SIMULATION \*\*\*\*\*

```
      TF=1.5E-3
```

C\*\*\*\*\* CALL THE SOLVER \*\*\*\*\*

```
      CALL RK78RG(T,X)
      END
```

C\*\*\*\*\*

C\*\*\*\*\*

```

SUBROUTINE PROUT(T,X,F)
DIMENSION X(20),F(20)
COMMON/BLK1/RS,RA,AL,ALARM,AMUTL,CAP,AMASS,
*      DMDX,V0
COMMON/BLK2/W0,WMAG1,WMAG2,WCAP,WMV2,
*      WMAMU,PACC,VI
COMMON/MISC/TF,DT,DTMAX,IP,N

```

```

WM=WMAMU+WMAG1+WMAG2
RLOSS=X(4)+X(5)
FORCE = AMASS * PACC
EBAL=W0-WCAP-WMAG1-WMAG2-WMV2-X(4)-X(5)-WMAMU

```

```

WRITE(8,145) T,X(7),X(6),PACC,FORCE,AMUTL,DMDX
WRITE(10,145)T,X(1),X(1)**2,X(2),X(2)**2,PACC,EBAL
WRITE(10,145)W0,WCAP,WM,RLOSS,WMV2,EBAL

```

145 FORMAT(7(1X,E10.4))

```

RETURN
END

```

C\*\*\*\*\*

C\*\*\*\*\*

```

SUBROUTINE DERIVS(T,X,F)
DIMENSION X(20),F(20)
DIMENSION ALIND(2,2),BERI(2),AX(2)
COMMON/BLK1/RS,RA,AL,ALARM,AMUTL,CAP,AMASS,
*      DMDX,V0
COMMON/BLK2/W0,WMAG1,WMAG2,WCAP,WMV2,
*      WMAMU,PACC,VI
COMMON/MISC/TF,DT,DTMAX,IP,N

```

```

C***** CALL SUBROUTINE AMUTUAL TO COMPUTE MUTUAL
C
S=X(7)
CALL AMUTUAL(S,AMUTL1,DMDX1)
AMUTL=AMUTL1
DMDX=DMDX1
C*****
ALIND(1,1)=AL
ALIND(1,2)=AMUTL
ALIND(2,1)=ALIND(1,2)
ALIND(2,2)=ALARM

BERI(1)=X(3)-X(1)*RS-DMDX*X(2)*X(6)
BERI(2)=-X(2)*RA-DMDX*X(1)*X(6)

CALL LSLRG(2,ALIND,2,BERI,1,AX)

F(1)=AX(1)
F(2)=AX(2)

F(3)=(-1.0/CAP)*X(1)

PACC=(1.0/AMASS)*(X(1)*X(2)*DMDX)

F(7)=X(6)

F(6)=PACC

F(4)=X(1)*X(1)*RS
F(5)=X(2)*X(2)*RA

WMAG1=0.5*AL*X(1)*X(1)

```

WMAG2=0.5\*ALARM\*X(2)\*X(2)

WCAP=0.5\*CAP\*X(3)\*X(3)

WMV2=0.5\*AMASS\*X(6)\*X(6)

WMAMU=X(2)\*X(1)\*AMUTL

RETURN

END

C\*\*\*\*\*

C\*\*\*\*\*

C SUBROUTINE AMUTUAL

C Program determines mutual inductance between

C two coaxial circular coils as a function

C of axial position for a series of positions along the axis

C\*\*\*\*\*

SUBROUTINE AMUTUAL(S,AMUTL1,DMDX1)

COMMON/BLK3/RADA,RADS,STATR,STATC,ARMR,

\* ARMC,INCRA,INCRS,NUM1,N2,COILCTR

PARAMETER (PI = 3.141592)

REAL MM,MMGRAD,MUT,K,MU,NUM1,N2,M,

\* MGRAD,INCRA,INCRS,FILS

REAL I,J,L,N,X,XX,RA,RS,RAA,RSS

RA = RADA

RS = RADS

A = AINT(STATC/2.)

B = AINT(STATR - 1.)

C = AINT(ARMC/2.)

D = AINT(ARMR - 1.)

FILS = STATR \*STATC \*ARMR \*ARMC

MU = 4.\*PI\*1E-7

M = 0.

MGRAD = 0.

DO 20 L = 0., D,1.

DO 30 J = 0., B,1.

DO 40 N = -C, C,1.

DO 50 I = -A, A,1.

RAA = RA - L\*INCRA

RSS = RS + J\*INCRS

XX = XL + I\*INCRS + N\*INCRA

K = ((4.\*RAA\*RSS)/(XX\*\*2 + (RAA + RSS)\*\*2))\*\*.5

QQC = (1. - K\*\*2)\*\*.5

BB = 1.

ELPTCK = CEL(QQC, 1., 1., BB)

BB = QQC\*\*2.

ELPTCE = CEL(QQC, 1.,1., BB)

```
MM=(2.*MU/K)*SQRT(RAA*RSS)*((1.-.5*K**2.)*ELPTCK -  
* ELPTCE)
```

```
COEFF=(MU*K*XX)/(4.*(1.-K**2)*(RAA*RSS)**.5)  
MMGRAD=COEFF*((2.*(1.-K**2)*ELPTCK)-((2.-K**2)*ELPTCE))
```

```
M = MM + M  
MGRAD = MMGRAD + MGRAD
```

```
50 CONTINUE  
40 CONTINUE  
30 CONTINUE  
20 CONTINUE
```

```
AMUTL1 = NUM1*N2*(M/FILS)  
DMDX1 = NUM1*N2*(MGRAD/FILS)
```

```
RETURN  
END
```

```
C*****
```

```

C***** FUNCTION CEL *****
C      FUNCTION TO DETERMINE ELLIPTIC INTEGRALS OF
C      FIRST AND SECOND KINDS
C*****

```

```

      FUNCTION CEL(QQC, PP, AA, BB)
      PARAMETER (CA= .0003, PIO2=1.57079632)
      IF(QQC.EQ.0.) PAUSE 'FAILURE IN CEL'
      QC=ABS(QQC)
      A = AA
      B=BB
      P=PP
      E=QC
      EM=1.
      IF(P.GT.0.)THEN
      P=SQRT(P)
      B=B/P
      ELSE
      F=QC*QC
      Q=1. -F
      G=1. -P
      F=F - P
      Q=Q*(B-A*P)
      P=SQRT(F/G)
      A=(A-B)/G
      B=-Q/(G*G*P) + A*P
      ENDIF
1      F=A
      A=A + B/P
      G=E/P
      B=B + F*G

```

```

B=B + B
P=G + P
G=EM
EM=QC + EM
IF(ABS(G-QC).GT.G*CA)THEN
QC=SQRT(E)
QC=QC + QC
E=QC*EM
GO TO 1
ENDIF
CEL= PIO2*(B + A*EM)/(EM*(EM+P))
RETURN
END

```

C\*\*\*\*\*

C\*\*\*\*\*

```

SUBROUTINE RK78RG(TX,X)
C SEVENTH ORDER RUNGE-KUTTA INTEGRATION WITH
C STEPSIZE CONTROL
C THE REFERENCE FOR THIS INTEGRATOR IS NASA TR-287
C PROGRAM MODIFIED BY RON GREENE ---1971
C PROGRAM MODIFIED BY BILL BIRD ---1977
COMMON/MISC/TF,DT,DTMAX,IP,N
DIMENSION ALPH(13),B(13,12),CH(13)
DIMENSION X(20),F(20)
DIMENSION XDUM(20)
DIMENSION F1(20),F2(20),F3(20),F4(20),F5(20),F6(20),F7(20),
1F8(20),F9(20),F10(20),F11(20),F12(20),F13(20)
EQUIVALENCE (F2,F4),(F3,F5,F11)
EQUIVALENCE(B21,B31,B41,B51,B61,B71,B81,B91,B101,B111,B121,

```

```

*      B131),(
2  B43,B53),(B64,B74,B94,B104,B114),(B65,B75,B85,B95,B105,B115),
3  (B76,B86,B96,B106,B116,B126,B136),(B87,B97,B107,B117,B137),
4  (B98,B108,B118,B128,B138),(B119,B139),(B1110,B1310)
DATA (ALPH(I),I=1,13)/
*      0 , .740740740741E-01, .111111111111E+00,
* .166666666667E+00, .416666666667E+00, .500000000000E+00,
* .833333333333E+00, .166666666667E+00, .666666666667E+00,
* .333333333333E+00, .100000000000E+01,      0 ,
* .100000000000E+01/
DATA (B(I),I=1,54)/
*      0 , .740740740741E-01, .277777777778E-01,
* .416666666667E-01, .416666666667E+00, .500000000000E-01,
* -.231481481481E+00, .103333333333E+00, .200000000000E+01,
* -.842592592593E+00, .581219512195E+00, .146341463415E-01,
* -.433414634146E+00,      0 ,      0 ,
* .833333333333E-01,      0 ,      0 ,
*      0 ,      0 ,      0 ,
*      0 ,      0 ,      0 ,
*      0 ,      0 ,      0 ,
*      0 ,      0 , .125000000000E+00,
* -.156250000000E+01,      0 ,      0 ,
*      0 ,      0 ,      0 ,
*      0 ,      0 ,      0 ,
*      0 ,      0 ,      0 ,
*      0 , .156250000000E+01, .250000000000E+00,
* .115740740741E+01,      0 , -.883333333333E+01,
* .212962962963E+00, -.207926829268E+01,      0 ,
* -.207926829268E+01,      0 ,      0 /
DATA (B(I),I=55,108)/
*      0 ,      0 ,      0 ,
* .200000000000E+00, -.240740740741E+01, .271111111111E+00,

```



```

*      0 ,      0 , .100000000000E+01/

*      0 ,      0 ,      0 ,
*      0 ,      0 , .323809523810E+00,
* .257142857143E+00, .257142857143E+00, .321428571429E-01,
* .321428571429E-01,      0 , .488095238095E-01,
* .488095238095E-01/
DATA N,ERPS,TOL,TOLT/20,1.E-12,1.E-05,1.E-06/
C 4 FEB 77 VERSION
T=TX
IS=0
IR=0
9  IF(ABS(DT).GE.ABS(TF-T)) DT=TF-T
    IF(MOD(IS,IP).NE.0) GO TO 888
    CALL DERIVS(T,X,F)
    CALL PROUT(T,X,F)
888 DO 20 I=1,N
20  XDUM(I)=X(I)
    TS=T+ALPH( 1)*DT
    CALL DERIVS(TS,X,F1)
30  CONTINUE
    B21=B(2,1)*DT
    TS=T+ALPH( 2)*DT
    DO 42 I=1,N
42  X(I)=B21*F1(I) + XDUM(I)
    CALL DERIVS(TS,X,F2)
    B31=B(3,1)*DT
    B32=B(3,2)*DT
    TS=T+ALPH( 3)*DT
    DO 43 I=1,N
43  X(I)=B31*F1(I) + B32*F2(I) + XDUM(I)
    CALL DERIVS(TS,X,F3)

```

```
B41=B(4,1)*DT
TS=T+ALPH( 4)*DT
DO 44 I=1,N
44  X(I)=B41*F1(I) + B43*F3(I) + XDUM(I)
    CALL DERIVS(TS,X,F4)
    B51=B(5,1)*DT
    B53=B(5,3)*DT
    TS=T+ALPH( 5)*DT
    DO 45 I=1,N
45  X(I)=B51*F1(I) + B53*(F3(I) - F4(I)) + XDUM(I)
    CALL DERIVS(TS,X,F5)
    B61=B(6,1)*DT
    B64=B(6,4)*DT
    B65=B(6,5)*DT
    TS=T+ALPH( 6)*DT
    DO 46 I=1,N
46  X(I)=B61*F1(I) + B64*F4(I) + B65*F5(I) + XDUM(I)
    CALL DERIVS(TS,X,F6)
    B71=B(7,1)*DT
    B74=B(7,4)*DT
    B75=B(7,5)*DT
    B76=B(7,6)*DT
    TS=T+ALPH( 7)*DT
    DO 47 I=1,N
47  X(I)=B71*F1(I) + B74*F4(I) + B76*F6(I) + B75*F5(I) + XDUM(I)
    CALL DERIVS(TS,X,F7)
    B81=B(8,1)*DT
    B85=B(8,5)*DT
    B86=B(8,6)*DT
    B87=B(8,7)*DT
    TS=T+ALPH( 8)*DT
    DO 48 I=1,N
```

```

48  X(I)=B87*F7(I) + B81*F1(I) + B86*F6(I) + B85*F5(I) + XDUM(I)
    CALL DERIVS(TS,X,F8)
    B91=B(9,1)*DT
    B94=B(9,4)*DT
    B95=B(9,5)*DT
    B96=B(9,6)*DT
    B97=B(9,7)*DT
    B98=B(9,8)*DT
    TS=T+ALPH( 9)*DT
    DO 49 I=1,N
49  X(I)=B97*F7(I) + B91*F1(I) + B98*F8(I) + B94*F4(I) + B96*F6(I)
    1  + B95*F5(I) + XDUM(I)
    CALL DERIVS(TS,X,F9)
    B101=B(10,1)*DT
    B104=B(10,4)*DT
    B105=B(10,5)*DT
    B106=B(10,6)*DT
    B107=B(10,7)*DT
    B108=B(10,8)*DT
    DO 50 I=1,N
50  X(I)=-B32*F9(I) + B104*F4(I) + B107*F7(I) + B101*F1(I) + B108*F8(I)
    *   1) + B106*F6(I) + B105*F5(I) + XDUM(I)
    CALL DERIVS(TS,X,F10)
    B111=B(11,1)*DT
    B114=B(11,4)*DT
    B115=B(11,5)*DT
    B116=B(11,6)*DT
    B117=B(11,7)*DT
    B118=B(11,8)*DT
    B119=B(11,9)*DT
    B1110=B(11,10)*DT
    TS=T+ALPH(11)*DT

```

```

DO 51 I=1,N
F4(I)=B114*F4(I)+B115*F5(I)
51 X(I)=B119*F9(I) + B1110*F10(I) + B117*F7(I) + B118*F8(I)
1   +B111*F1(I)+F4(I)+B116*F6(I)+XDUM(I)
CALL DERIVS(TS,X,F11)
B121=B(12,1)*DT
B126=B(12,6)*DT
B128=B(12,8)*DT
DO 52 I=1,N
TS=T+ALPH(12)*DT
52 X(I)=B121*(F1(I) - F7(I)) + B128*(F8(I) - F9(I))
1   + B126*(F6(I) - F10(I)) + XDUM(I)
CALL DERIVS(T,X,F12)
B131=B(13,1)*DT
B136=B(13,6)*DT
B137=B(13,7)*DT
B138=B(13,8)*DT
B139=B(13,9)*DT
B1310=B(13,10)*DT
TS=T+ALPH(13)*DT
DO 53 I=1,N
53 X(I)=B139*F9(I) + B1310*F10(I) + B131*F1(I) + B137*F7(I)
1   +B138*F8(I)+F12(I)*DT+F4(I)+B136*F6(I)+XDUM(I)
CALL DERIVS(TS,X,F13)
C6=CH(6)*DT
C7=CH(7)*DT
C9=CH(9)*DT
C12=CH(12)*DT
DO 100 I=1,N
100 X(I)=XDUM(I)+(C6*F6(I)+C7*(F7(I)+F8(I))+C9*(F9(I)+F10(I))+C12*
1   (F12(I)+F13(I)))
C ESTIMATE NEW STEP SIZE

```

```
ER=0.0
DO 150 J=1,N
A=X(J)
IF(ABS(A).LT.ERPS) GO TO 150
ES=ABS((F1(J)+F11(J)-F12(J)-F13(J))/A)
IF(ES.GT.ER) ER=ES
150 CONTINUE
160 ER=ER*ABS(C12)+1.0E-20
170 DT1=DT
175 DT=TOLT/ER
DT=DT1*DT**.125
IF(DT.GT.DTMAX) DT = DTMAX
IF(ER-TOL) 7,7,8
8 IR=IR+1
GO TO 30
7 CONTINUE
C TOLERANCE IS PASSED
C CHECK VARIABLES TO MODIFY TIME STEP OR
C SWITCH CODE FLAGS
CALL XCHECK(T,X,F,DT1,ICK)
GO TO (5,8,180,21)ICK
180 CONTINUE
T=T+DT1
TIME=T
10 IF(TF-T) 5,5,6
6 IS=IS-1
GO TO 9
5 CONTINUE
CALL DERIVS(T,X,F)
CALL PROUT(T,X,F)
21 WRITE(6,22)IS,IR
22 FORMAT(/8X,I5,5X,I2)
```

```

      CALL SECOND(AA)
      WRITE(6,23)AA
23   FORMAT(* *,8X,E10.3)
      RETURN
      END

```

```

C*****
C*****
      SUBROUTINE XCHECK(T,X,F,DT1,ICK)
      DIMENSION X(20),F(20)
      COMMON/BLK1/RS,RA,AL,ALARM,AMUTL,CAP,
*           AMASS,DMDX,V0
      COMMON/BLK2/W0,WMAG1,WMAG2,WCAP,WMV2,
      WMAMU,PACC,VI
      COMMON/MISC/TF,DT,DTMAX,IP,N

      XBARR=0.2
      TP=T+DT1
      CALL DERIVS(TP,X,F)
      XXX1=(X(7)-XBARR)/XBARR
C   IF(XXX1.GE.-1.000E-03) GO TO 1
      ICK=3
      RETURN
1   IF(XXX1.GT.1.000E-03) GO TO 2
      T=T+DT1
      TIME=T
      CALL DERIVS(T,X,F)
      CALL PROUT(T,X,F)
      ICK=4
      RETURN
2   DT=DT1/2.
      ICK=2

```

```
RETURN  
CALL DERIVS(T,X,F)  
CALL PROUT(T,X,F)  
ICK=4  
RETURN  
END
```

```
C *****
```

## Appendix C

### TABULATED RESULTS

This appendix contains the tabulated simulation results for the coilgun selected in chapter 5.

Coil 1 Simulation Parameters
VI = 0.
RS = 1.598E-3
AL = 9.836E-6
RA = 3.0390E-3
ALARM = 9.23E-6
CAP = 2.50E-3
V0 = 20.0E3
AMASS = 3.4
STAT = 11.
ARM = 13.
COILCTR = -.04125
RADA = .04525
RADS = .05375
STATR = 3.
STATC = 3. * STAT
ARMR = 3.
ARMC = 3. * ARM
INCRA = .0025
INCRS = .0025
NUM1 = 11
N2 = 13
DT = 5.0E-6

Table B-1

Coil 1 Kinematic Data				
Time	Position	Velocity	Acceleration	Force
0.0000E+00	0.0000E+00	0.0000E+00	0.0000E+00	0.0000E+00
0.3500E-04	0.1106E-04	0.1255E+01	0.1060E+06	0.3605E+06
0.7000E-04	0.1701E-03	0.9478E+01	0.3863E+06	0.1313E+07
0.1050E-03	0.8104E-03	0.2921E+02	0.7437E+06	0.2529E+07
0.1400E-03	0.2356E-02	0.6089E+02	0.1046E+07	0.3557E+07
0.1750E-03	0.5165E-02	0.1004E+03	0.1176E+07	0.3998E+07
0.2100E-03	0.9392E-02	0.1406E+03	0.1088E+07	0.3699E+07
0.2450E-03	0.1494E-01	0.1746E+03	0.8366E+06	0.2844E+07
0.2800E-03	0.2150E-01	0.1986E+03	0.5313E+06	0.1806E+07
0.3150E-03	0.2871E-01	0.2123E+03	0.2696E+06	0.9167E+06
0.3500E-03	0.3627E-01	0.2185E+03	0.9866E+05	0.3354E+06
0.3850E-03	0.4396E-01	0.2203E+03	0.1744E+05	0.5928E+05
0.4200E-03	0.5168E-01	0.2204E+03	-.2839E+04	-.9652E+04
0.4550E-03	0.5939E-01	0.2204E+03	0.3752E+04	0.1276E+05
0.4900E-03	0.6711E-01	0.2208E+03	0.1548E+05	0.5263E+05
0.5250E-03	0.7485E-01	0.2215E+03	0.2388E+05	0.8119E+05
0.5600E-03	0.8261E-01	0.2224E+03	0.2725E+05	0.9264E+05
0.5950E-03	0.9041E-01	0.2233E+03	0.2649E+05	0.9007E+05
0.6300E-03	0.9825E-01	0.2242E+03	0.2318E+05	0.7880E+05
0.6650E-03	0.1061E+00	0.2249E+03	0.1873E+05	0.6368E+05
0.7000E-03	0.1140E+00	0.2255E+03	0.1416E+05	0.4816E+05
0.7350E-03	0.1219E+00	0.2259E+03	0.1008E+05	0.3426E+05
0.7700E-03	0.1298E+00	0.2262E+03	0.6736E+04	0.2290E+05
0.8050E-03	0.1377E+00	0.2264E+03	0.4193E+04	0.1426E+05
0.8400E-03	0.1457E+00	0.2265E+03	0.2373E+04	0.8067E+04
0.8750E-03	0.1536E+00	0.2266E+03	0.1143E+04	0.3885E+04
0.9100E-03	0.1615E+00	0.2266E+03	0.3589E+03	0.1220E+04
0.9450E-03	0.1694E+00	0.2266E+03	-.1099E+03	-.3738E+03
0.9800E-03	0.1774E+00	0.2266E+03	-.3700E+03	-.1258E+04
0.1015E-02	0.1853E+00	0.2266E+03	-.4998E+03	-.1699E+04
0.1050E-02	0.1932E+00	0.2266E+03	-.5528E+03	-.1880E+04
0.1080E-02	0.2000E+00	0.2266E+03	-.5626E+03	-.1913E+04

Table B-2

Coil 1 Current Data				
Time	$I_s$	$I_s^2$	$I_a$	$I_a^2$
0.0000E+00	0.0000E+00	0.0000E+00	0.0000E+00	0.0000E+00
0.3500E-04	0.9809E+05	0.9622E+10	-.5397E+05	0.2913E+10
0.7000E-04	0.1879E+06	0.3529E+11	-.1025E+06	0.1051E+11
0.1050E-03	0.2620E+06	0.6864E+11	-.1408E+06	0.1982E+11
0.1400E-03	0.3135E+06	0.9830E+11	-.1636E+06	0.2678E+11
0.1750E-03	0.3381E+06	0.1143E+12	-.1677E+06	0.2811E+11
0.2100E-03	0.3357E+06	0.1127E+12	-.1536E+06	0.2360E+11
0.2450E-03	0.3108E+06	0.9660E+11	-.1265E+06	0.1601E+11
0.2800E-03	0.2700E+06	0.7292E+11	-.9355E+05	0.8751E+10
0.3150E-03	0.2192E+06	0.4804E+11	-.6091E+05	0.3710E+10
0.3500E-03	0.1623E+06	0.2633E+11	-.3265E+05	0.1066E+10
0.3850E-03	0.1018E+06	0.1037E+11	-.1054E+05	0.1111E+09
0.4200E-03	0.3974E+05	0.1579E+10	0.5362E+04	0.2875E+08
0.4550E-03	-.2213E+05	0.4898E+09	0.1604E+05	0.2573E+09
0.4900E-03	-.8159E+05	0.6657E+10	0.2273E+05	0.5164E+09
0.5250E-03	-.1362E+06	0.1855E+11	0.2644E+05	0.6989E+09
0.5600E-03	-.1836E+06	0.3370E+11	0.2797E+05	0.7824E+09
0.5950E-03	-.2215E+06	0.4907E+11	0.2795E+05	0.7811E+09
0.6300E-03	-.2483E+06	0.6165E+11	0.2685E+05	0.7211E+09
0.6650E-03	-.2627E+06	0.6899E+11	0.2507E+05	0.6284E+09
0.7000E-03	-.2640E+06	0.6971E+11	0.2288E+05	0.5236E+09
0.7350E-03	-.2523E+06	0.6368E+11	0.2052E+05	0.4210E+09
0.7700E-03	-.2283E+06	0.5212E+11	0.1814E+05	0.3292E+09
0.8050E-03	-.1931E+06	0.3731E+11	0.1587E+05	0.2520E+09
0.8400E-03	-.1487E+06	0.2210E+11	0.1379E+05	0.1902E+09
0.8750E-03	-.9710E+05	0.9428E+10	0.1195E+05	0.1427E+09
0.9100E-03	-.4105E+05	0.1685E+10	0.1037E+05	0.1075E+09
0.9450E-03	0.1670E+05	0.2790E+09	0.9069E+04	0.8224E+08
0.9800E-03	0.7329E+05	0.5371E+10	0.8042E+04	0.6468E+08
0.1015E-02	0.1259E+06	0.1585E+11	0.7276E+04	0.5294E+08
0.1050E-02	0.1720E+06	0.2959E+11	0.6748E+04	0.4553E+08
0.1080E-02	0.2046E+06	0.4186E+11	0.6464E+04	0.4178E+08

Table B-3

**Coil 46 Simulation Parameters**

VI = 2111.  
RS = 132.2E-6  
AL = .731E-6  
RA = 3.0390E-3  
ALARM = 9.23E-6  
CAP = 2.50E-3  
V0 = 20.0E3  
AMASS = 3.4  
STAT = 11.  
ARM = 13.  
COILCTR = .03375  
RADA = .04525  
RADS = .05375  
STATR = 3.  
STATC = 3. \* STAT  
ARMR = 3.  
ARMC = 3. \* ARM  
INCRA = .0025  
INCRS = .0025  
NUM1 = 3  
N2 = 13  
DT = 5.0E-7

Table B-4

Coil 46 Kinematic Data				
Time	Position	Velocity	Acceleration	Force
0.0000E+00	0.0000E+00	0.2111E+04	0.0000E+00	0.0000E+00
0.3500E-05	0.7388E-02	0.2111E+04	-.1982E+05	-.6738E+05
0.7000E-05	0.1478E-01	0.2111E+04	-.7824E+05	-.2660E+06
0.1050E-04	0.2216E-01	0.2110E+04	-.1364E+06	-.4637E+06
0.1400E-04	0.2955E-01	0.2110E+04	-.9822E+05	-.3340E+06
0.1750E-04	0.3693E-01	0.2110E+04	0.1124E+06	0.3821E+06
0.2100E-04	0.4432E-01	0.2111E+04	0.4488E+06	0.1526E+07
0.2450E-04	0.5171E-01	0.2113E+04	0.7603E+06	0.2585E+07
0.2800E-04	0.5911E-01	0.2116E+04	0.9448E+06	0.3212E+07
0.3150E-04	0.6653E-01	0.2120E+04	0.9977E+06	0.3392E+07
0.3500E-04	0.7395E-01	0.2123E+04	0.9562E+06	0.3251E+07
0.3850E-04	0.8139E-01	0.2126E+04	0.8590E+06	0.2921E+07
0.4200E-04	0.8883E-01	0.2129E+04	0.7345E+06	0.2497E+07
0.4550E-04	0.9629E-01	0.2131E+04	0.6009E+06	0.2043E+07
0.4900E-04	0.1038E+00	0.2133E+04	0.4695E+06	0.1596E+07
0.5250E-04	0.1112E+00	0.2135E+04	0.3478E+06	0.1182E+07
0.5600E-04	0.1187E+00	0.2136E+04	0.2415E+06	0.8212E+06
0.5950E-04	0.1262E+00	0.2136E+04	0.1571E+06	0.5341E+06
0.6300E-04	0.1336E+00	0.2137E+04	0.9852E+05	0.3350E+06
0.6650E-04	0.1411E+00	0.2137E+04	0.6130E+05	0.2084E+06
0.7000E-04	0.1486E+00	0.2137E+04	0.3813E+05	0.1296E+06
0.7350E-04	0.1561E+00	0.2137E+04	0.2368E+05	0.8051E+05
0.7700E-04	0.1636E+00	0.2137E+04	0.1464E+05	0.4976E+05
0.8050E-04	0.1710E+00	0.2137E+04	0.8959E+04	0.3046E+05
0.8400E-04	0.1785E+00	0.2137E+04	0.5399E+04	0.1836E+05
0.8750E-04	0.1860E+00	0.2137E+04	0.3175E+04	0.1080E+05
0.9100E-04	0.1935E+00	0.2137E+04	0.1799E+04	0.6116E+04
0.9400E-04	0.1999E+00	0.2137E+04	0.1055E+04	0.3588E+04

Table B-5

Coil 46 Current Data				
Time	$I_s$	$I_s^2$	$I_a$	$I_a^2$
0.0000E+00	0.0000E+00	0.0000E+00	0.0000E+0	0.0000E+0
0.3500E-05	0.1596E+06	0.2546E+11	-.2843E+05	0.8085E+09
0.7000E-05	0.3457E+06	0.1195E+12	-.6528E+05	0.4261E+10
0.1050E-04	0.5513E+06	0.3039E+12	-.1084E+06	0.1175E+11
0.1400E-04	0.7551E+06	0.5702E+12	-.1516E+06	0.2299E+11
0.1750E-04	0.9264E+06	0.8583E+12	-.1862E+06	0.3466E+11
0.2100E-04	0.1042E+07	0.1086E+13	-.2053E+06	0.4214E+11
0.2450E-04	0.1099E+07	0.1208E+13	-.2082E+06	0.4335E+11
0.2800E-04	0.1113E+07	0.1240E+13	-.1991E+06	0.3964E+11
0.3150E-04	0.1103E+07	0.1216E+13	-.1830E+06	0.3348E+11
0.3500E-04	0.1080E+07	0.1166E+13	-.1636E+06	0.2678E+11
0.3850E-04	0.1053E+07	0.1109E+13	-.1433E+06	0.2054E+11
0.4200E-04	0.1027E+07	0.1055E+13	-.1233E+06	0.1521E+11
0.4550E-04	0.1003E+07	0.1006E+13	-.1044E+06	0.1089E+11
0.4900E-04	0.9822E+06	0.9646E+12	-.8681E+05	0.7535E+10
0.5250E-04	0.9640E+06	0.9292E+12	-.7098E+05	0.5038E+10
0.5600E-04	0.9478E+06	0.8983E+12	-.5719E+05	0.3271E+10
0.5950E-04	0.9324E+06	0.8694E+12	-.4570E+05	0.2089E+10
0.6300E-04	0.9162E+06	0.8394E+12	-.3647E+05	0.1330E+10
0.6650E-04	0.8974E+06	0.8054E+12	-.2912E+05	0.8478E+09
0.7000E-04	0.8750E+06	0.7656E+12	-.2323E+05	0.5396E+09
0.7350E-04	0.8481E+06	0.7193E+12	-.1848E+05	0.3414E+09
0.7700E-04	0.8166E+06	0.6668E+12	-.1461E+05	0.2133E+09
0.8050E-04	0.7802E+06	0.6087E+12	-.1144E+05	0.1308E+09
0.8400E-04	0.7390E+06	0.5461E+12	-.8825E+04	0.7787E+08
0.8750E-04	0.6932E+06	0.4805E+12	-.6664E+04	0.4441E+08
0.9100E-04	0.6429E+06	0.4134E+12	-.4870E+04	0.2371E+08
0.9400E-04	0.5966E+06	0.3559E+12	-.3572E+04	0.1276E+08

Table B-6

Coil 91 Simulation Parameters
VI = 2985.
RS = 132.2E-6
AL = .731E-6
RA = 3.0390E-3
ALARM = 9.23E-6
CAP = 2.50E-3
V0 = 20.0E3
AMASS = 3.4
STAT = 11.
ARM = 13.
COILCTR = .05
RADA = .04525
RADS = .05375
STATR = 3.
STATC = 3. * STAT
ARMR = 3.
ARMC = 3. * ARM
INCRA = .0025
INCRS = .0025
NUM1 = 3
N2 = 13
DT = 5.0E-7

Table B-7

Coil 91 Kinematic Data				
Time	Position	Velocity	Acceleration	Force
0.0000E+00	0.0000E+00	0.2985E+04	0.0000E+00	0.0000E+00
0.3500E-05	0.1045E-01	0.2985E+04	-.1550E+05	-.5269E+05
0.7000E-05	0.2089E-01	0.2985E+04	-.7587E+05	-.2580E+06
0.1050E-04	0.3134E-01	0.2984E+04	-.1723E+06	-.5857E+06
0.1400E-04	0.4179E-01	0.2984E+04	-.1820E+06	-.6189E+06
0.1750E-04	0.5223E-01	0.2983E+04	0.7990E+05	0.2717E+06
0.2100E-04	0.6267E-01	0.2984E+04	0.5123E+06	0.1742E+07
0.2450E-04	0.7312E-01	0.2987E+04	0.7950E+06	0.2703E+07
0.2800E-04	0.8358E-01	0.2990E+04	0.8518E+06	0.2896E+07
0.3150E-04	0.9405E-01	0.2993E+04	0.7743E+06	0.2633E+07
0.3500E-04	0.1045E+00	0.2995E+04	0.6410E+06	0.2180E+07
0.3850E-04	0.1150E+00	0.2997E+04	0.4929E+06	0.1676E+07
0.4200E-04	0.1255E+00	0.2999E+04	0.3491E+06	0.1187E+07
0.4550E-04	0.1360E+00	0.3000E+04	0.2219E+06	0.7546E+06
0.4900E-04	0.1465E+00	0.3000E+04	0.1270E+06	0.4319E+06
0.5250E-04	0.1570E+00	0.3001E+04	0.7098E+05	0.2413E+06
0.5600E-04	0.1675E+00	0.3001E+04	0.4031E+05	0.1371E+06
0.5950E-04	0.1780E+00	0.3001E+04	0.2330E+05	0.7923E+05
0.6300E-04	0.1885E+00	0.3001E+04	0.1365E+05	0.4642E+05
0.6650E-04	0.1990E+00	0.3001E+04	0.8073E+04	0.2745E+05
0.6687E-04	0.2001E+00	0.3001E+04	0.7634E+04	0.2595E+05

Table B-8

Coil 91 Current Data				
Time	$I_s$	$I_s^2$	$I_a$	$I_a^2$
0.0000E+00	0.0000E+00	0.0000E+00	0.0000E+00	0.0000E+00
0.3500E-05	0.1367E+06	0.1868E+11	-.2108E+05	0.4444E+09
0.7000E-05	0.3070E+06	0.9427E+11	-.5330E+05	0.2840E+10
0.1050E-04	0.5158E+06	0.2661E+12	-.9757E+05	0.9521E+10
0.1400E-04	0.7437E+06	0.5531E+12	-.1480E+06	0.2190E+11
0.1750E-04	0.9328E+06	0.8701E+12	-.1877E+06	0.3522E+11
0.2100E-04	0.1030E+07	0.1060E+13	-.2011E+06	0.4044E+11
0.2450E-04	0.1043E+07	0.1088E+13	-.1903E+06	0.3620E+11
0.2800E-04	0.1017E+07	0.1033E+13	-.1674E+06	0.2802E+11
0.3150E-04	0.9820E+06	0.9644E+12	-.1413E+06	0.1998E+11
0.3500E-04	0.9534E+06	0.9089E+12	-.1160E+06	0.1345E+11
0.3850E-04	0.9349E+06	0.8740E+12	-.9277E+05	0.8606E+10
0.4200E-04	0.9269E+06	0.8592E+12	-.7224E+05	0.5218E+10
0.4550E-04	0.9279E+06	0.8609E+12	-.5497E+05	0.3021E+10
0.4900E-04	0.9348E+06	0.8739E+12	-.4156E+05	0.1727E+10
0.5250E-04	0.9435E+06	0.8902E+12	-.3171E+05	0.1006E+10
0.5600E-04	0.9503E+06	0.9030E+12	-.2444E+05	0.5973E+09
0.5950E-04	0.9530E+06	0.9083E+12	-.1896E+05	0.3596E+09
0.6300E-04	0.9508E+06	0.9039E+12	-.1477E+05	0.2180E+09
0.6650E-04	0.9429E+06	0.8890E+12	-.1150E+05	0.1323E+09
0.6687E-04	0.9417E+06	0.8868E+12	-.1120E+05	0.1254E+09

Table B-9

## ENDNOTES

### Chapter 1

<sup>1-1</sup>S. C. Rashleigh and R. A. Marshall, "Electromagnetic Acceleration of Macroparticles to High Velocities," Journal of Applied Physics 49 (April 1978), 2540-2. Rashleigh and Marshall built a rail gun that launched 12.7 millimeter cubes of lexan to velocities up to 5.9 kilometers per second.

<sup>1-2</sup>Harry D. Fair, Jr., "Electromagnetic Propulsion: A New Initiative," IEEE Transactions on Magnetics 18 (January 1982), 5.

<sup>1-3</sup>Mack W. Dowdy, "Comparative Analyses," chap in Gun Propulsion: Emerging Army Technologies (Jet Propulsion Laboratory, JPL D-3294, August 1986), 7-3 -- 7-4. Propellant impetus definition. Propellant impetus order of magnitude base upon table 7-2.

<sup>1-4</sup>Ibid., 7-31 -- 7-33. Maximum breech pressures of  $10^5$  pounds per square inch were assumed in the analyses of advanced artillery, armor, and air defense guns.

<sup>1-5</sup>Department of Civil and Mechanical Engineering, United States Military Academy, Mechanical Design (West Point, NY: USMA Text, 1991), 8-1 -- 8-6. Including modified figures 8-1 and 8-2.

<sup>1-6</sup>John P. Barber, "The Acceleration of Macroparticles and a Hypervelocity Accelerator," (Ph.D. diss, Australian National University, 1972), 30-31.

<sup>1-7</sup>Harry D. Fair, Phil Coose, Carolyn Meinel, and Derek Tidman, "Electromagnetic Earth-to-Space Launch," IEEE Transactions on Magnetics 27 (January 1991), 10.

<sup>1-8</sup>Fair, "Electromagnetic Propulsion," 4.

1-9M. L. Spann, S. B. Pratap, W. F. Weldon, and W. A. Walls  
"Rotating Machines -- Power Supplies for the Next Generation of EM  
Accelerators," IEEE Transactions on Magnetics 27 (January 1991),  
344.

1-10John T. Bosma and Carolyn Meinel, Electromagnetic Launch  
Systems: New Opportunities in Electromagnetic Propulsion Markets  
Vol 1 (Albuquerque, NM: Cardinal Communications Corp., 1989), 21-  
22.

1-11Donald N. Gower, "Present Gun Propulsion Base," chap in  
Gun Propulsion: Emerging Army Technologies (Jet Propulsion  
Laboratory, JPL D-3294, August 1986), 3-9.

1-12Fair, et al., "Electromagnetic Earth-to-Space Launch," 10-11.

1-13M. R. Palmer and R. X. Lenard, "A Revolution in Access to  
Space Through Spinoffs of SDI Technology," IEEE Transactions on  
Magnetics 27 (January 1991), 13-15.

1-14D. P. Bauer, J. P. Barber, and H. F. Swift, "Application of  
Electromagnetic Accelerators to Space Propulsion," IEEE Transactions  
on Magnetics 18 (January 1982), 170-175.

1-15J. L. Upshaw and J. P. Kajs, "Micrometeoroid Impact  
Simulations Using a Railgun Electromagnetic Accelerator," IEEE  
Transactions on Magnetics 27 (January 1991), 607.

1-16J. M. Schroeder, J. H. Gully, and M. D. Driga,  
"Electromagnetic Launchers for Space Applications," IEEE  
Transactions on Magnetics 25 (January 1989), 505-506.

1-17Bosma and Meinel, Electromagnetic Launch Systems: New  
Opportunities in Electromagnetic Propulsion Markets Vol 1, 187-188.

1-18Ibid., 188-189.

## Chapter 2

2-1Herbert H. Woodson and James R. Melcher, Electromechanical Dynamics Part I, (Malabar, Florida: Robert Krieger Publishing, 1990), B12-B19. The magnetic field system simplification is justified based upon Maxwell's equations.

2-2Ibid., 60. In lumped parameter systems, experience has shown that the system can be considered lossless without introducing unacceptable error.

2-3Ibid., 18-19.

2-4Ibid., 63-64.

2-5Ibid., 67-69. The relationship between force and energy is developed.

2-6William R. Smythe, Static and Dynamic Electricity, (New York, NY: Hemisphere Publishing Co., 1989), 332-333. Derivation of magnetic field energy.

2-7Ibid, 342-343.

2-8Woodson and Melcher, Electromechanical Dynamics, 72-76.

2-9Ibid., 64-65.

2-10Ibid., 76. Magnetic energy version of figure 3.1.8.

2-11Ibid., 72-73. The relationship between force and coenergy is developed.

2-12Smythe, Static and Dynamic Electricity, 342.

2-13Ibid., 581-582. Derivation of the Lorentz force law from Maxwell's equations.

2-14This is a modified file illustration from the Center for Electromechanics at the University of Texas at Austin.

2-15Woodson and Melcher, Electromechanical Dynamics, 322-323. This idealized system is adapted from problem 6.12.

2-16William H. Hayt, Engineering Electromagnetics, 5th ed., (New York, NY: McGraw-Hill Book Co., 1989), 228-229.

2-17R. J. Hayes and R.C. Zowarka, "Experimental Results From CEM-UTS Single Shot 9 MJ Railgun," IEEE Transactions on Magnetics 27 (January 1991): 36.

2-18George L. Jackson, Lloyd K. Farris, and Michael M. Tower, "Electromagnetic Railgun Extended-Life Bore Material Tests Results," IEEE Transactions on Magnetics 22 (November 1986): 1542-3. Overview of barrel wear mechanisms.

2-19 Hayes and Zowarka, "Experimental Results CEM Railgun," 34. CEM reconditions its railgun after each launch to repair launch damage.

2-20Smythe, Static and Dynamic Electricity, 335. Complete derivation of the mutual inductance between coaxial filamentary coils.

2-21Frederick W. Grover, Inductance Calculations: Working Formulas and Tables, (New York, NY: D. Van Nostrand Co., 1946), 2-3.

2-22Albert Y. Wu, "Parameter Studies for Traveling Wave Coaxial Launchers," IEEE Transactions on Magnetics 27 (January 1991): 618.

2-23V. N. Bondaletov and E. N. Ivanov, "Ultrahigh Axial Acceleration of Conducting Rings," Soviet Physics: Technical Physics 22 (February 1977): 232-234.

2-24David Halliday and Robert Resnick, Fundamentals of Physics 3d ed., (New York, NY: John Wiley and Sons, 1988), 647-648.

2-25T. J. Tucker and R. P. Roth, EBWI: A Computer Code for the Prediction of the Behavior of Electrical Circuits Containing Exploding Wire Elements, April 1978, Sandia National Laboratory, SAND 75-0041, 24-25.

2-26J. A. Andrews, D. A. Bresie, S. K. Ingram, and M. E. Davis, Development of a DC Coaxial Accelerator RF 110, (Austin, TX: University of Texas at Austin, Government Contract Report, August 1991): 33. Long solenoid used as an upper bound for axial magnetic flux density

2-27Paul Lorrain, Dale P. Corson, and Francois Lorrain, Electromagnetic Fields and Waves, 3rd ed., (New York: W. H. Freeman and Co., 1988), 355-356.

2-28W. F. Weldon, "A Taxonomy of Electromagnetic Launchers," IEEE Transactions on Magnetics 25 (January 1989): 591-592.

2-29M. D. Driga and W. F. Weldon, "Induction Launcher Design Considerations," IEEE Transactions on Magnetics 25 (January 1989): 153.

2-30M. D. Driga, W. F. Weldon, and H. H. Woodson, "Coaxial Electromagnetic Launchers," IEEE Transactions on Magnetics 22 (November 1986): 1454.

2-31Ibid., 1455.

2-32Driga and Weldon, "Induction Launcher Design Considerations," 153.

2-33Weldon, "A Taxonomy of Electromagnetic Launchers", 591.

2-34Kenelm McKinney and Peter Mongeau, "Multiple Stage Pulsed Induction Acceleration," IEEE Transactions on Magnetics 20 (March 1984): 239-242.

2-35David G. Elliott, "Traveling Wave Induction Launchers," IEEE Transactions on Magnetics 25 (January 1989): 159-163.

2-36Z. Zabar, Y. Naot, L. Birenbaum, E. Levi, and P. N. Joshi, "Design and Power Conditioning for the Coilgun," IEEE Transactions on Magnetics 25 (January 1989): 627-631.

2-37Z. Zabar, X. N. Lu, J. L. He, L. Birenbaum, E. Levi, S. B. Kuznetson, and M. D. Nahemow, "Test Results for Three Prototype Models of a Linear Induction Launcher," IEEE Transactions on Magnetics 27 (January 1991): 558-562.

2-38M. W. Ingram, J. A. Andrews, and D. A. Bresie, "An Actively Switched Pulsed Induction Accelerator," IEEE Transactions on Magnetics 27 (January 1991): 591-595.

2-39J. A. Andrews, D. A. Bresie, S. K. Ingram, and M. E. Davis, Development of a DC Coaxial Accelerator RF 110, (Austin, TX: University of Texas at Austin, Government Contract Report, August 1991): 73.

2-40M. D. Driga and W. F. Weldon, "Induction Launcher Design Considerations," IEEE Transactions on Magnetics 25 (January 1989): 153-158.

2-41Center for Electromechanics, The University of Texas at Austin, Development of a DC Coaxial Accelerator RF 81 (Austin, TX: Government Contract Report, January 1989): 11-41.

2-42 Samuel K. Ingram, "Theoretical Analysis of a Collapsing Field Accelerator," (Technical Paper prepared for presentation at 6th Electromagnetic Launch Symposium, April 1992, Center for Electromechanics at the University of Texas at Austin, 1991): 1-5.

### Chapter 3

3-1 Kenlem McKinney and Peter Mongeau, Multiple Stage Pulsed Induction Acceleration," IEEE Transactions on Magnetics 20 (March 1984) 239. Per stage stored energy to kinetic energy conversion greater than 50 percent is a realistic.

3-2 M. D. Driga, W. F. Weldon, and H. H. Woodson, "Coaxial Electromagnetic Launchers," IEEE Transactions on Magnetics 22 (November 1986): 1454 and 1457. Energy efficiency for induction motor starting is less than 50 percent. Conceptual rising frequency generator powered launcher with 28 percent efficiency.

3-3 M. F. Rose "Compact Capacitor Powered Railgun Systems," IEEE Transactions on Magnetics 22 (November 1986), 1717. Expected system efficiency of 30 percent.

3-4 M. W. Ingram, J. A. Andrews, and D. A. Bresie, "An Actively Switched Pulsed Induction Accelerator," IEEE Transactions on Magnetics 27 (January 1991), 593. Predicted overall performance of two pulsed induction launchers 23 and 33 percent.

3-5 D. A. Bresie, J. A. Andrews, and S. W. Ingram, "Parametric Approach to Linear Induction Accelerator Design," IEEE Transactions on Magnetics 27 (January 1991), 390. Linear Induction Accelerators designed with efficiencies ranging from 20 to 40 percent.

3-6 Samuel K. Ingram, "Theoretical Analysis of a Collapsing Field Accelerator," 5. Overall example system efficiency 28 percent.

3-7J. H. Gully, "Power Supply Technology for Electric Guns," IEEE Transactions on Magnetics 27 (January 1991), 330. Figure 2.

3-8William F. Weldon, "Pulsed Power Packs a Punch," IEEE Spectrum 22 (March 1985) 62. Some of the information is dated but the table provides a basis for comparing energy storage devices.

3-9J. H. Gully, "Power Supply Technology for Electric Guns," 331. Including modified table 3.

3-10J. D. Sterrett, J. R. Lippert, M. R. Palmer, N. E. Johnson, and M. C. Altstatt, "Design of a Battery Power Supply for the Electromagnetic Gun Experimental Research Facility," in Digest of Technical Papers of the 6th IEEE Pulsed Power Conference held in Arlington, VA, 29 June - 1 July 1987, ed. Bernard Berstein and Peter Turchi (New York: IEEE), 42-45. U.S. Air Force Armament Laboratory railgun power supply consisted of a series parallel arrangement of 16,128 lead acid batteries.

3-11Harvey N. Seiger, "Lithium/Cobalt Sulfide Pulse Power Battery," in Proceedings of the 34th International Power Sources Symposium held in Cherry Hill, NJ, 25-28 June 1990 by the IEEE, (New York: IEEE, 1990) 334.

3-12R. L. Laughlin, J. H. Gully, K. E. Nalty, and R. C. Zowarka, "System Design of the Ultrahigh Velocity GEDI Experiment," IEEE Transactions on Magnetics 22 (November 1986) 1578-1580.

3-13R. C. Zowarka, J. P. Kajs, S. B. Pratap, J. H. Price, and W. F. Weldon, "A New Approach to a High Efficiency Inductive Store," IEEE Transactions on Magnetics 27 (January 1991) 385-386.

3-14J. R. Laghari, and W. J. Sarjeant, "Energy Storage Pulsed Power Capacitor Technology." in Proceedings of the 34th International Power Sources Symposium held in Cherry Hill, NJ, 25-28 June 1990 by the IEEE, (New York: IEEE, 1990) 380. Figure 1. This figure inspired similar figures for other energy storage devices.

3-15Ibid., 381.

3-16W. J. Sarjeant, "Trip Report: Electromagnetic Power Supplies and Launchers Workshop, 9-11 January 1991," (23 January 1991) Institute for Advanced Technology, University of Texas at Austin, 5-6.

3-17Weldon, "Pulsed Power Packs a Punch," 62.

3-18Weldon, "Pulsed Power Packs a Punch," 62.

3-19This is a file illustration (view graph no. 26) from CEM, UT Austin.

3-20Paul Lorrain and Dale R. Corson, Electromagnetic Fields and Waves, 2d ed., (San Francisco, CA: W. H. Freeman and Co., 1970), 662-664.

3-21William F. Weldon, "Electromechanics Course," EE397K in-class lecture notes, The University of Texas at Austin, Summer 1991.

3-22W. F. Weldon, M. D. Driga, and H. H. Woodson, U. S. Patent No. 4,200,831, April 29, 1980, "Compensated Pulsed Alternator," 1-2.

3-23M. L. Spann, S. B. Pratap, M. D. Werst, A. W. Walls, and W. G. Fulcher, "Compulsator Research at the University of Texas at Austin -- An Overview," IEEE Transactions on Magnetics 25 (January 1989) 529-531.

3-24Weldon, "Pulsed Power Packs a Punch," 60. Figure 1c combined with file illustration (view graph no. 3616) from CEM, UT at Austin.

3-25Spann, et al., "Compulsator Research at UT - Austin," 530. Modified version of figure 1a.

3-26Ibid. 530.

3-27 This is a file illustration (view graph no. 3619) from CEM, UT Austin.

3-28 This is a file illustration (view graph no. 3621) from CEM, UT Austin.

3-29 Spann, et al., "Compulsator Research at UT - Austin," 530.

3-30 This is a file illustration (view graph no. 3617) from CEM, UT Austin.

3-31 Spann, et al., "Compulsator Research at UT - Austin," 530. Including modified version of figure 1b.

3-32 M. D. Driga and H. D. Fair, "Advanced Concepts for Electromagnetic Launcher Power Supplies Incorporating Magnetic Flux Compression," IEEE Transactions 27 (January 1991), 351-353. A clear and simple explanation of flux compression.

3-33 J. H. Gully, "Power Supply Technology for Electric Guns," 332.

3-34 M. D. Driga and W. F. Weldon, "Induction Launcher Design Considerations," IEEE Transactions on Magnetics 25 (January 1989) 155-157. Describes mechanical and electrical variants of the rising frequency generator. Including modified figure 4.

3-35 M. D. Driga, H. H. Woodson, and W. F. Weldon, "Electromagnetic Induction Launchers," IEEE Transactions on Magnetics 22 (November 1986), 1455. Describes mechanical and electrical variants of the rising frequency generator.

3-36 J. H. Gully, "Power Supply Technology for Electric Guns," 329. Figure 1.

3-37 Emanuel M. Honig, "Induction Energy Storage Circuits," in Opening Switches, ed. A. Guenther and M. Kristiansen (New York: Plenum Press, 1987), 5. From Table 1.

3-38 D. Bhasavanich, S. S. Hitchcock, P. M. Creely, R. S. Shaw, H. G. Harmon, and J. T. Naff, "Development of a Compact, Higher-Energy Spark Gap Switch and Trigger Generator System," in Digest of Technical Papers 8th International Pulsed Power Conference held in San Diego, CA 16-19 June 1991, ed. K. Prestwich and R. White (New York, IEEE), 343.

3-39 R. F. Thelen and J. H. Price, "Pulsed Power Electronics in the 9 Megajoule EM Range Gun System," in Digest of Technical Papers 8th International Pulsed Power Conference held in San Diego, CA, 16-19 June 1991, ed. K. Prestwich and R. White (New York, IEEE), 146.

3-40 J. A. Andrews, D. A. Bresie, S. K. Ingram, and M. E. Davis, Development of a DC Coaxial Accelerator RF-110 (Austin, TX: Center for Electromechanics at the University of Texas at Austin, Government Contract Report, August 1991). 27.

3-41 T. R. Burkes, J. P. Craig, M. O. Hagler, M. Kristiansen, and W. M. Portnoy, "A Review of High-Power Switch Technology," Transactions on Electron Devices 10 (October, 1979), 1402. Including figure 2.

3-42 Ibid., 1405. Includes figure 7.

3-43 R. Kihara, D. B. Cummings, K. S. Leighton, and A. P. Shulski, "Commercial High Current Ignitron Development," in Digest of Technical Papers 7th IEEE Pulsed Power Conference, held in Monterey, CA, 11-14 June, 1989 ed. B. H. Berstein and J. P. Shannon (New York, IEEE), 18-21. Ignitron dimensions estimated from scale in figure 3.

3-44 "Tentative NL-9000 Data Sheet," Richardson Electronics, Ltd, Lafox, IL, Undated.

3-45Bhasavanich, et al., "Development of a Compact, Higher-Energy Spark Gap Switch and Trigger Generator System," 343-344.

3-46Honig, "Induction Energy Storage Circuits," 30-36. Includes figure 28.

3-47Thelen and Price, "Pulsed Power Electronics in the 9 Megajoule EM Range Gun System," 148.

3-48Information from CEM Viewgraph 2227.1 describing the SCR used to build the switch referred to in note 3-39.

3-49Honig, "Induction Energy Storage Circuits," 8-10.

3-50K. H. Schoenbach, M. Kristiansen, and G. Schaefer, "A Review of Opening Switch Technology for Inductive Energy Storage," Proceedings of the IEEE 72 (August 1984), 1037.

3-51Ibid., 1027-8.

3-52Ibid., 1024-7.

3-53John P. Barber, "Advances in Opening Switch Technology at IAP Research," IEEE Transactions on Magnetics 25 (January 1989), 68-69.

3-54Honig, "Induction Energy Storage Circuits," 9-11.

3-55Ibid., 23-26.

3-56J. H. Price, D. A. Badger, and R. A. Lee, "Design and Testing of High Current, High Voltage Hexapolar Flexible Cables for Pulsed Power Applications," in Digest of Technical Papers 8th International Pulsed Power Conference held in San Diego, CA 16-19 June 1991, ed. K. Prestwich and R. White (New York, IEEE), 150-155.

3-57D. R. Peterson, J. H. Price, W. F. Weldon, R. C. Zowarka, C. W. G. Fulcher, and J. H. Hahne, "Design and Operation of a High-energy Railgun Facility," IEEE Transactions on Magnetics 25 (January 1989), 439-440.

#### Chapter 4

4-1Samuel K. Ingram, "Theoretical Analysis of a Collapsing Field Accelerator," (Technical Paper prepared for presentation at 6th Electromagnetic Launch Symposium, April 1992, Center for Electromechanics at the University of Texas at Austin, 1991): 4-5.

4-2D. A. Bresie, J. A. Andrews, and S. W. Ingram, "Parametric Approach to Linear Induction Accelerator Design," IEEE Transactions on Magnetics 27 (January 1991), 390-391. Including table 1.

#### Chapter 5

5-1David Elliott, "Panel Estimates of Size, Weight, Power, and Cooling for 18 Missions," in Electric Gun Propulsion and Power Conditioning Panel of the Electric Gun System Study to David C. Hardison. Study Director, David Elliott, ed., JPL Laboratories, JPL D-6272, 15 May 1989, 2-1 and 2-5. The missions were specified in the final report of the Threat, Projectiles, Fire Control, and Terminal Effects Panel, California Research and Technology, Inc., Pleasanton, CA, November 1988.

5-2Christopher Foss, ed., Jane's Armour and Artillery, 11th ed., (Alexandria, VA: Jane's Defence Data, 1990), 144. Hull height is not specifically listed but is estimated to be 1.5 meters.

5-3"Data Sheet: Type KM High Energy Density Pulsed Discharge Capacitors," Aerovox Inc., New Bedford, MA, Undated.

5-4James F. Young and Robert S. Shane, ed., Materials and Processes 3rd ed., (New York: Marcel Dekker, Inc., 1985), 796. Table 15-4.

5-5"Periodic Table of Elements," Catalog No. S-18806 (Skokie IL: Sargent Welch Scientific Co., 1980) 1-2.

5-6J. A. Andrews, D. A. Bresie, S. K. Ingram, and M. E. Davis, Development of a DC Coaxial Accelerator RF 110, (Austin, TX: University of Texas at Austin, Government Contract Report, August 1991): 15. Fabrication considerations make a 1 mm air gap realistic for coilguns regardless of bore size.

5-7William H. Hayt and Jack E. Kemmerly, Engineering Circuit Analysis 4th ed., (New York, NY: McGraw-Hill Book Co., 1986), 440-441.

5-8Frederick W. Grover, Inductance Calculations: Working Formulas and Tables, (New York, NY: D. Van Nostrand Co., 1946), 105 and 94.

5-9A.W. Goodman, Analytic Geometry and the Calculus 3rd ed., (New York: MacMillian Publishing Co., Inc., 1974), 683-684.

5-10Grover, Inductance Calculations: Working Formulas and Tables, 149-151.

## Appendix A

A-1Frederick W. Grover, Inductance Calculations: Working Formulas and Tables, (New York, NY: D. Van Nostrand Co., 1946), 89-90.

## Appendix B

B-1 This computer code was substantially prepared by Sunil Murthy based upon equations that I provided him. I wrote the sub-routines to calculate the mutual inductance and mutual inductance gradients.

B-2 William H. Press, Brian P. Flannery, Saul A. Teukolsky, and William T. Vetterling, Numerical Recipes: The Art of Scientific Computing (Fortran Version), (New York: Cambridge University Press, 1989), 183-188. Source for the code for determining Elliptic Integrals of the first and second kind.

B-3 Erwin Fehlberg, Classical Fifth-, Sixth-, Seventh-, and Eighth-order Runge-Kutta Formulas with Step-size Control, NASA Technical Report TR R-287 (Washington, DC: National Aeronautics and Space Administration, October 1968), 52-67. This reference is the source of the Runge-Kutta Integrator upon which the integrator sub-routine is based. The sub-routine RK78RG is a Center for Electromechanics file code.

## BIBLIOGRAPHY

- Aerovox Inc. "Data Sheet: Type KM High Energy Density Pulsed Discharge Capacitors." New Bedford, MA, Undated.
- Andrews, J. A., D. A. Bresie, S. K. Ingram, and M. E. Davis. Development of a DC Coaxial Accelerator RF 110. Austin, TX: University of Texas at Austin, Government Contract Report, August 1991.
- Barber, John P. "Advances in Opening Switch Technology at IAP Research." IEEE Transactions on Magnetics 25 (January 1989), 68-71.
- Barber, John P. "The Acceleration of Macroparticles and a Hypervelocity Accelerator." Ph.D. diss., Australian National University, 1972.
- Bauer, D. P., J. P. Barber, and H. F. Swift. "Application of Electromagnetic Accelerators to Space Propulsion." IEEE Transactions on Magnetics 18 (January 1982): 170-175.
- Bhasavanich, D., S. S. Hitchcock, P. M. Creely, R. S. Shaw, H. G. Harmon, and J. T. Naff. "Development of a Compact, Higher-Energy Spark Gap Switch and Trigger Generator System." In Digest of Technical Papers 8th International Pulsed Power Conference held in San Diego, CA, 16-19 June 1991, edited by K. Prestwich and R. White, 343-345. New York: IEEE, 1991.
- Bondaletov, V. N., and E. N. Ivanov. "Ultrahigh Axial Acceleration of Conducting Rings." Soviet Physics: Technical Physics 22 (February 1977): 232-234.

Bosma, John T., and Carolyn Meinel. Electromagnetic Launch Systems: New Opportunities in Electromagnetic Propulsion Markets Vol. 1. Albuquerque, NM: Cardinal Communications Corp., 1989

Bresie, D. A., J. A. Andrews, and S. W. Ingram. "Parametric Approach to Linear Induction Accelerator Design." IEEE Transactions on Magnetics 27 (January 1991), 390-393.

Burkes, T. R., J. P. Craig, M. O. Hagler, M. Kristiansen, and W. M. Portnoy. "A Review of High-Power Switch Technology." Transactions on Electron Devices 10 (October, 1979), 1401-11.

Center for Electromechanics, The University of Texas at Austin. Development of a DC Coaxial Accelerator RF 81. Austin, TX: Government Contract Report, January 1989: 11-41.

Department of Civil and Mechanical Engineering, United States Military Academy. Mechanical Design. West Point, NY: USMA Text, 1991.

Dowdy, Mack W. "Comparative Analyses." Chap. in Gun Propulsion: Emerging Army Technologies. Jet Propulsion Laboratory, JPL D-3294, August 1986.

Driga, M. D., and H. D. Fair. "Advanced Concepts for Electromagnetic Launcher Power Supplies Incorporating Magnetic Flux Compression." IEEE Transactions on Magnetics 27 (January 1991), 350-355.

Driga, M. D., and W. F. Weldon. "Induction Launcher Design Considerations." IEEE Transactions on Magnetics 25 (January 1989): 153-158.

- Driga, M. D., W. F. Weldon, and H. H. Woodson. "Coaxial Electromagnetic Launchers." IEEE Transactions on Magnetics 22 (November 1986): 1453-8.
- Elliott, David G. "Panel Estimates of Size, Weight, Power, and Cooling for 18 Missions." In Electric Gun Propulsion and Power Conditioning Panel of the Electric Gun System Study to David C. Hardison, Study Director, edited by David Elliott. JPL Laboratories, JPL D-6272, 15 May 1989.
- Elliott, David G. "Traveling Wave Induction Launchers." IEEE Transactions on Magnetics 25 (January 1989): 159-163.
- Fair, Harry D., Jr. "Electromagnetic Propulsion: A New Initiative." IEEE Transactions on Magnetics 18 (January 1982): 4-6.
- Fair, Harry D., Phil Coose, Carolyn Meinel, and Derek Tidman. "Electromagnetic Earth-to-Space Launch." IEEE Transactions on Magnetics 27 (January 1991): 9-16.
- Fehlberg, Erwin. Classical Fifth-, Sixth-, Seventh-, and Eighth-order Runge-Kutta Formulas with Step-size Control. NASA Technical Report TR R-287. Washington, DC: National Aeronautics and Space Administration, October 1968.
- Foss, Christopher, ed. Jane's Armour and Artillery Alexandria, VA: Jane's Defence Data, 1990.
- Goodman, A. W. Analytic Geometry and the Calculus 3rd ed. New York: MacMillian Publishing Co., Inc., 1974.
- Gower, Donald N. "Present Gun Propulsion Base." Chap. in Gun Propulsion: Emerging Army Technologies. Jet Propulsion Laboratory, JPL D-3294, August 1986.

- Grover, Frederick W. Inductance Calculations: Working Formulas and Tables. New York, NY: D. Van Nostrand Co., 1946.
- Gully, J. H. "Power Supply Technology for Electric Guns." IEEE Transactions on Magnetics 27 (January 1991), 329-334.
- Halliday, David, and Robert Resnick. Fundamentals of Physics 3d ed. New York, NY: John Wiley and Sons, 1988.
- Hayes, R. J., and R.C. Zowarka. "Experimental Results From CEM-UTS Single Shot 9 MJ Railgun." IEEE Transactions on Magnetics 27 (January 1991): 33-38.
- Hayt, William H. Engineering Electromagnetics, 5th ed. New York, NY: McGraw-Hill Book Co., 1989.
- Hayt, William H., and Jack E. Kemmerly. Engineering Circuit Analysis 4th ed. New York, NY: McGraw-Hill Book Co., 1986.
- Honig, Emanuel M., "Induction Energy Storage Circuits," in Opening Switches, ed. A. Guenther and M. Kristiansen, 1-48. New York: Plenum Press, 1987.
- Ingram, M. W., J. A. Andrews, and D. A. Bresie. "An Actively Switched Pulsed Induction Accelerator." IEEE Transactions on Magnetics 27 (January 1991): 591-595.
- Ingram, Samuel K. "Theoretical Analysis of a Collapsing Field Accelerator." (Technical Paper prepared for presentation at 6th Electromagnetic Launch Symposium, April 1992, Center for Electromechanics at the University of Texas at Austin, 1991): 1-5.

- Jackson, George L., Lloyd K. Farris, and Michael M. Tower. "Electromagnetic Railgun Extended-Life Bore Material Tests Results." IEEE Transactions on Magnetics 22 (November 1986): 1542-5.
- Kihara, R., D. B. Cummings, K. S. Leighton, and A. P. Shulski, "Commercial High Current Ignitron Development," In Digest of Technical Papers 7th IEEE Pulsed Power Conference, held in Monterey, CA, 11-14 June, 1989 ed. B. H. Berstein and J. P. Shannon, 18-21. New York: IEEE, 1989.
- Laghari, J. R., and W. J. Sarjeant. "Energy Storage Pulsed Power Capacitor Technology." In Proceedings of the 34th International Power Sources Symposium held in Cherry Hill, NJ, 25-28 June 1990 by the IEEE. New York: IEEE, 1990, 380-386.
- Laughlin, R. L., J. H. Gully, K. E. Nalty, and R. C. Zowarka. "System Design of the Ultrahigh Velocity GEDI Experiment." IEEE Transactions on Magnetics 22 (November 1986) 1578-1583.
- Lorrain, Paul, and Dale R. Corson. Electromagnetic Fields and Waves, 2d ed. San Francisco, CA: W. H. Freeman and Co., 1970.
- Lorrain, Paul, Dale P. Corson, and Francois Lorrain. Electromagnetic Fields and Waves, 3rd ed. New York: W. H. Freeman and Co., 1988.
- McKinney, Kenelm, and Peter Mongeau. "Multiple Stage Pulsed Induction Acceleration." IEEE Transactions on Magnetics 20 (March 1984): 239-242.
- Palmer, M. R., and R. X. Lenard. "A Revolution in Access to Space Through Spinoffs of SDI Technology." IEEE Transactions on Magnetics 27 (January 1991): 11-20.

Peterson, D. R., J. H. Price, W. F. Weldon, R. C. Zowarka, C. W. G. Fulcher, and J. H. Hahne. "Design and Operation of a High-energy Railgun Facility." IEEE Transactions on Magnetics 25 (January 1989), 438-442.

Press, William H., Brian P. Flannery, Saul A. Teukolsky, and William T. Vetterling. Numerical Recipes: The Art of Scientific Computing (Fortran Version). New York: Cambridge University Press, 1989.

Price, J. H., D. A. Badger, and R. A. Lee. "Design and Testing of High Current, High Voltage Hexapolar Flexible Cables for Pulsed Power Applications." In Digest of Technical Papers 8th International Pulsed Power Conference held in San Diego, CA, 16-19 June 1991, edited by K. Prestwich and R. White, 150-155. New York: IEEE, 1991.

Rashleigh, S. C., and R. A. Marshall. "Electromagnetic Acceleration of Macroparticles to High Velocities." Journal of Applied Physics 49 (April 1978): 2540-2.

Richardson Electronics, Ltd. "Tentative NL-9000 Data Sheet." Lafox, IL, Undated.

Rose, M. F. "Compact Capacitor Powered Railgun Systems." IEEE Transactions on Magnetics 22 (November 1986), 1717-21.

Sargent Welch Scientific Co. "Periodic Table of Elements." Catalog No. S-18806. Skokie, IL, 1980.

Sarjeant, W. J., "Trip Report: Electromagnetic Power Supplies and Launchers Workshop, 9-11 January 1991." (23 January 1991) Institute for Advanced Technology, University of Texas at Austin.

Schoenbach, K. H., M. Kristiansen, and G. Schaefer. "A Review of Opening Switch Technology for Inductive Energy Storage." Proceedings of the IEEE 72 (August 1984), 1019-1040.

Schroeder, J. M., J. H. Gully, and M. D. Driga. "Electromagnetic Launchers for Space Applications." IEEE Transactions on Magnetics 25 (January 1989): 504-507.

Seiger, Harvey N. "Lithium/Cobalt Sulfide Pulse Power Battery." In Proceedings of the 34th International Power Sources Symposium held in Cherry Hill, NJ, 25-28 June 1990 by the IEEE. New York: IEEE, 1990, 334-338.

Smythe, William R. Static and Dynamic Electricity. New York, NY: Hemisphere Publishing Co., 1989.

Spann, M. L., S. B. Pratap, M. D. Werst, A. W. Walls, and W. G. Fulcher. "Compulsator Research at the University of Texas at Austin -- An Overview." IEEE Transactions on Magnetics 25 (January 1989) 529-537.

Spann, M. L., S. B. Pratap, W. F. Weldon, and W. A. Walls. "Rotating Machines -- Power Supplies for the Next Generation of EM Accelerators." IEEE Transactions on Magnetics 27 (January 1991): 344-349.

Sterrett, J. D., J. R. Lippert, M. R. Palmer, N. E. Johnson, and M. C. Altstatt. "Design of a Battery Power Supply for the Electromagnetic Gun Experimental Research Facility." In Digest of Technical Papers of the 6th IEEE Pulsed Power Conference held in Arlington VA 29 June - 1 July 1987, edited by Bernard Bernstein and Peter Turchi, 42-45. New York: IEEE, 1987.

- Thelen, R. F., and J. H. Price. "Pulsed Power Electronics in the 9 Megajoule EM Range Gun System." In Digest of Technical Papers 8th International Pulsed Power Conference held in San Diego, CA, 16-19 June 1991, edited by K. Prestwich and R. White, 146-149. New York: IEEE, 1991.
- Tucker, T. J., and R. P. Roth. EBWI: A Computer Code for the Prediction of the Behavior of Electrical Circuits Containing Exploding Wire Elements. Sandia National Laboratory, SAND 75-0041, April 1978.
- Upshaw, J. L. and J. P. Kajs. "Micrometeroid Impact Simulations Using a Railgun Electromagnetic Accelerator," IEEE Transactions on Magnetics 27 (January 1991), 607.
- Weldon, W. F. "A Taxonomy of Electromagnetic Launchers." IEEE Transactions on Magnetics 25 (January 1989): 591-592.
- Weldon, W. F., M. D. Driga, and H. H. Woodson, U. S. Patent No. 4,200,831, April 29, 1980, "Compensated Pulsed Alternator."
- Weldon, William F. "Pulsed Power Packs a Punch." IEEE Spectrum 22 (March 1985) 59-66.
- Woodson, Herbert H., and James R. Melcher. Electromechanical Dynamics Part I. Malabar, Florida: Robert Krieger Publishing, 1990.
- Wu, Albert Y. "Parameter Studies for Traveling Wave Coaxial Launchers." IEEE Transactions on Magnetics 27 (January 1991): 617-622.
- Young, James F., and Robert S. Shane, ed. Materials and Processes 3rd ed. New York: Marcel Dekker, Inc., 1985.

Zabar, Z., X. N. Lu, J. L. He, L. Birenbaum, E. Levi, S. B. Kuznetson, and M. D. Nahemow. "Test Results for Three Prototype Models of a Linear Induction Launcher." IEEE Transactions on Magnetics 27 (January 1991): 558-562.

Zabar, Z., Y. Naot, L. Birenbaum, E. Levi, and P. N. Joshi. "Design and Power Conditioning for the Coilgun." IEEE Transactions on Magnetics 25 (January 1989): 627-631.

Zowarka, R. C., J. P. Kajs, S. B. Pratap, J. H. Price, and W. F. Weldon. "A New Approach to a High Efficiency Inductive Store." IEEE Transactions on Magnetics 27 (January 1991): 384-389.

## VITA

Karl Edward Reinhard was born at Camp Hanford, Washington, on 18 August, 1960, the son of Donald Robert and Mary Helen Reinhard. He received his Bachelor of Science Degree from the United States Military Academy, West Point, New York in 1982 and was commissioned in the United States Army. In the following year, he completed the Ordnance Officer Basic Course and Explosive Ordnance Disposal School. His first assignment was as Executive Officer of the 47th Ordnance Detachment (Explosive Ordnance Disposal (EOD)) at Fort Hood, Texas from July 1983 to September 1984. He commanded the 94th Ordnance Detachment (EOD) at Fort Carson, Colorado from September, 1984 to June 1986.

Following the Ordnance Officer Advanced Course, Captain Reinhard served in Germany first as Operations Officer of Miesau Army Depot. Subsequently, he commanded Headquarters and Headquarters Company, 60th Ordnance Group (Ammunition) from December 1987 to June 1989. He then served on the Group staff until his return to the United States and entry into the Graduate School of the University of Texas at Austin in June 1990.

Captain Reinhard's next assignment will be as an instructor in the Department of Electrical Engineering and Computer Science at the United States Military Academy.

Permanent Address:

805 Hercules Place  
Colorado Springs, Colorado 80906

This thesis was typed by Karl E. Reinhard